Studying cellular and molecular pathways underlying Inflammatory Bowel Disease pathogenesis in humans by CRISPR/Cas9 genetic engineering in human cells and mice.

Final report for the Marshall Plan Scholarship

Submitted by

Laura-Sophie Frommelt, BSc

Yale University

Yale School of Medicine

Department of Immunobiology

Supervisor: Dr. Richard Flavell, Dr Manolis Roulis

Leopold-Franzens-University Innsbruck

Institute of Zoology

Department of Evolutionary and Developmental Biology

Supervisor: Ass. Prof. Dr. Peter Ladurner

Index

1 Introduction

1.1 Inflammatory bowel diseases (IBD)

Inflammatory bowel diseases (IBD) represent a heterogenous group of inflammatory and ulcerative diseases that cause chronic inflammation at various sites in the gastrointestinal tract (GI-tract). People with IBD suffer from intermittent or persistent symptoms such as diarrhea, abdominal pain, severe internal cramps, rectal bleeding, fever, malnutrition, and weight loss. Prolonged inflammation of the intestines results in severe damage to the GI-tract and increases the risk of developing colorectal cancer. IBD may also cause extraintestinal complications including anemia, arthritis, osteoporosis, ocular disorders, inflammatory skin and liver diseases (Kirsner 2001; Ephgrave 2007).

Research studies show that incidents and prevalence of IBD have increased worldwide in recent decades (Shivananda et al. 1996; Russel 2000; Lakatos 2006; M'Koma 2013). The diseases occur mainly in developed countries and currently affect up to 1.6 million people in the US and 2.2 million in Europe. Although people of any racial or ethnic group may be affected, people of Northern European and Anglo-Saxon descent have an increased risk of developing IBD (Basu et al. 2005). These diseases affect people of both sexes equally and can occur at any age form early childhood to beyond the sixth decade of life (Ruel et al. 2014). An increased incidence of IBD in families can be observed indicating a genetic component of these diseases.

Although major scientific advances have led to a better understanding of the underlying mechanisms of IBD, their exact etiology is still unknown. The current hypothesis assumes a complex interplay between genetic, environmental and intestinal microbial factors with the host immune system (see fig. 1[A]). Intestinal inflammation and associated mucosal lesions are caused by dysregulated auto-inflammatory immune responses triggered by the intestinal microbiome and unidentified environmental factors (i.e. food particles or stress) in people with a multifactorial genetic predisposition (Souza and Fiocchi 2016; Manichanh et al. 2012; Lakatos 2006). The immune responses include an excessive release of inflammatory mediators such as cytokines, interleukins (IL) and tumor necrosis factor (TNF) (Fujino et al. 2003). Susceptibility genes can contribute to the pathogenesis by causing abnormal mucosal immune reactions, poor epithelial barrier function or changes in the composition of the intestinal microbiome (Walfish and Ching Companioni 2019).

IBD are generally diagnosed by performing endoscopy with tissue biopsy of pathological lesions in combination with evaluation of inflammatory markers in stool and blood samples (Haas et al. 2016). Since there is no cure for IBD, various types of medications are used to control inflammation, relieve associated symptoms and maintain remission: anti-inflammatory drugs (5-aminosalicylates, corticosteroids), immunomodulating and biologic agents (immunesuppressive and anticytokine drugs), antibiotics and probiotics, stress management and surgery (Sohrabpour et al. 2010).

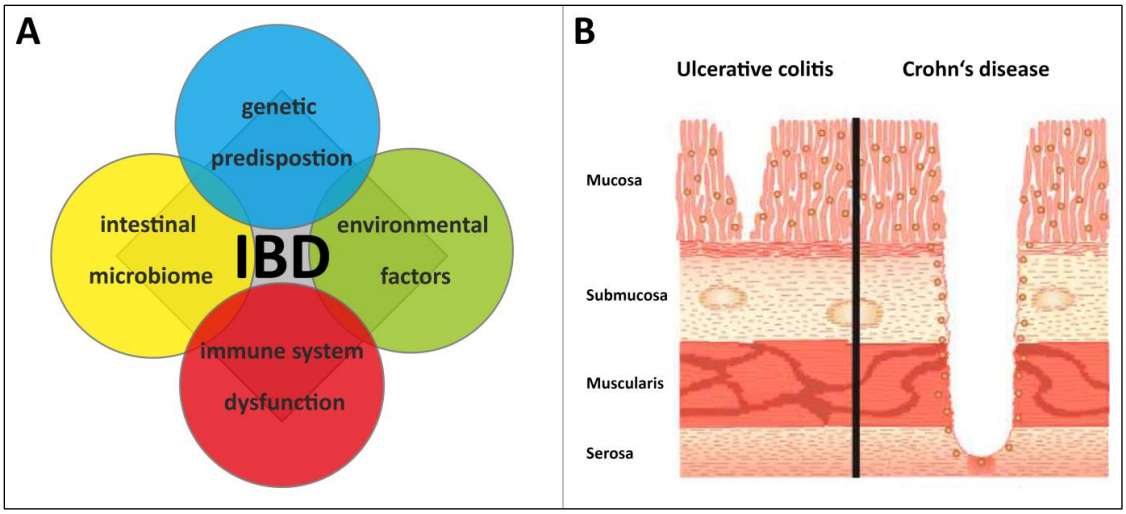

Figure 1: Inflammatory bowel diseases. [A] The pathological interaction of genetic predisposition, environmental factors and dysregulated immune system results in chronic inflammation of the gastrointestinal tract. **[B]** The two major types of IBD, ulcerative colitis and Crohn's disease can be distinguished by location and nature of inflammatory changes. Ulcerative colitis causes inflammation and ulcers in the mucosa and submucosa of rectum and colon, whereas Crohn's disease can affect any part of the GI-tract and causes transmural (mucosa to submucosa) lesions. Image 1[B] is modified after IBD-smartypance.com

The two main types of IBD, ulcerative colitis (UC) and Crohn's disease (CD), are characterized by similar clinical symptoms (chronic diarrhea and abdominal pain) but differ in distribution pattern and nature of the inflammatory changes (see fig. 1 [B]).

- Ulcerative colitis: This disease is usually chronic, with repeated flare-ups interrupted by remissions. The mucosal inflammation typically begins in the rectum and can spread continuously to proximal segments of the colon, but hardly ever extends into the ileum. In addition, UC usually causes shallow ulcers in the innermost layers (mucosa and submucosa) of the colonic wall. Early in the disease, the mucous membrane is reddened and becomes increasingly granular and friable during the course of the disease. The loss of the normal vascular pattern is often associated with scattered hemorrhagic areas, resulting in bloody diarrhea, abdominal pain and cramps (Kirsner 2001; Torres et al. 2012)

- Crohn's disease: This inflammatory bowel disease can affect any part of the GI-tract, from the mouth to the anus, but in most cases it occurs in the terminal ileum and proximal colon (35% ileum alone, 20% colon alone, 40% ileum + colon, 5% other areas). The rectum, however, is almost never affected. The granulomatous inflammation in CD is often discontinuous, affecting some segments of the intestinal tract, while other areas remain completely unaffected (skip areas). In the early stages of the disease, focal crypt inflammation and abscesses can be observed. Over time, inflammation and mucosal lesions spread transmural (mucosa to serosa), leading to deep longitudinal and traverse ulcers, lymphedema and thickening of the intestinal wall. The characteristic cobblestone appearance of the intestine in CD can be observed. Common complications in CD are intestinal blockage due to scarring, and abscesses, internal and external fistulas and perforation caused by deep ulcers penetrating through the intestinal wall (Rubin et al. 2012; Ha and Khalil 2015; Stange and Wehkamp 2016).

The development of animal models of colitis to mimic clinical symptoms or genetic predisposition of both forms of IBD has led to a better understanding of the molecular mechanisms underlying these diseases (Chassaing et al. 2014; Chen et al. 2016; Das et al. 2017; Eichele and Kharbanda 2017; Reinoso Webb et al. 2018). Furthermore, genome-wide association studies (GWAS) have helped to identify numerous candidate genes and non-coding genomic regions involved in IBD and underscore the importance of environmental factors, in particular the intestinal microbiome (Duchmann et al. 1995; Duerr et al. 2006; Huyghe et al. 2019; Manichanh et al. 2012). Ongoing research in genetics, immunology, geographic epidemiology and microbiology focuses on improving current treatment, seeking new targets for developing more effective drugs, discovering new diagnostic tools and extending our knowledge of the etiology of these complex diseases.

1.2 Genome-wide association studies and enhanceropathy

A person's susceptibility to many common complex diseases, such as IBD, is determined by a combination of genetic predisposition and environmental factors. The main objective of human genetics is to identify these genetic risk factors associated with diseases in order to gain a better understanding of molecular mechanisms underlying diseases, identify possible new drug targets and disease biomarkers, and pave the way for personalized medicine. Genome-wide association studies (GWAS) represent a powerful and emerging technology for genome-wide analysis of genetic variations using whole-genome sequencing or genome-wide single nucleotide polymorphisms (SNPs) arrays (e.g. Illumina Immunochip) in large case-control cohorts. To date, more than 240 susceptibility loci, often with annotated target genes, have been discovered for both major forms of IBD, UC and CD, based on GWAS (Jostins et al. 2012b; Huang et al. 2017; Iida et al. 2018; Lange et al. 2017). This underscores the importance of genetics for the pathology of IBD and could explain the inheritance of these diseases, which is particularly evident in CD. The functional analysis of IBD-genes showed that they are involved either in the regulation of the immune system (*IRGM*, *ATG16L1,IL-10*, integrins), in epithelial barrier function or in the control of microbial composition and growth in the intestine (*NOD2*/*CARD15*) (Liu and Stappenbeck 2016; Iida et al. 2018). Furthermore, several IBD-SNPs were found to overlap with risk loci of other non-intestinal autoimmune diseases such as psoriasis, ankylosing spondylitis and multiple sclerosis (Verstockt et al. 2018)

GWAS are based on the systematic scanning of the entire genome of many individuals to detect statistically relevant genotype-phenotype association. They compare DNA sequence variations, mostly SNPs, across the entire genome in large case (people with the disease) – control (healthy people) populations, allowing identification of variants that occur with a significantly altered frequency in the case cohort (Verstockt et al. 2018). Commonly, SNP-chips or arrays are used which enable testing of several hundred thousand to millions of SNPs across the entire genome in a single experiment. SNPs that are overrepresented in the case cohort are believed to be involved in disease etiology and are therefore referred to as disease-associated risk loci (see Fig. 2[A]). These SNPs, however, do not necessarily cause the disease, but can be inherited with the true causal variant(s) due to strong linkage disequilibrium (Altshuler et al. 2008; Momozawa et al. 2018b).

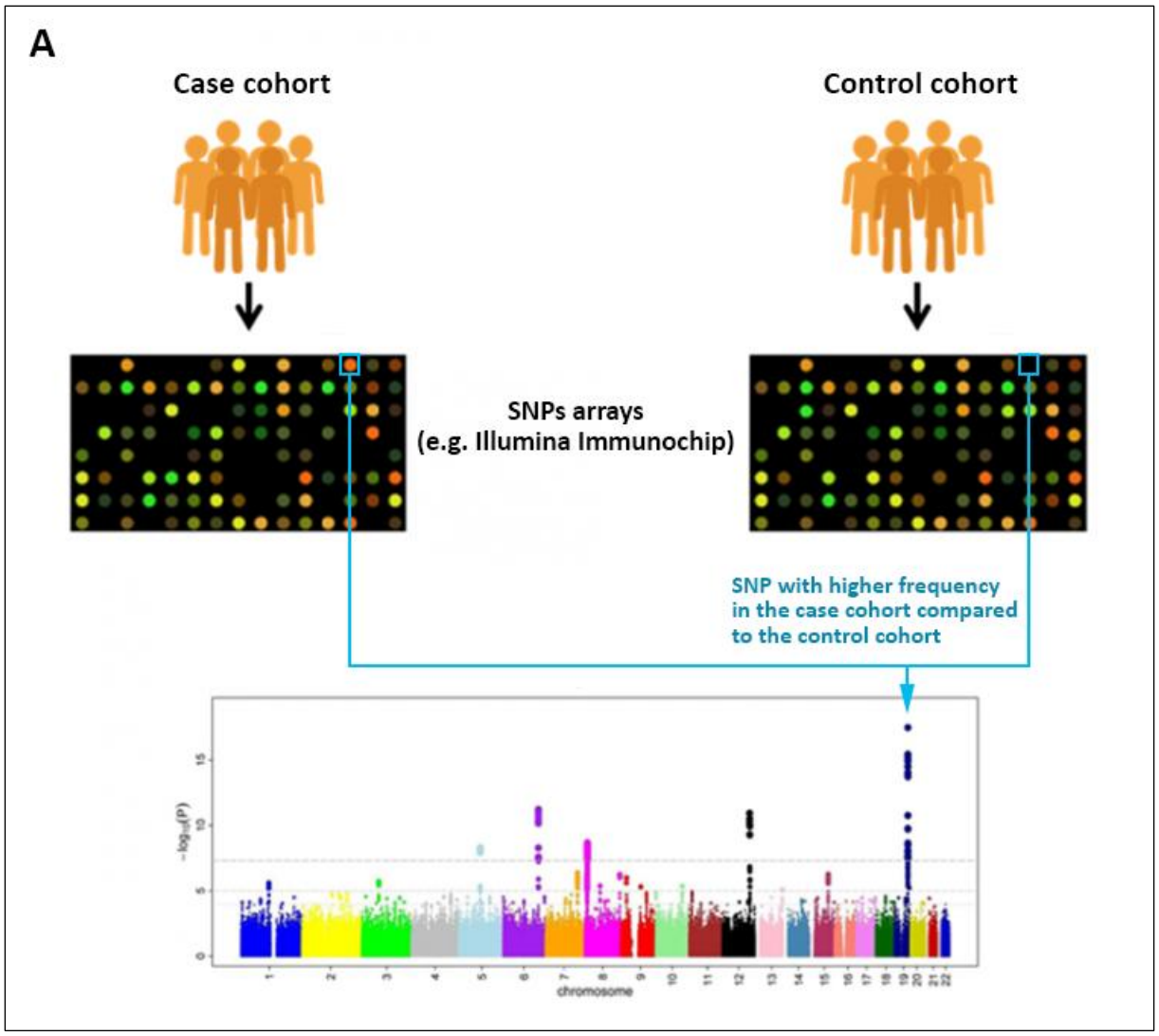

Figure 2: Diagram of genome-wide association study (GWAS). [A] The case-control setup of GWAS is used in the study of complex diseases to identify disease associated variants using an array-based genotyping method (adapted from EMBL-EBI).

Over the past decade, case-control GWAS of multifactorial diseases have identified over 3.500 risk loci of genome-wide significance, associated with one or more complex diseases (Tam et al. 2019). These risk loci typically span around 250 kb and numerous SNPs due to linkage disequilibrium patterns in the human genome. Therefore, for the vast majority of GWAS-hits, the causative variants, annotated target genes and biological consequences are still unknown. Current efforts in biomedicine focus predominantly on post-GWAS experiments, such as statistical fine-mapping and functional studies or epigenetic, epidemiological and bioinformatic analyses. (Edwards et al. 2013; Verstockt et al. 2018). Fine-mapping studies of risk loci that refine the list of possible associated variants and thus minimize the relevant genomic region, showed that most causal SNPs are located in non-coding regions of the genome, making biological interpretation difficult (Tam et al. 2019). Among those SNPs, many map to *cis*-regulatory elements (promoters, enhancers and insulators) as they feature transcription-factor (TF) binding sites and dense clusters of H3K4me1 and H3K27ac, epigenetic markers for open chromatin and active enhancer elements (Edwards et al. 2013). Regulatory risk variants may be involved in disease pathogenesis by perturbing the expression levels of their target gene(s) in disease relevant cell types and tissues (Momozawa et al. 2018b). Enhancers can interact with their target promoters regardless of their position, orientation or distance as they can be brought into close proximity by looping mechanisms of the DNA sequence (Bulger and

Groudine 2011b). Studies have shown that enhancers regulate both the expression of neighboring genes adjacent to the enhancer region (Khor et al. 2011) and distal genes millions of bp away (Verstockt et al. 2018). This poses a challenge to assign newly found disease-associated enhancer elements to their target genes. The increasing incidence of enhancer dysfunction (enhanceropathy) in human diseases, however, makes it necessary to analyze the regulatory potential of disease-associated genetic variants located within enhancer regions. Chromosome conformation capture technologies (3C-5C), CRISPR-interference and gene expression analyses in adequate mouse models are promising tools for the functional analysis these enhancer regions. (Rickels and Shilatifard 2018a).

1.3 Prostaglandin E2-EP4 signaling is involved in inflammatory bowel diseases and colorectal cancer

The *PTGER4* gene, encoding prostaglandin E_2 (PGE_2) receptor protein 4 (EP4), was identified by several independent GWAS as annotated candidate gene of risk loci associated with IBD and CRC (Jostins et al. 2012a; Libioulle et al. 2007; Huyghe et al. 2019). In addition, EP4 receptors have been shown to be highly expressed in pathologic conditions, such as colorectal cancer, inflammatory bowel disease, rheumatoid arthritis or ankylosing spondylitis (Hull et al. 2004; Yokoyama et al. 2013; Konya et al. 2013). The importance of the prostaglandin E_2 signaling pathway in chronic inflammation is underscored by another high ranked IBD- risk locus, the *PTGS2* gene (Liu et al. 2015). It encodes the enzyme cyclooxygenase 2 (COX-2), which mediates PGE_2 synthesis. Moreover, non-steroidal anti-inflammatory drugs (NSAIDs) like 5-aminosalicylates, which inhibit COX-activity and thus reduce PGE_2 production, are frequently used for the symptomatic treatment of flair-ups in IBD (Konya et al. 2013)and arthritis (Park et al. 2006) as well as for the prevention and therapy of CRC (Gupta and Dubois 2001). While the accelerating effect of the PGE_2-EP4 signaling cascade in CRC-initiation and progression (promoting cell proliferation and angiogenesis) is well-established (Hull et al. 2004), the exact role of this signaling pathway in IBD is still unclear and controversially discussed.

PGE_2-EP4 signaling exerts both anti-inflammatory and pro-inflammatory effects in chronic intestinal diseases. For example, Morteau et al. (2000) and Kabashima et al. (2002) have shown that COX-1-, COX-2-, and EP4-deficient mice developed severe augmented colitis compared to their WT-controls in the chemically induced dextran sodium sulfate (DSS)-model of colitis, indicating anti-inflammatory actions of the PGE_2-EP4 pathway. Furthermore, similar results were obtained with EP4-agonists (ameliorated colitis) and -antagonists (severe colitis) in murine colitis models supporting the hypothesis that the PGE_2-EP4 cascade is important for gastrointestinal homeostasis and mucosal barrier integrity (Konya et al. 2013). Kaufmann and Taubin (1987) and Felder et al. (2000) have shown in clinical studies that NSAIDs, which are commonly used as first-line therapy in UC treatment, can reactivate quiescent IBD. In addition, Nakase et al. (2010) conducted a clinical pilot study in patients suffering from UC with an EP-agonist that led to an improvement in clinical symptoms and histological scores, underlining the potential protective effect of the PGE_2-EP4 axis in IBD.

In contrast to the beneficial effects of PGE_2 in IBD mediated by the EP4-receptor, Libioulle et al. (2007) have shown, for example, that the causative genetic variants of the *PGTER4*-risk locus cause an increase in *PTGER4* transcription, suggesting a disease-promoting, pro-inflammatory role of PGE_2-EP4 signaling in CD. Also in different mouse models of colitis (e.g. trinitrobenzene sulfonic acid-

induced colitis, T-cell dependent transfer colitis model) the negative effect of the PGE_2-EP4 signaling pathway on disease progression were shown (Sheibanie et al. 2007; Maseda et al. 2018). The EP4-KO and mPGES-KO mice (mPGES catalyses the last step of PGE_2 synthesis) performed significantly better in colitis models compared to their WT-controls. These negative proinflammatory effects may be attributed to the major role of the PGE_2-EP4 axis in T-cell development, differentiation and function. It not only leads to an increased IL-23 secretion of dendritic cells and the associated accumulation of proinflammatory IL-17-producing T_h17 cells (Sheibanie et al. 2007), but also reduces the amount of T_{reg}-cells in the intestine (Maseda et al. 2018).

The numerous complex and seemingly contradictory effects mediated by the PGE_2-EP4 signaling cascade in inflammation may be explained by the local concentrations of PGE_2 and other low-affinity ligands (=other prostanoids), the expression pattern of EP4, and the various signal transduction pathways activated by EP4 (Kalinski 2012) (see Fig. 3). Moreover, PGE_2-EP4 functions found in animal studies do not necessarily have to be present in humans, as EP4-functions may vary according to species. It will therefore be important to further clarify the precise molecular mechanisms involved in EP4-mediated pathophysiological effects in humans and mice.

1.3.1 Prostaglandin E_2 signaling via its protein receptor 4 (EP4)

Arachidonic acid, a 20 carbon-chain polyunsaturated fatty acid, found in mammalian cell membranes, serves as a key substrate for the synthesis of prostanoids (prostaglandins + thromboxanes), a family of potent bioactive lipid mediators (Hanna and Hafez 2018). First, arachidonic acid is released from cell membrane phospholipids by the enzymatic activity of phospholipase A_2 (see Fig. 3[A]). The fatty acid is then converted into PGG_2 and further reduced to PGH_2 by cyclooxygenase-1 and/or -2 (COX-1, COX-2). The two COX-enzymes are the rate limiting factors in the synthesis of prostanoids and exhibit different expression patterns. COX-1 is the constitutive isoform expressed in most tissues under standard conditions. In contrast, COX-2 expression is normally restricted to the gastrointestinal mucosa, endothelium, kidneys and brain, but can be induced in response to various stimuli, many of which are pathological (proinflammatory, oncogenic) (Zidar et al. 2009). The intermediate PGH_2 is converted by cell-specific synthases into the different prostaglandins PGE_2, PGI_2, PGD_2, $PGF_{2\alpha}$ or thromboxane A2 (TXA_2). The PGE_2 molecule is the most common prostanoid in humans and is synthesized by three isoforms of the PGE synthase (microsomal PGE synthase-1 and -2 (mPGES-1/2); and cytosolic PGE synthase (cPGES-1)). These enzymes are predominately expressed in fibroblasts, monocytes and epithelial cells and endothelial cells. The degradation of PGE_2 is controlled by the enzyme 15-PGDH. PGE_2 signals in an autocrine and/or paracrine manner through four prostaglandin E_2 receptors (EP1-4). The receptors feature distinct tissue distribution and signal transduction pathways, which contribute to the different biological effects of PGE_2.

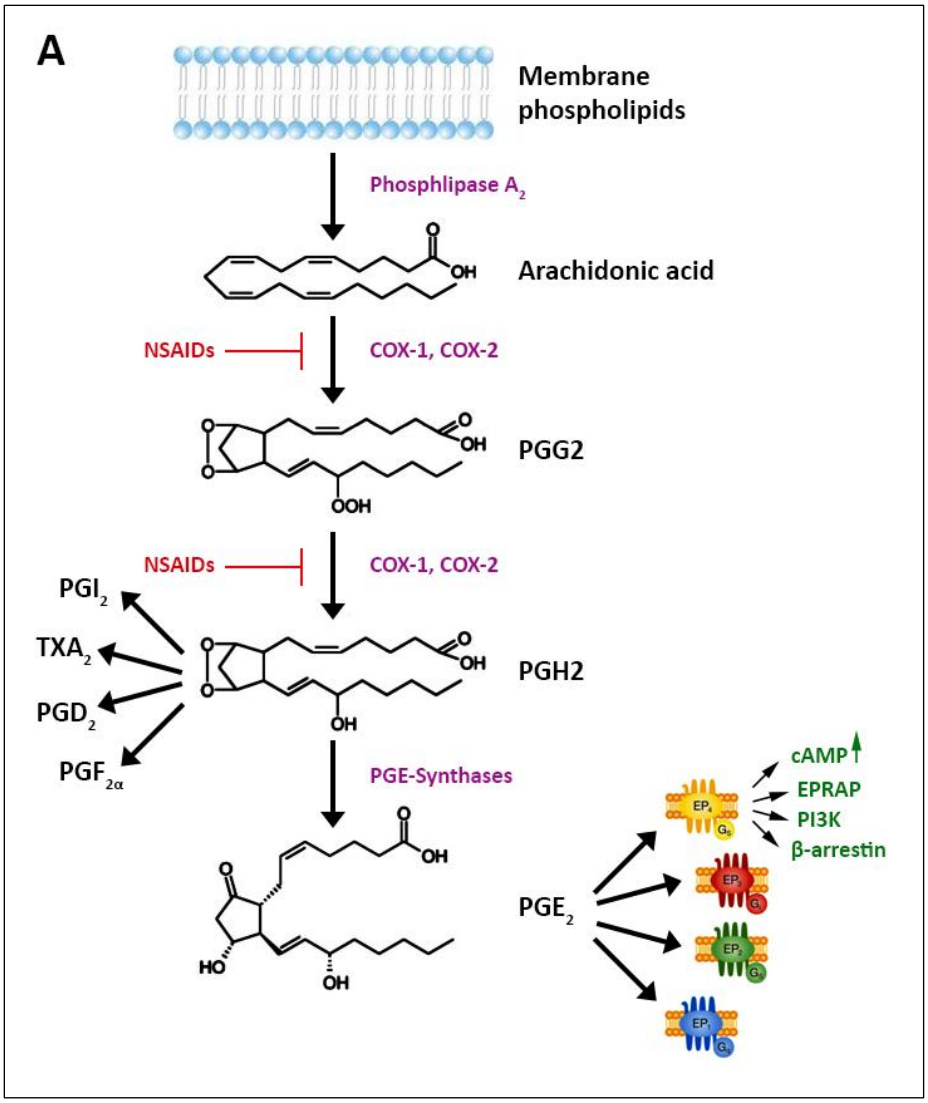

Figure 3: Prostaglandin E_2 synthesis and signaling pathways via PGE_2 receptor 4 (EP4) (adapted from Konya et al. (2013)).

The EP4 receptor is the most widely expressed PGE_2 receptor and is found on the plasma and nuclear membranes of cells of the gastrointestinal tract, hematopoietic tissues and associated immune cells (leukocytes, monocytes, macrophages) as well as the osteoarticular and cardiovascular systems (Yokoyama et al. 2013). EP4 is a high-affinity receptor for PGE_2, therefore low concentrations of PGE2 are sufficient for effective signaling. It is a $G_{\alpha s}$-protein coupled receptor upstream of several signaling cascades. The binding of PGE_2 (or other low-affinity ligands) to the EP4-receptor activates:

- adenylate cyclase, leading to an increase in the cellular level of cyclic adenosine monophosphate (cAMP), which in turn activates numerous cAMP-dependent signaling molecules, e.g., PKA (protein kinase A), Epac (exchange factor activated by cAMP), AMPK (PKA-independent AMP-activated protein kinase) and CREB (cAMP-responsive element-binding protein) or its repressor analog ICER (inducible cAMP early repressor). It has been shown that the cAMP signaling pathway regulates inflammatory responses (Bos 2003), angiogenesis (Zhang and Daaka 2011), vascular relaxation (Hristovska et al. 2007) and responses to bacterial infections (Hazan-Eitan et al. 2006).

Furthermore, the cAMP/PKA-signal axis can also interact with Wnt signaling via the glycogen synthase kinase-3 (GSK-3) pathway thereby regulating cellular proliferation, differentiation, migration and regeneration (Goessling et al. 2009).

- phosphatidylinositol 3-kinase (PI3K)/ERK (extracellular signal-regulated kinase)/Akt (Protein kinase B) signaling cascade, which regulates cellular differentiation and mitogenesis as well as migration and metastasis in colorectal carcinoma (Buchanan et al. 2006).
- Prostaglandin E receptor 4-associated protein (EPRAP), which stabilizes the p105 subunit of NF-κB and thus prevents the activation of NF-κB and MEK (mitogen-activated protein kinase). This results in a reduced secretion of proinflammatory cytokines and transcription inhibition of elements that regulate inflammation, cell growth and cell survival (Markovič et al. 2017).
- G-protein-coupled receptor kinases (GRKs) to bind to the C-terminus of the receptor protein and to phosphorylate it. These P- residues attract β-arrestin, which initiates rapid desensitization of the receptor by receptor internalization (Desai and Ashby 2001). In colorectal cancer, the PI3K signaling cascade can also be activated by β-arrestin via activation of the epidermal growth factor receptor (EGFR) (Buchanan et al. 2006).

The diverse biological function mediated by EP4 receptor proteins may be explained by the diverse signal transduction pathways activated by the binding of its ligand PGE_2. It is not yet clear whether the pathways act in concert or in alternating manner and which factors and molecular mechanisms are required for the activation of the respective signaling pathways (e.g. ligands, physiological or pathophysiological conditions) (Konya et al. 2013). Therefore, both EP4 receptor agonists and antagonists might represent useful new classes of compounds for the treatment of IBD, CRC, rheumatoid arthritis, osteoporosis and other autoimmune diseases.

1.4 Functional analysis of genetic variants associated with inflammatory bowel diseases and colorectal cancer

1.4.1 Preliminary experimental results

Several independent GWAS have identified a risk locus upstream of the *PTGER4* gene on chromosome 5 significantly associated with ulcerative colitis and Crohn's diseases in population-datasets of different ethnic backgrounds: Caucasian, East Asian, Indian and Iranian descent and African-American and Ashkenazi Jews (Libioulle et al. 2007; Jostins et al. 2012a; Momozawa et al. 2018a; Liu et al. 2015; Brant et al. 2017) (see Fig. 4[A]). In addition, a recently performed GWA-study identified the same genomic region as a common variant in people with colorectal cancer (Huyghe et al. 2019) and others found it to be associated with auto-immune diseases such as ankylosing spondylitis, arthritis (both extraintestinal manifestations of IBD) and multiple sclerosis (Ellinghaus et al. 2016; Rodriguez-Rodriguez et al. 2015).

A

Phenotype	Chromosome: Position (hg19 (Mb))	SNP	Candidate genes	p-value
CD	Chr.16:50.66	rs2066847	*NOD2, ADCY7*	5.86E-209
IBD	Chr.1:67.68	rs11209026	*IL23R, IL12RB2*	8.12E-161
UC	Chr.6:32.595	rs6927022	*HLA-DQB1, HLA-DRB1, HLADQA1, HLA-DRA*	4.71E-133
IBD	**Chr.5:40.38**	**rs11742570**	***PTGER4***	**1.81E-82**
CD	Chr.2:234.145	rs12994997	*ATG16L1, INPP5D*	4.14E-70

B

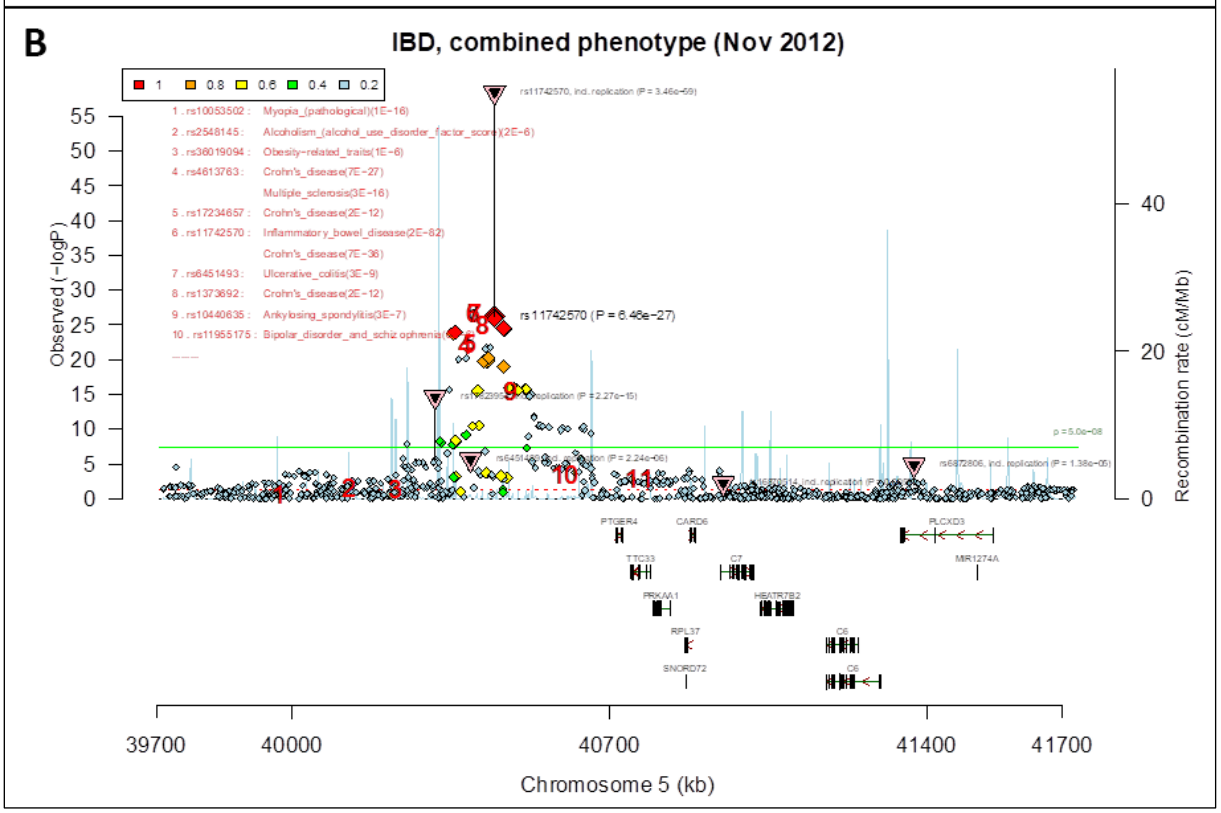

Figure 4: Genome-wide association studies show a significant association of the *PTGER4* locus with inflammatory bowel diseases. [A] Ranking of genes according to their IBD-association significance**.** The top SNP for the *PTGER4* risk locus is ranked fourth (adapted from Cho and Brant (2011) and Jostins et al. (2012a). **[B]** The Ricopili plot displays several SNPs with strong evidence of IBD-association in high linkage disequilibrium. They SNPs are located in a non-coding genomic region adjacent to the *PTGER4* gene on chromosome 5 (adapted from Jostins et al. (2012a)). IBD= inflammatory bowel diseases.

Like the vast majority of risk loci found by GWAS, these IBD-association variants (SNPs) also lie in a non-coding region of the genome (Rickels and Shilatifard 2018b). The fine-mapping study identified further IBD-associated SNPs (>100 SNPs) and limited the area of the risk locus to a range of approx. 400 kp (40.250.000-40.650.000) adjacent to the gene *PTGER4* (see Fig. 4[B] and Fig. 5[A] boxes A,B and C). As can be clearly seen in Figure 4 [B], the top SNP is in high linkage disequilibrium with several other disease-associated SNPs, so that they are most likely inherited together in a block-wise manner, which explains the substantial amount of disease associated variants.

Previous unpublished work by the Flavell laboratory has shown that the *Ptger4*-risk locus overlay with extensive areas of histone 3 lysine 27 acetylation (H3K27ACs), a well-established epigenetic marker for active enhancer elements (Farh et al. 2015; Creyghton et al. 2010). Three main clusters of H3K27 acetylation were revealed, located in a 250 kb region (40.380.000-40.630.000) within the risk locus (see Fig 5[A]). The acetylation clusters were found predominantly in disease-relevant tissues and cell types (intestinal tissues and immune cells), suggesting a putative enhancer function of this

specific region in the aforementioned tissues. A homology analysis between humans and mice via genomic alignment showed that the genomic sequence of the risk locus and nine histone acetylation peaks are highly conserved between these two species, at least in intestinal tissues. In the mouse genome, however, H3K27Ac peaks appear in reverse order within a 100 kb region (5.380.000-5.480.000) on the murine chromosome 15. HiChIP data of the ubiquitously expressed transcription factor (TF) Yin Yang 1 (YY1) in human T-cells (Weintraub et al. 2017), showed a direct linkage of the first H3K27Ac cluster (40.380.000-40.480.000) containing five conserved peaks with the *PTGER4* gene. Altogether, this underscores the hypothesis that this risk locus harbors putative enhancer elements that regulate the expression of neighboring genes in humans and mice (Schernthanner 2019).

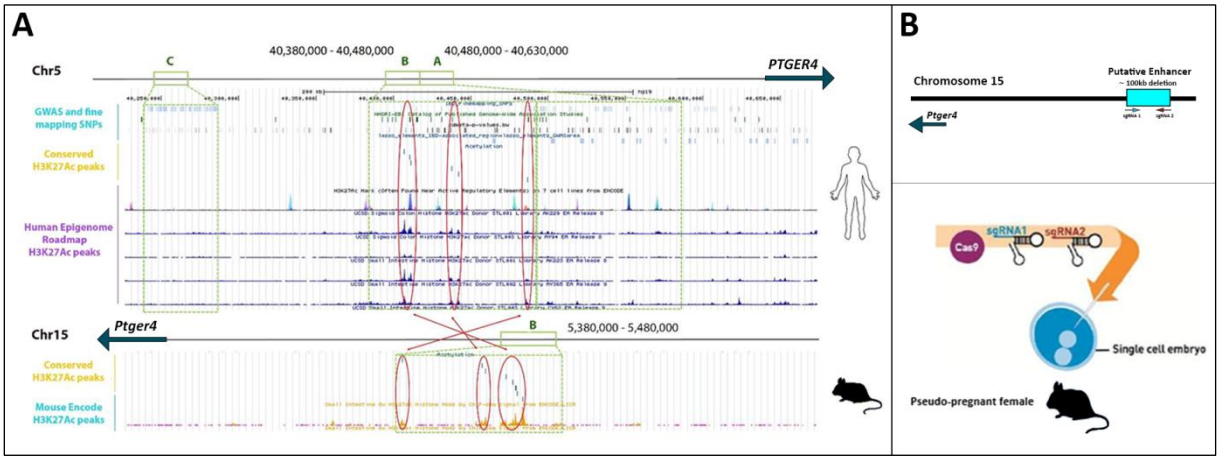

Figure 5: The IBD-risk locus upstream of PTGER4 in humans and mice. [A] Genomic assembly of the 400 kb risk locus upstream of the *PTGER4* gene of humans and mice. Three main cluster ofH3K27Ac-peaks (red circles) within the risk locus are conserved between humans and mice **[B]** An approx. 100 kb region containing putative enhancer elements located upstream of *Ptger4* was eliminated from the mouse genome using the CRISPR/Cas9 system. Two single-guide RNAs (sgRNAs) and the enzyme Cas9 were injected into zygotes and implanted into pseudo-pregnant female mice.

Due to its close proximity to humans and the conserved enhancer elements between the two species, the mouse was chosen as a model organism to study the activity, function and effect of these putative enhancer elements *in vitro* and *in vivo*. A new knock-out mouse line was created – the Ptger4-Enhancer-KO (Enh-KO) mice. The CRISPR-Cas9 system was used to ablate a ~100 kb region upstream of *Ptger4* containing all nine conserved acetylation peaks and several IBD-associated SNPs. Two single-guide RNAs (sgRNAs) and the enzyme Cas 9were injected into murine zygotes and implanted into pseudo-pregnant mice (see Fig. 5[B]). Heterozygous Enh-KO mice were backcrossed to wildtype animals prior to breeding for homozygous Enh-KO mice.

1.4.2 Aims of this master thesis

As with most IBD-risk loci found by GWAS, the causal gene/s at this associated site are not yet identified or functionally characterized. Therefore, the first aim of this master thesis was:

- to find the causative genes by identifying a correlation between the enhancer region and the expression levels of neighbouring genes: *Ptger4*, *Ttc33*, *Prkaa1*, *Card6*, and *C7*. Thereby, simultaneously validating that the risk locus indeed harbors active enhancer elements.

Since enhancers often show spatiotemporal activity patterns in a tissue and cell type specific manner (Corradin and Scacheri 2014) the second goal of the project was:

- to investigate the activity and expression pattern generated by these enhancer elements. The main focus hereby was on tissue and cell types that might play a role in IBD: intestinal cells and tissues (crypts, organoids, mesenchymal cells, duodenum, ileum, colon) as well as immune cells and tissues (Bone-marrow derived macrophages, T-cells, mesenteric lymph nodes, spleen and thymus).

Enhancer activity can often be stimulated or repressed by various factors even in fully differentiated cells. These factors interact with transcription factors (TFs), cofactors or chromatin structure (Kaikkonen et al. 2013; Ostuni et al. 2013). Thus, the third aim of the thesis was:

- to determine putative stimuli of the enhancer elements. Since this genomic region is associated with IBD and CRC, intestinal microbial factors may interact with the enhancer region. Therefore, lipopolysaccharides (LPS) located in the outer membrane of gram-negative bacteria were used as possible stimuli for the enhancer elements. In addition, the entire intestinal microbiome was tested as stimuli by comparing expression levels of target genes in germ-free and colonized mice.

This risk locus is associated with both major forms of IBD, ulcerative colitis and Crohn's disease, and this genetic predisposition to IBD may be due to a perturbation of the enhancer activity or function. To test this hypothesis another goal of the project was:

- to investigate the role of the enhancer region in two murine IBD-models(1) Dextran sodium sulfate (DSS) that mimics pathophysiology of ulcerative colitis and (2) T-cell dependent transfer colitis model that features many pathological characteristics of Crohn's disease.

2 Material and Methods

2.1 Cells and cell culture

2.1.1 Mesenchymal cells of the small intestine

Intestinal mesenchymal cells (IMCs), excluding lymphocytes and endothelial cells, consist mainly of fibroblasts and myofibroblasts, but also include pericytes, stromal stem cells and smooth muscle cells. For this master thesis, IMCs derived from Enh-WT and –KO mice were used to shed some light on the role of the Ptger4-enhancer in mesenchymal cells by analyzing and comparing the Ptger4 expression in IMCs of both genotypes. For details about the method see Koliaraki and Kollias (2016) and Tao et al. (2016)

<u>In the animal procedure room</u>

- Two mice per genotype (Ptger4-Enhancer-WT and –KO) were selected for the isolation of IMCs.
- The first mouse was euthanized by CO_2-asphyxiation. Cervical dislocation was performed to ensure the death of the animal.
- The abdomen of the mouse was sprayed with 70% ethanol.

- Surgical scissors were used to make an incision at the top of the abdomen and the skin was pulled down towards the hind legs to expose the peritoneum and the underlying intestines.
- The peritoneum was carefully opened and the intestine was removed from the cavity. The last 2/3 of the small intestine (around 8 cm) was harvested and placed in a Petri dish filled with ice-cold PBS.
- The intestine was flushed repeatedly with ice-cold PBS using a 10 ml syringe equipped with a dulled 20G needle to extrude luminal content and food debris. A set of tweezers was used to remove fat and connective tissue.
- The small intestine was first cut longitudinally and then into 0.5-1 cm pieces. The tissue pieces were transferred into a 50 ml falcon tube with sterile DMEM-complete medium (Dulbecco's Modified Eagle Medium (Gibco) supplemented with 10% FBS (Gibco); 2mM L-glutamine (Gibco) and 100µg/ml Pen/Strep (Gibco)) on ice for transportation from the animal experiment room to the tissue culture room.
- <u>In the tissue culture room</u>
- The medium was removed and the tissue pieces were washed with ice-cold PBS by vigorously shaking the tube, removing the supernatant and adding new PBS. This step was repeated 5-10 times until the supernatant was clear.
- For the first digestion step 25-30 ml HBSS/EDTA/DTT solution were added to each tube and incubated at 4°C on a shaking platform for 15 minutes.(HBSS supplemented with 1mM EDTA (ethylenediaminetetraacetic acid Sigma-Aldrich), 1mM DTT (dithiothreitol, ThermoScientific), 2% FBS and 2% HEPES (4-(2-hydroxyethyl)-1-piperazineethanesulfonic acid, Gibco)
- The tubes were shaken vigorously after incubation to release the intestinal epithelial cells. The supernatant was discarded and new HBSS/EDTA/DTT solution was added. The digestion step was repeated 2-4 times until only few epithelial cells were set free by the shaking process and the supernatant no longer appeared cloudy.
- The tissue pieces were washed with PBS (w/o Ca^{2+} and Mg^{2+}) to remove residual HBSS/EDTA/DTT solution completely to prevent inhibition of the enzymatic reactions by EDTA in the next step.
- For the second digestion step 25 ml of DMEM-10/Collagenase/Dispase/DNAse solution were added to each tube and incubated at 37°C at 200 rpm in a shaker incubator for 45-60 minutes. (DMEM supplemented with 10% FBS, 200u/ml Collagenase XI (Sigma), 0.1mg/ml Dispase and 50u/ml DNAse II type V (Sigma)).
- The incubation was stopped when the supernatant became cloudy and the tissue looked stringy and more transparent. The tubes were shaken vigorously to set the mesenchymal cells free, and the supernatant was filtered through a sterile 70 µm strainer to remove large tissue debris, followed by centrifugation at 200 g at 4°C for 5 minutes.
- The cell pellets were washed with PBS containing 2% sorbitol and the tubes were spun again with the same setting. The addition of sorbitol, a sugar alcohol, to the tubes led to a higher density of the mixture and thus to the sole pelleting of living cells in the centrifugation step. The remaining tissue and cell debris and other contaminations were in the supernatant, which was decanted.
- The remaining cell pellets were re-suspended in 15 ml of DMEM complete medium and seeded in T-75 cell culture flasks (one flask per genotype). The cells were grown in a humidified incubator with 5% CO_2 at 37°C.
- The next day the supernatant containing non-adherent cells was removed and new DMEM complete medium was added.

- Subculture and lysis of cells for RNA isolation
- On the 5th day, the cells reached ~90% confluency and were passaged into T-175 flasks. The cells were first washed with PBS and then trypsinized and splitted in a ratio of 1:2 for the subculture. From then on the cells were passaged every 3-4 days.
- The cells of the third passage are normally negative for hematopoietic cells and, thus were used for RNA isolation. Three 10 cm dishes per genotype were seeded with 2x10^6 cells and incubated over night to allow fibroblasts to attach to the dish. The next day the supernatant was decanted and the cells washed with ice-cold PBS and lysed using 1 ml of Trizol® per dish. The cells were harvest with a cell scraper and the Trizol®-cell mixture was transferred into microcentrifuge tubes and stored at -80°C until RNA isolation and purification was performed.

2.1.2 Bone marrow derived macrophages (BMDMs)

BMDMs are primary macrophage cells isolated from the bone marrow of adult mice. They differentiate *in vitro* from myeloid precursor cells in the presence of the M-CSF growth factor (macrophage colony-stimulating factor). The main advantages of BMDMs cultures are their homogeneity, ability to proliferate, high cell numbers and a relatively long lifespan of up to three weeks. These properties make differentiated BMDMs an excellent model for the investigation of different mechanisms in primary cell cultures, especially in the field of immunology and cell biology.

For this master thesis, unstimulated Enh-WT, -Het and –KO BMDMs were used to investigate the impact of the Ptger4 enhancer on gene expression at steady state in cells of the innate immune system. In addition, BMDMs were stimulated with lipopolysaccharides (LPS) for 1, 3, 6 or 10 hours study the effect of LPS-stimulation on Ptger4 expression in activated macrophages. For details about the method see Weischenfeldt and Porse (2008) and Marim et al. (2010).

In the animal procedure room

- Three mice per genotype (WT, HET and KO) were selected for the isolation of BMDMs.
- The first mouse was sacrificed by CO_2 asphyxiation. Cervical dislocation was performed to ensure the death of the animal.
- Abdomen and hind legs of the mouse were sprayed with 70% ethanol
- Surgical scissors were used to make an incision at the top of each hind leg. The skin was pulled down towards the paw to expose the leg muscles.
- The muscle tissue was removed from the bones using scissors and tweezers. Tibia and femur bones were cut at both ends to free them from pelvic- and foot bones.
- The exposed bones were placed into 50 ml falcon tubes containing sterile HBSS (Hank's balanced salt solutions, Gibco) on ice for transportation from the animal facility room to the tissue culture room.

In the tissue culture room

- The tibias/femurs were sterilized with 70% ethanol. Therefore, a petri dish was filled with ethanol and the bones were submerged for around 10 seconds.
- The sterilized bones were transferred into a clean petri dish filled with sterile HBSS.
- Tibia and femur were separated by cutting the knee joint with a new razor blade. The epiphyses of all bones were removed to make the bone marrow cavity accessible, again using the razor blade.

- The bones were flushed with HBSS using a 5 ml syringe with an attached 26G needle to extrude bone marrow into a fresh petri dish.
- To obtain a homogenized single-cell suspension the bone marrow plugs were gently pipetted up and down several times with a 1000 µl pipette.
- The single-cell suspensions were transferred to labeled 50 ml falcon (one per genotype) tube and centrifuged at 1200 rpm for 10 minutes.
- The supernatant was discarded and the cell pellets were resuspended in 5 ml ACK-lysis buffer (ammonium-chloride-potassium) and incubated for 5 min at RT to lyse the red blood cells.
- Around 10-15 ml of fresh RPMI medium (Roswell Park Memorial Institute medium, Gibco) was added to each tube to stop the lysis reaction and the tubes were spinned again at 1200 rpm for 10 min
- The supernatant was discarded. To wash the cell pellets, they were resuspended in 10 ml of RPMI medium and centrifuged again at the same settings.
- The supernatant was discarded and the cell pellets were resuspended in 45ml RPMI complete medium (RPMI-1640 supplemented with 10% fetal bovine serum (FBS; Gibco); 2mM L-glutamine (Gibco) and 100µg/ml Pen/Strep (Gibco)).
- Nine large tissue culture dishes (150mm) were seeded per genotype. Therefore, 5 ml of the cell suspension and 25 ml of RPMI complete medium were added to each cell culture dish. The lineage specific growth factor M-CSF that causes myeloid progenitor cells to proliferate and differentiate into macrophages, was pipetted to each dish in a 1:4000 dilution (à 7.5 µl).
- The cells were grown in a humidified incubator with 5% CO_2 at 37°C for nine days.

<u>Washing of the cells at day 3 and day 6 after isolation of BMDMs</u>

- The used cell culture medium was replaced by fresh one. The supernatants of the cell culture dishes containing non-adherent cells were pooled into 50 ml falcon tubes (one tube per genotype) and centrifuged at 1200 rpm for 10 min.
- Around 25 ml of fresh RPMI complete medium was added to each dish.
- After centrifugation, the supernatant was discarded and the cell pellets were resuspended in 45 ml of RPMI complete medium containing M-CSF (1:4000 dilution). Then, 5 ml of the respective cell suspension was added to the corresponding dishes and they were put back into the incubator.

<u>Re-plating of the cells for LPS-stimulation at day 8 after isolation of BMDMs</u>

- First, the efficiency of the differentiation was assessed by bright-field microscopy.
- Then, the medium of the cell culture dishes was decanted and the adherent cells were washed with around 15 ml of phosphate-buffered saline (PBS) per dish.
- In order to detach the cells, 3 ml of trypsin (Gibco) was added to each dish and distributed evenly by short swiveling. The dishes were placed in the 37°C incubator for at least 10 minutes as BMDMs are difficult to tryppsinize.
- After detachment of the cells, 15 ml RPMI was added to stop the trypsin reaction and the cells were counted manually using a Neubauer chamber.
- In 60 mm cell culture dishes, 1x10^6 cells per dish were seeded in 2 ml of RPMI-complete medium. The cell amount of the KO-genotype was sufficient to plate ten dishes, while the amount of WT and HET cells was sufficient for 15 dishes. Therefore, duplicates for each

timepoint of the stimulation experiment were seeded for the KO-genotype, and triplicates for the WT- and HET-genotype.

- The plates were incubated for another day in a humidified incubator with 5% CO_2 at 37°C.

LPS-stimulation and harvesting of the cells

- First, the 0h timepoint of the LPS-stimulation experiment was harvested. Therefore, the medium of cell culture dishes (2xKO, 3xWT, 3xHET) was decanted and the cells were washed with 2 ml of ice cold PBS. To lyse the cells, 1 ml of TRIzol® (Invitrogen) was added directly to each dish on ice and a cell scraper was used to harvest the cells into the TRIzol®. After pipetting up and down several times with a P1000 pipette the resulting lysates were transferred into labeled microcentrifuge tubes and stored at -80°C until RNA isolation and purification was performed.
- For all other timepoints (1h, 3h, 6h and 10h of stimulation) the BMDMs were stimulated by adding 10 ng/ml LPS (20 ng LPS in total) to each cell culture dish. The plates were then placed back in the incubator for 1, 3, 6 or 10 hours. At the indicated timepoints, eight dishes (2xKO, 3xWT, 3xHET) were removed from the incubator and the stimulated cells were harvested and lysed. This process was performed in the exact same way as for the 0h timepoint and all samples were stored at -80°C.

2.1.3 Intestinal Crypts and Organoids

Intestinal organoids represent an *in vitro* multi-cellular, organotypic 3D culture system with strong physiological relevance to the adult intestine compared to conventional monolayer cell cultures. They not only consist of all cell types found in an adult intestinal epithelium but also feature a polarized epithelium, a crypt-villus organization and a functional lumen. Moreover, intestinal organoids recapitulate most inter- and intra-epithelial cell dynamics that occur *in vivo* making them a powerful *in vitro* tool in various areas of the biomedical research field.
Intestinal organoids can be genetically manipulated with the CRISPR/Cas9 system, retro- or lentiviral infection methods and electroporation. Co-culture systems with various autologous cell types (e.g. intestinal fibroblasts) or bacteria are another advantage of this model system. The large number of experimental tools to which these cultures are amenable further expand the usefulness and field of application of intestinal organoids.
Intestinal organoid cultures are used to investigate the development and function of normal and tumorigenic intestinal epithelium, to model intestinal diseases and to study mucosal physiology, intestinal regeneration, host-microbiome interaction and stem cell properties and dynamics. Moreover, they are used for testing newly developed drugs and food supplements as well as for regenerative therapy approaches (Lee et al. 2018; Rahmani et al. 2019).

For this master thesis, intestinal crypts and organoids derived from Ptger4-Enh-WT and –KO mice were used to study the effect of the enhancer on the expression of the Ptger4 gene in the intestinal epithelium by qPCRs. Throughout the procedure all pipettes, pipette tips and tubes were pr-wetted with PBS+2%FBS before manipulating intestinal pieces and crypts to prevent the tissue pieces from sticking to the surface of the pipettes and tips. For details about the method see STEMCELL Technologies Inc. (2016) and Swiatecka and Mackie (2015).

In the animal procedure room

- One mouse per genotype (Ptger4-Enh-WT and –KO) were selected for the isolation of intestinal crypts.
- The first mouse was euthanized by CO_2-asphyxiation. Cervical dislocation was performed to ensure death of the animal.
- The last 20 cm of the small intestine was harvested, placed in a Petri-dish and flushed with cold PBS. Fat and connective tissue were removed with tweezers.
- The entire length of the intestine was cut open with surgical scissors and the tissue was splayed open using tweezers. Mucous and villi were carefully scraped off with a coverslip.
- With tweezers the washed intestinal tissue was held over a 50 ml falcon tube filled with cold HBSS and the intestine was cut into 2-4 mm pieces which fell into the buffer.
- The tubes (one tube per genotype) were put on ice for transportation from the animal experiment room to the tissue culture room

<u>In the tissue culture room</u>

- The tissue pieces were washed by pipetting up and down three times with a 10 ml serological pipette. After the intestinal pieces settled by gravity the supernatant was carefully removed and ~15 ml of cold PBS were added to the tissue fragments. This washing step was repeated for at least 15-20 times or until the supernatant was almost clear.
- The tissue pieces were resuspended in 25 ml of PBS/EDTA/FBS (PBS supplemented with 5mM ETDA and 0.2%FBS) to isolate the crypts. The tubes were incubated for 30 min at 4°C and 20 rpm on a shaking platform.
- After the incubation time, the supernatant was removed and 10 ml of cold PBS+0.2%FBS were added to the tubes. They were shaken vigorously to set the intestinal crypts free and the supernatant was removed and passed through a 70 µm cell strainer into a new 50 ml falcon tube (fraction 1). Fraction 1 was put on ice and the step was repeated five times to generate fractions 2-6.
- To assess the quality of each fraction 1 ml of each suspension was added to the individual wells of a 6-well plate. The fraction samples were analyzed for enrichment of intact crypts (small, folded sections of an epithelial monolayer) using an inverse microscope. The samples were added back to the respective fraction, afterwards.
- The three fractions (usually fraction 3-5) with the best crypts-debris ratio were selected, combined and washed several times before being used for plating intestinal organoid cultures.
- The other three fractions (usually fraction 1,2 and 6) were combined to isolate RNA from intestinal crypts. The combined solution was splitted equally between three tubes (á 1 ml) and the crypts were spun down at 290xg for 5 min at 4°C. The supernatant was removed and 1 ml of Trizol® was added to lyse the intestinal cells. After pipetting up and down a couple of times with a P1000 pipette the lysates were stored at -80°C until RNA isolation and purification were performed.
- For the first washing step of the combined fraction solutions for the organoid cultures, the tubes were centrifuged at 200xg for 3 min at 4°C. The supernatant containing single cells was aspirated and the pelleted intestinal crypts were resuspended in 10 ml of PBS+0.2%FBS and transferred into pre-coated 15 ml tubes. The washing step was repeated 2-3 times with reduced centrifugation speed (100xg, 50xg and 30xg) to clear most single cells from the samples.

- After the washing steps, the number of crypts per ml was calculated. For an accurate assessment of crypt numbers six 10 µl-drops of each suspension were pipetted onto the lid of a 6-well plate. The intact crypts in each drop were counted with an inverse microscope. The mean of all six calculated values was used to determine the number of crypts per ml (=mean x 100).
- The volumes containing approx. 2000-3000 crypts were transferred into pre-coated 15 ml falcon tubes and centrifuged for 5 min at 4°C with 200xg. The supernatant was removed and the pellets were resuspended in 500 µl of PBS+0.2%FBS. The dissolved crypts were transferred into pre-coated microcentrifuge tubes and spun down at 200xg. The supernatant was removed as much as possible to avoid dilution of Matrigel® in the next step.
- For six organoid domes 150 µl of complete IntestiCult™ Organoid Growth Medium (IC-medium) at RT and 150 µl of ice-cold Matrigel® Matrix were added to both pellets. (number of domes x 25µl of IC-medium and Matrigel). (IntestiCult™ Organoid Growth Medium supplemented with 5% of Supplement 1, 5% of supplement 2 and 100u/100µg per ml Pen/Strep). The intestinal crypts were carefully resuspended by pipetting slowly up and down to prevent the introduction of air bubbles.
- The organoid domes were placed in the twelve central wells of a pre-warmed non-tissue culture treated 24-well plate by carefully pipetting 50 µl of the crypt-Matrigel® suspension of each genotype into the middle of six adjacent wells. The plate wasn't moved for 1-2 min to allow initiation of the solidification process of the Matrigel® before incubating the domes at 37°C for 5-10 minutes.
- To each well with a fully solidified dome 500 µl of pre-warmed IC-medium was added by gently pipetting the medium down the wall of the well. To all empty wells 500 µl of distilled water (Gibco) was added to reduce evaporation effects.
- The plate was put in a 37°C incubator with 5% CO_2 atmosphere. After 2-4 days the isolated intestinal crypts should have formed organoids.

<u>Exchanging of medium, passaging of intestinal organoid cultures and RNA isolation</u>

- The medium was exchanged once a week by removing the existing medium and replacing it with 500 µl of fresh IC-medium.
- The organoids were passaged every 7-10 days after seeding with a split ratio between 1:2 and 1:6 according to their growth performance. For the splitting process, the culture medium was carefully removed and 700 µl Gentle Cell Dissociation Reagent (GCDR) at RT was added to the top of each dome to be passaged. After 1 min of incubation, the GCDR was pipetted up and down with a P1000 pipette to break up the domes and organoids. The organoid suspension was transferred to a pre-coated microcentrifuge tube and incubated on a shaking platform at 20 rpm for 10 min at RT. The tubes were centrifuged at 290xg for 5 min at 4°C to pellet the organoid fragments, the supernatant containing Matrigel®, dead cells and single cells was removed and the pellets were washed with 1 ml of PBS+0.2%FBS. The tubes were spun again at the same speed and the supernatant was as much as possible. IC-medium and Matrigel® Matrix were added to the pellets and the domes were pipetted into a new 24-well plate like described before.
- Three domes per genotype of passage 3 were used to extract RNA for qPCR analysis of Ptger4 gene expression. For this, the medium of the respective domes was removed and 700 µl of GCDR was added to each well to break up the domes. After 10 min of incubation on a shaking platform the organoid fragments were pelleted by centrifugation at 290xg for 5 min. The

supernatant was removed and the intestinal cells of the organoid pieces were lysed with 500 µl of RLT-buffer. The lysates were stored at -80°C until RNA extraction using the Quigen-RNA-Micro kit was peformed.

- Mouse – Mammalian model organism
- In biomedical research the house mouse *Mus musculus* is the most commonly used mammalian model organism. For a century, mice have been intensively used to elucidate the mechanisms underlying human diseases and to test and improve novel drug therapies. Mice are small, have a short generation time (around 10 weeks) and an accelerated life span (2-3 years), which makes them a space-, time- and cost-effective model organism for research. In addition, the close proximity to humans and the possibility of genetically modifying the mouse genome enables the creation of mouse strains that precisely mimic human diseases by introducing the disease-causing mutation(s) into the mouse genome.
- Mice with a C57BL/6 genetic background were used for all *in vivo* experiments. The C57BL/6 strain is the most widely used inbred strain of laboratory mice and its genome was sequenced in 2002. For the enhancer-project, the CRISPR-Cas9 technology was used to create a Ptger4-Enhancer knock-out (Enh-KO) mouse line. In this master thesis the Enh-WT and –KO mice were used to study *in vivo* the function of the enhancer region in different cell types and tissues. Furthermore, the effect of this targeted enhancer on the course of experimentally induced colitis was investigated (DSS-induced colitis model and T-cell dependent transfer colitis model)
- Normally, five littermates were group housed in an individually ventilated cage under a controlled photoperiod (12:12-h light dark cycle) in the animal holding room. They were provided with food pellets and autoclaved drinking water *ad libitum* as well as bedding and nesting material. If extensive barbering or fighting behavior occurred, the animals were separated into different cages. Co-housed littermates were used as controls for all experiments. The animal experiment were conducted by specially trained and authorized persons and approved by the Yale School of Medicine Institutional Animal Care and Use Committee (IACUC), and were in accordance with Yale's Animal Program and the Animal Welfare Act Regulations (AWAR). This ensured animal welfare and minimized possible pain, suffering and anxiety for the mice during the experiments.

2.2 Mice – Mammalian model organism

In biomedical research the house mouse *Mus musculus* is the most commonly used mammalian model organism. For a century, mice have been intensively used to elucidate the mechanisms underlying human diseases and to test and improve novel drug therapies. Mice are small, have a short generation time (around 10 weeks) and an accelerated life span (2-3 years), which makes them a space-, time- and cost-effective model organism for research. In addition, the close proximity to humans and the possibility of genetically modifying the mouse genome enables the creation of mouse strains that precisely mimic human diseases by introducing the disease-causing mutation(s) into the mouse genome.

Mice with a C57BL/6 genetic background were used for all *in vivo* experiments. The C57BL/6 strain is the most widely used inbred strain of laboratory mice and its genome was sequenced in 2002. For the enhancer-project, the CRISPR-Cas9 technology was used to create a Ptger4-Enhancer knock-out (Enh-KO) mouse line. In this master thesis the Enh-WT and –KO mice were used to study *in vivo* the

function of the enhancer region in different cell types and tissues. Furthermore, the effect of this targeted enhancer on the course of experimentally induced colitis was investigated (DSS-induced colitis model and T-cell dependent transfer colitis model)

Normally, five littermates were group housed in an individually ventilated cage under a controlled photoperiod (12:12-h light dark cycle) in the animal holding room. They were provided with food pellets and autoclaved drinking water *ad libitum* as well as bedding and nesting material. If extensive barbering or fighting behavior occurred, the animals were separated into different cages. Co-housed littermates were used as controls for all experiments. The animal experiment were conducted by specially trained and authorized persons and approved by the Yale School of Medicine Institutional Animal Care and Use Committee (IACUC), and were in accordance with Yale's Animal Program and the Animal Welfare Act Regulations (AWAR). This ensured animal welfare and minimized possible pain, suffering and anxiety for the mice during the experiments.

2.2.1 Tissue sampling – isolation of various tissues

For the Ptger4-expression analysis experiments in tissues and the germ-free vs. colonized mice experiment, it was necessary to collect all types of tissues: parts of the gastrointestinal tract (duodenum, ileum, colon), organs of the immune system (spleen, thymus, MLN), as well as kidney, liver and lung tissue of Ptger4-Enhancer-WT and –KO mice. The tissue harvesting procedure was performed as quickly as possible to preserve the integrity of the RNA.

- All mice were euthanized by CO_2-asphyxiation. Cervical dislocation was performed to ensure the death of the animals.
- The abdomen of the mice was sprayed with 70% ethanol.
- Using surgical scissors, an incision was made at the top of the abdomen and the skin was pulled apart to expose the peritoneum and the underlying intestines.
- The peritoneum was carefully opened with scissors and the intestine was removed from the cavity. First, the mesenteric lymph nodes were collected and flash frozen. Duodenum, ileum and colon were placed in a Petri-dish with ice-cold PBS and flushed repeatedly to extrude luminal contents with a 10 ml syringe equipped with a dulled 20G needle. The tissue pieces were transferred into special snap freezing tubes (Eppendorf) and flash frozen by immersion in liquid nitrogen.
- The spleen was harvested next. It is a bean-shaped dark red organ located on the left side of the abdominal cavity at the level of the thorax.
- One of the kidneys and one of the many liver lobes was collected and snap-frozen.
- To isolate the lung and thymus, it was necessary to open the thorax with surgical scissors. The thymus is located directly above the heart in the midline of the thoracic cavity. It is a milky white tissue and has two lobes, one on each side of the midline. One lung lobe and the entire thymus were collected and flash frozen.
- All samples were transferred to special snap-freezing tubes (Eppendorf) and immersed in liquid nitrogen to allow flash freezing. In the lab, the tubes were removed from the bucket of liquid nitrogen and stored at -80°C until RNA isolation was conducted.
- It is important that tissue samples are immediately frozen in liquid nitrogen and stored at -80°C to prevent unwanted changes in the gene expression profile of cells due to RNA degradation.

2.2.2 Dextran sulfate sodium (DSS)-induced colitis in mice

Dextran sodium sulfate (DSS) is a water-soluble, negatively charged sulfated polysaccharide with anticoagulant properties and is used for the chemical induction of experimental colitis in mice. DSS-induced colitis is relatively simple, fast and inexpensive to perform and therefore a widely used model of experimental colitis in mice. It mimics clinical and histopathological features of human IBD, in particular of ulcerative colitis (UC), and is used to study the pathogenesis and etiology of these diseases as well as genetic predisposition, immune mechanisms and the role of the microbiome in IBD. In addition, the model is also used in preclinical studies to test and improve therapeutic options.

Acute, chronic and relapsing models of colitis can be easily achieved by changing DSS concentration duration and frequency of administration. Onset and severity of DSS-induced colitis are affected by several factors: DSS itself (concentration, molecular weight, duration and frequency of DSS-administration, manufacturer and batch) genetics of the animals (strain susceptibility, gender, gene mutations) and microbiological factors (microbiological state of the animals, composition of the microbiome, housing conditions) (Eichele and Kharbanda 2017; Perše and Cerar 2012; Yan et al. 2009)

Acute experimental colitis was induced in male and female Ptger4-Enhancer-WT and –KO mice by administration of DSS for 7 days followed by a 7-day recovery period with regular water. The experiment was performed to elucidate the role of the deleted Ptger4 enhancer and associated less abundant Ptger4-receptor protein in the pathogenesis of DSS-induced colitis. For more details about the method see Chassaing et al. (2014) and Das et al. (2017).

- Seven Enhancer-WT and seven Enhancer-KO littermates were selected for this experiment and co-housed in mixed groups of 4-5 mice. All mice were weighed before DSS treatment and average group weight was equilibrated to eliminate significant weight differences between groups. The weight of the mice should be around 20 g. However, two of the female mice were slightly lighter, weighing 18.5-19.0 g.
- A 1.5% (w/v) DSS solution was prepared by dissolving the DSS powder in autoclaved drinking water. The bottle was shaken vigorously until the DSS was dissolved and the solution appeared clear.
- The cage water bottles were filled with approx. 250 ml of the DSS-solution and offered *ad libitum* as exclusive drinking water source to mice. The DSS-solution was administered in the first 7 days, followed by autoclaved drinking water for another 7 days.
- Each mouse was weighed daily in a blind manner to evaluate disease activity. To obtain further information on their health status, the animals were also examined for signs of diarrhea, fecal and rectal bleeding and behavioral changes.
- At the end of the experiment the mice were euthanized according to the guidelines of the ethic committee.
  Humane endpoints of the experiment: (1) body weight loss of more than 30% of initial weight (2) severe and bloody diarrhea, accompanied by behavioral abnormalities such as hunched posture, ruffled fur, reduced mobility and piloerection. In both cases, the animal was sacrificed before the end of the experiment to minimize its suffering.
- A weight curve was created and statistically analyzed using Prism to determine the effect of DSS-induced colitis on the two different genotypes (ENH-WT and ENH-KO mice).

2.2.3 T-cell dependent transfer colitis experiment

For the T-cell dependent model of colitis, effector T-cells ($CD4^+$, $CD45RB^{high}$) from Enh-WT- and KO mice were isolated, purified and transferred to recombinase activating gene-deficient ($RAG^{-/-}$) recipient mice. This experiment was conducted to see whether the knock-out of the Ptger4-enhancer region alters the onset and severity of induced colitis.

<u>In the animal procedure room</u>

- Six-weeks-old male and female Enh-WT and –KO mice were selected for the isolation of naïve T-cells (Enh-WT: 2x m+f; Enh-KO: 1x m, 2x f). In general, T-cells from one animal are sufficient to inject $5x10^5$to $1x10^6$ naïve T-cells into 4-5 recipient mice.
- The mice were euthanized by CO_2-asphyxiation. A cervical dislocation was performed to ensure the death of the animals.
- With surgical scissors an incision was made at the top of the abdomen and the skin was completely pulled apart to expose the body cavity with the internal organs.
- The brachial and axillary peripheral lymph nodes and the spleen were collected for each mouse (see Fig. 6 for location information) and transferred to a 50 ml falcon tube containing ice-cold HBSS.
- The tissue parts were transported on ice to the laboratory for T-cell isolation.

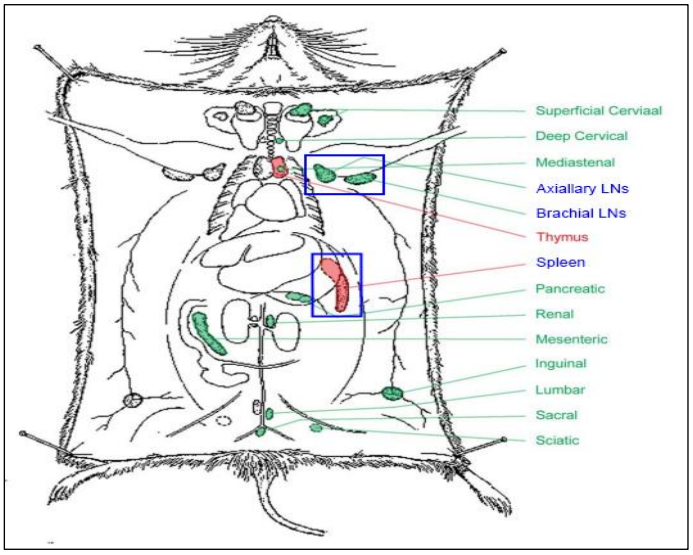

Figure 6: Organs of the immune system. The position of the spleen, axillary and brachial lymph nodes is highlighted by blue squares. Image modified from: The virtual mouse necropsy.

<u>Isolation of T-cells</u>

- The tissue parts were placed on a 70 µm cell strainer (Falcon) on a 50 ml falcon tube. The tissues were gently pressed through the strainer using a syringe plunger. Fat tissue, aggregates and debris couldn't pass through the filter and were disposed of.
- For the washing step, 20 ml FACS-buffer (PBS+2%FBS+0.5mM EDTA) were added to the resulting single cell suspensions and the tubes were spun for 5 min at 1500 rpm at 4°C.
- The supernatant was discarded and the cell pellets were resuspended in 4 ml ACK-lysis buffer by pipetting up- and down to destroy the erythrocytes.
- To stop the reaction, 15-20 ml of FACS-buffer were added and the tubes were centrifugated.

- The supernatant was discarded and the clotted erythrocytes were removed with a P1000 pipette tip. The cell pellets were resuspended in 500 µl FACS-buffer.
- T-cells were enriched by immunomagnetic negative selection using the EasySepTM Mouse T-Cell Isolation Kit (Stemcell) according to the manufacturer's instructions (STEMCELL Technologies Inc. 2019).
- The clear media containing the isolated T-cells were transferred to new FACS-tubes and they were spun for 5 min at 1500 rpm at 4°C

Purification of naïve T-cells

- The cells were stained with FITC-anti-CD45RB^{high} antibody (Bioscience), PB-anti CD4 antibody (Bioscience) and PE-Cy7-anti-TCR-β antibody (Bioscience) to label the naïve T-cells. For the antibody-premix (AB-premix) all three ABs were diluted 1:200 in 1 ml FACS-buffer. For the compensation controls, 200 µl FACS-buffer, 50 µl Enh-WT cell suspension and 1 µl of the respective antibody were pipetted into FACS tubes. For the unstained control, only FACS-buffer and cell suspension were added to a FACS tube.
- The supernatant was discarded and each T-cell pellet was resuspended in around 240 µl of the antibody premix.
- The FACS-tubes were incubated for 30 min on a shaking plattform in the cold room (4°C).
- The cells were washed with 1 ml FACS-buffer and pelleted by centrifugation.
- The supernatant was discarded and the cell pellets were resuspended in 500 µl (samples) and 200 µl (compensation controls) FACS-buffer, respectively.
- The cell sorting for naïve CD4^{+} CD45RB^{high} T-cells was performed by the Yale's core facility for cell sorting (>95% purity).

Injection of naïve T-cells into RAG$^{-/-}$-mice

- The sorted CD4+ CD45RBhigh T-cells were spun at 1500 rpm for 5 min at 4°C to pelletize the cells.
- The supernatant was discarded and the cell pellets were resuspended in 700 µl PBS and transferred to labeled microcentrifuge tubes. The FACS- tubes were rinsed with an additional 500 µl of PBS to obtain as many cells as possible.
- The tubes were centrifuged, the supernatant was discarded and the pellets were resuspended in the appropriate volume of ice-cold PBS to obtain 5x106 cells per ml. The tubes were placed on ice.

In the animal room

- The RAG-/--mice (12x male, 11x female mice) were weighed and marked by cutting specific parts of their ears.
- The T-cells were well resuspended before an insulin syringe was filled with the T-cell suspension.
- Each mouse was properly restrained in a standard hand hold with the head tilted downwards, and 5x105 naïve T-cells in 100 µl PBS were slowly injected intra peritoneal (i.p.). The needle was therefore inserted into the lower right quadrant of the abdomen to reduce the likelihood of penetrating any organs. The plunger was slightly withdrawn to check for accidental organ puncture (yellow fluid – bladder; greenish brown fluid – intestine or cecum). If there was no reflux, the cell suspension was injected into the peritoneal cavity.

- Special attention was paid to gender matching, i.e. naïve T-cells of female Enhancer-mice were injected into female RAG-/--mice and cells of male Enhancer-mice were injected into male RAG-/--mice.
- Around the same number of recipient animals was injected with Enh-WT T-cells as with Enh-KO T-cells: WT: 7x m, 6x f; KO: 5x m+f

Pathological scoring of colitis

- The body weight of the animals was measured once aweek for the entire experiment, as weight loss is a well-established indicator of the onset and course of colitis.
- Endoscopy was performed from week 6-10 to additionally analyze histologic changes of the colon due to colitis, as some mice do not lose weight but may still develop classic pathological lesions.
- At the end of the experiment (week 10), the mice were sacrificed and the T-cell infiltration of the colon was investigated by flow cytometry.
- The same humane endpoints were applied as in the DSS- colitis model.

2.2.3.1 Endoscopy

The mice of the transfer colitis experiment were subjected to an endoscopy of the distal gastrointestinal tract from week 6 to week 10. Endoscopy is a powerful method to examine the gastrointestinal system for inflammatory or neoplastic changes not only in humans but also in mice. Over a decade ago, prior to the development of the endoscopy tool for small animals, the possibilities to monitor development and activity of colitis in mice were limited to (1) indirect methods, like weight loss, food and water intake, presence of blood in the feces and feces consistence, and (2) *post mortem* analysis of histological sections. High resolution endoscopy, however, allows direct and detailed visualization of the colonic mucosa in the living animal at any time point given during an experiment. Therefore, endoscopy enabled the monitoring and scoring of the pathological alterations in the inflamed colon in the course of the transfer colitis experiment.

Endoscopy in mice is not only a relatively safe and quick to perform method, it is also easily reproducible and results in the reduction of costs and animal numbers per experiment. The procedure can be safely used for mice with very severe colitis and weight loss. Nevertheless it requires a certain amount of training to carry out endoscopic procedures in small laboratory animals. Therefore, a well trained graduate student, Hao Xu, helped me perform all endoscopies for this transfer colitis experiment.

The used endoscopic system consists of a rigid Storz® telescope with an endoscopic sheath, a powerful light source to illuminate the surface of colon, an air pump to insufflate the GI-tract, a digital camera to record the endoscopy, a monitor to display the images and a tape recorder to save the video files. The rigid nature of the telescope unit allows examination of the distal colon only due to the colonic flexure which cannot be passed with the rigid scope. Fortunately, in the transfer colitis model the distal area is particularly affected. The camera takes 25 pictures per second, creating a large pool of picture to analyze the extent of the inflammation in the colon later on (Neurath et al. 2010) For details about the method see Becker et al. (2006), Brückner et al. (2014) and Kodani et al. (2013).

Setup of the endoscopic device

- The endoscopy sheath and the telescope lens were sterilized and cleaned with water and 70% ethanol.
- The camera and the rigid telescope were assembled and connected to the endoscopic workstation composed of the monitor and the tape recorder.
- The light source and the air pump were attached to the endoscopic sheath. The air flow was adjusted using the corresponding valve. It was set to a continuous and slow flow (~one bubble/second) to avoid strong inflation of the GI-tract which could cause injury to the animal (from respiratory distress to death of the animal).
- A paper towel was wrapped around the endoscopic tube and the focus of the camera was manually adjusted so that the surface of the paper towel, which simulates the colonic surface, was in focus.

Anesthetize the mice

- The mice of the first cage were put in a leak-proofed anesthetic chamber and inhalation anesthesia was induced by administrating 2-3% isoflurane in 100% oxygen.
- As soon as the animals were fully anesthetized (approx. 1 min), the first mouse was taken out of the chamber and positioned on the clean work surface with its ventral side up. The mouse needed to be deeply anesthetized to prevent movement during endoscopy that may result in injury to the intestinal mucosa by the endoscopic device. Therefore, effectiveness of anesthesia was tested by checking the reflexes through toe pinching. If no pedal retraction occurred and no change in respiratory rate was observed, the endoscopic procedure was started.

Endoscopic standard procedure

- If possible, feces which could have impaired vision during endoscopy, was removed from the rectal tube by gently squeezing the lower abdominal area of the mouse.
- The rigid endoscope was carefully inserted through the after and slowly introduced up to the right colonic flexure (about 4 cm from the anus) but not further to avoid perforation of the colon. If feces or blood led to smearing of the optical lens, the endoscope was withdrawn, cleaned and reintroduced.
- Once the colonic flexure was reached, the endoscope was slowly withdrawn and the recording was started. The intestinal mucosa was examined for inflammatory changes of the intra-luminal surroundings while the endoscope was retracted. The recording was stop when the anus was reached.
- The endoscope was removed and the anesthetized mouse was placed on a paper towel to protect it from inhaling bedding material. As soon as the animal regained consciousness it was put back in its cage. The animal was monitored closely until it fully recovered from the endoscopic procedure and the associated anesthesia.

Analyzing data and scoring of the colitis activity

- The well-established and quantitative colitis scoring system MEICS (murine endoscopic index of colitis severity) was used to evaluate the pathologic tissue changes in the colon in the course of colitis. It consists of five parameters: Thickening of the bowel wall, changes in the pattern of the vascular system, mucosal granularity, stool consistency and presence of fibrin.

The latter, however, was not included in the assessment of the transfer colitis mice, as fibrin is mainly found in the recovery phase after colitis.

- Each parameter was evaluated individually (score between 0 and 3) and then combined to a total score between 0 (no signs of inflammation) and 12 (signs of very severe inflammation). Mice not affected by colitis had a total score of 0-3.
- The results of the endoscopy were compared with the weight curve values and presented in a graph using Prism. The latter was also used to calculate whether there was a significant difference between the colitis scores of the two experimental groups (WT vs. KO).

2.2.3.2 Flow cytometry analysis of colonic immune cell infiltration

At the end of the T-cell dependent transfer colitis model, the mice were sacrificed and the colon was removed. Infiltrated T-cells of the colonic tissue were isolated and stained for surface proteins of effector T-cells and intracellular production of cytokines. Flow cytometry was used to determine the percentage of pathogenic T_h1-and T_h17-cells derived from the transferred naïve T-cells.

In the animal procedure room

- The mice were euthanized by placing them in the CO_2-chamber for 3 minutes, followed by cervical dislocation to ensure death of the animals.
- The abdomen of the first mouse was sprayed with 70% ethanol and the abdominal cavity was carefully opened with surgical scissor.
- The intestine was removed and the entire colon was collected by cutting at the cecal-colon junction and the colon-rectal junction. Large pieces of connective tissue and mesenteric fat were removed with tweezers.
- The harvested colon was placed in a well of a 12-well plate containing ice-cold RPMI complete medium and the plate was put on ice until the colon of all mice was collected.

In the laboratory

Washing

- The colon was opened longitudinally and food particles, fecal debris and mucous was carefully scraped off with the backside of the scissors. The colonic tissue was washed three times by flushing it with cold PBS.
- Each colon piece was placed in 1 ml RPMI complete medium in a 12-well plate.

Digestion

- To start the first step of tissue digestion, 25 ml of pre-warmed digestion buffer-1 (DB-1) was added to 50° ml falcon tubes and the colon pieces were transferred from the RPMI medium to the digestion buffer. (DB-1: HBSS + 10% FBS, 10mM HEPES-buffer and 5mM DTT). The tubes were incubated for 30° min at 37°C and 220 rpm in the shaker incubator.
- After incubation, the tubes were shaken vigorously to release the epithelial cells.
- The cloudy supernatants containing the epithelial cells were passed through a steel strainer on a petri dish to separate tissue pieces from the single cell suspension.
- The filtrated supernatants were poured back into the 50 ml falcon tubes, the cell strainers were rinsed with 5 ml PRMI medium and the tubes were stored at 4°C.

- For the second digestion step, the colon pieces were minced with surgical scissor and transferred into 15 ml falcon tubes containing with 5 ml of pre-warmed digestion buffer-2 (DB-2: 25 ml RPMI medium + 12.5 mg dispase, 37.5 mg collagenase II + 300 µl FBS).
- The tubes were incubated for 30 min at 37°C and 220 rpm in the shaker incubator. Afterwards, the tubes were shaken vigorously to dissolve the tissues, and the solutions were pooled with the purified supernatants from the first digestion step.
- The tubes were centrifuged for 5 min at 1500 rpm and 4°C to pelletize the cells and the supernatant was decanted.

Enrichment and purification of T-cells by Percoll® Gradient Centrifugation

- For the lower phase, 4 ml of 100% Percoll solution (90ml Percoll® + 10 ml 10xPBS) were added to the tube.
- The cell pellets were resuspended in 5 ml of 40% Percoll solution (40 ml 100% Percoll solution + 60 ml FACS buffer) and the Percoll-cell mixtures were slowly added on top of the lower phase without disturbing the phase interface.
- The tubes were centrifuged for 20 min at 1500 rpm (accel: 0; break: 2) and 4°C to enrich the T-cells in the phase interface.
- Most of the upper phase was removed with a serological pipette and discarded. The phase interface containing the T-cells was collected and filtered through a filter paper into a 15 ml falcon tube. The filter paper was rinsed with an additional 2 ml of FACS buffer.
- The falcon tubes were filled to the rim with FACS buffer and centrifuged at 1650 rpm for 6 min at 4°C. The supernatant was completely removed using a P1000 pipette.

Re-activation and cell surface staining of T-cells

- The cell pellets were resuspended in 3 ml of the re-activation medium (Click's medium + PMA (1:2000), Ionomycin (1:2000) and Golgi-Stop (1:2000)).
- The tubes were incubated for 3 hours at 37°C in a tissue culture incubator. The screw-cap of the tubes was not completely closed to allow the exchange of gases (oxygen, CO_2).
- After incubation, the cells were pelletized by centrifugation at 1650 rpm for 5 min and the supernatant was completely removed.
- The cells were stained with Alexa700-anti-CD45.2-antibody, PB-anti-CD4-antibdoy and PE-Cy7-anti-TCR-β-antibody by resuspending the cells in the staining solution. For the staining solution, all three ABs were diluted 1:500 in FACS buffer.
- The tubes were incubated for 15 min at 37°C in a cell culture incubator.
- To stop the staining reaction 3 ml of FACS buffer were added to each tube to dilute down the ABs. The tubes were vortexed briefly and centrifuged at 1500 rpm for 5 min.

Fixation and intracellular staining

- The supernatant was removed and the cells were resuspended in 1 ml of 4% formaldehyde fixing solution. The tubes were incubated at RT in the dark for 15 min.
- To stop the reaction, 3 ml FACS buffer were added to each tube and the cells were spun down at 1500 rpm for 5 min.
- The supernatant was completely removed and the cells were resuspended in 400 µl of permeabilization buffer (FACS buffer + 0.1% NP-40). The tubes were incubated at RT for 4 min to allow permeabilization of the cell membrane.

- To stop the reaction, 5 ml of FACS buffer were added to each tube and spun at 1200 rpm for 7 min at 4°C. The supernatant was discarded.
- Intracellular cytokines were stained with PE-anti-INF-γ-antibody and APC-anti-IL-17A-antibody by resuspending the cell pellets in 200 µl of intracellular staining solution. For the staining solution, the two ABs were diluted 1:200 in FACS buffer.
- The tubes were incubated for 30 min at 37°C in a cell culture incubator. To stop the reaction, 3 ml FACS buffer were added to each tube and the cells were spun down at 1200 rpm for 7 min at 4°C.
- The supernatant was completely removed and the cells were resuspended in 1 ml PBS.
- The unstained control and the single staining controls for all five antibodies were prepared with compensation beads.
- Compensation was performed on the flow cytometer for all fluorochromes used in the experiment. First, front and side scatter were used to select living single cells. Then all donor T-cells were selected by gating for CD45.2$^+$-cells. By using the fluorescence signal of CD4- and TCR-β antibodies, it was possible to gate for CD4$^+$ T-cells. The last step was to determine the proportion of T_h1 and T_h17-cells by checking for the intracellular production of INF-γ and IL-17 in CD4$^+$-cells.

2.3 Quantitative PCR analysis

2.3.1 RNA isolation

For this master thesis, RNA was isolated from various tissues (duodenum, small intestine, colon, mesenteric lymph nodes, spleen, thymus, liver, kidney and lung), cell types (BMDMs, IMCs) and intestinal crypts and organoids. The extracted RNA was purified and translated into cDNA, which in turn served as template for qPCRs. The qPCRs performed provided information on the relative expression of target genes (e.g. Pterg4 and adjacent genes) in tissues and cells of Ptger4-Enhancer-WT, -HET and –KO mice.

TRIzol™ Reagent (Invitrogen) was used to extract RNA from tissues, cells and intestinal crypts, whereas RNA from organoids was isolated using the RNeasy® Plus Micro-Kit (Qiagen).

TRIzol™ Reagent

The TRIzol™ reagent is a monophasic solution containing phenol and is used for the isolation of total RNA from cell and tissue samples. It is able to effectively inhibit RNase activity thereby maintaining the integrity of the isolated RNA during the extraction process. For more information about the procedure, see the manufacturer's protocol TRIzol™ Reagent (Thermo Fisher Scientific 2016). (Eurogentec 2008)

- First, the biological samples were lysed by adding TRIzol™ to the tissue pieces, cell culture plates or cell pellets.
- To homogenize the lysates, cell- TRIzol™ suspensions were pipette up and down several times, while tissue pieces were disrupted and homogenized with a tissue homogenizer to completely dissolve the cells and cell organelles.

- Chloroform was added to the samples and they were centrifuged to separate the homogenates into a colorless upper aqueous phase containing the RNA, an interphase, and a red lower organic phase containing the DNA and proteins.
- Solely the aqueous phase was transferred into a new tube and the contained RNA was precipitated with isopropanol and pelleted by centrifugation.
- The white gel-like RNA pellet was washed with 75% ethanol to remove impurities and then resuspended in RNase-free DEPC-water by pipetting up and down. The samples were incubated at 55°C in a heat block for 10 min to further solubilize the RNA pellet
- After measuring the concentration of the extracted RNA (µg RNA/ml) using the NanoDrop™ spectrophotometer, contaminating genomic DNA (gDNA) was eliminated with the TURBO DNase kit. It was also possible to store the isolated RNA at -80°C and perform the purification step at a later time.

RNeasy® Plus Micro Kit

The RNeasey® Plus Micro Kit is designed for extraction, purification and concentration of total RNA from small amounts of cells (max. $5x10^5$ cells - e.g. organoids) and tissue (max. 5 mg) using gDNA Eliminator and RNA extraction columns. The kit enables the parallel processing of multiple samples and, in contrast to TRIzol® RNA isolation, requires no toxic substances such as phenol and chloroform. All steps of the procedure were performed at RT. For more details about the method, see the manufacturer's protocol RNeasy® Plus Micro Handbook (Qiagen GmbH 2014).

- First, the pelleted intestinal organoids were lysed and disrupted by resuspension in highly denaturating buffer RLT Plus + β-mercaptoethanol (β-ME), which inactivated RNases and other proteins and thus prevented the degradation of RNA and the down- or upregulation of transcripts.
- The samples were passed through a QIAshredder spin column to homogenize the lysates by shearing gDNA and other high-molecular-weight cellular components.
- To effectively eliminate contaminating gDNA, the homogenized lysates were passed through gDNA Eliminator Mini spin columns and one volume of70% ethanol was added to the flow-through to provide optimal binding conditions for the RNA in the next step.
- The samples were load onto RNeasy MinElute® spin columns and centrifuged to bind the RNA to the spin column membranes.
- To remove cellular debris and other contaminates the spin column membranes were washed with buffer RW1, buffer RPE and 80% ethanol.
- After drying the membranes by centrifugation the purified RNA was eluted in RNase-free water and the RNA yield measured with a NanoDrop spectrophotometer. The extracted RNA was either transcribed immediately into cDNA or temporarily stored at -80°C.

2.3.2 Elimination of gDNA contaminations from RNA samples

The TURBO DNA-free™ Kit (Invitrogen) is designed to reduce the contamination of gDNA from extracted RNA samples to a level below the detection limit of qPCR. In addition, it also removes the introduced TURBO DNase™ enzyme and the divalent cations Mg^{2+} and Ca^2 from the samples, which would otherwise interfere with downstream procedures such as cDNA synthesis and qPCR. The TURBO DNA-free™ kit is free of toxic substances such as phenol and chloroform and represents an improvement over the classic DNaseI elimination of gDNA from RNA samples. For more information about the method see the manufacturer's protocol TURBO DNA-free™ Kit (Thermo Fisher Scientific).

For this master thesis, total RNA extracted from tissue, cell or crypt samples using the TRIzol® method was treated with the TURBO DNase- free™ kit following the standard protocol. Small 0.5 ml tubes were used for the reaction to facilitate pipetting of the supernatant after DNase inactivation treatment.

- Prior to treatment, the RNA-samples to be purified were diluted to 10 µg nucleic acid in a 50 µl total reaction volume.
- TURBO DNase™ buffer and TURBO DNase™ enzyme were added to the samples and mixed gently.
- The samples were incubated for 30 min at 37°C in a heat block to allow the enzyme to digest the contaminating gDNA.
- After incubation, the well resuspended DNase inactivation reagent was added to the tubes. The samples were incubated at RT for 5 minutes and mixed occasionally to redisperse the inactivation reagent.
- The tubes were centrifuged for 2 min at 1000xg and the supernatant containing the RNA was transferred to new tubes.
- After measuring the concentration of the purified RNA with a NanoDrop spectrophotometer, it was either directly transcribed into cDNA or temporarily stored at -80°C.

2.3.3 cDNA synthesis

All extracted and purified RNAs of this master thesis were reverse transcribed using the Thermo Scientific Maxima H Reverse Transcriptase kit. This kit is based on an advanced M-MuLV (Moloney Murine Leukemia Viurs) reverse transcriptase enzyme that features RNA and DNA-dependent polymerase activity, but no RNase H activity, ensuring a high yield of full length cDNA products within 30 minutes. The first strand cDNA synthesis was conducted according to the manufacturer's protocol for Maxima H Minus Reverse Transcriptase (Thermo Fisher Scientific). Oligo(dT) primers were used for the reaction, which bind to the poly-A tail of mRNAs, resulting in their increased transcription into cDNA.

- Template RNA (0.35-3.5 µg depending on experiment), oligo$(dT)_{16;20}$ primers and dNTPs were pipetted into sterile PCR-tubes on ice. The reaction volume was brought up to 14.5 µl with nuclease-free water.
- The tubes were incubated for 5 min at 65°C in a thermocycler to break up secondary structures and GC-rich templates.
- Subsequently, 5x RT Buffer, RNase Inhibitor and Maxima H Minus Reverse Transcriptase were added to the tubes on ice and gently mixed.
- The samples were incubated at 50°C for 45 min to allow the enzyme to transcribe the template RNA into cDNA. The enzyme was heat-inactivated by incubation at 85°C for 5 min.
- The resulting cDNA was either used directly as a template in qPCRs or temporarily stored at -20°C.

2.3.4 Quantitative PCR (qPCR)

Quantitative PCR is a method that combines the rapid amplification of nucleic acids with the detection and quantification of the amplicon in real time. It enables the precise quantification of gene expression levels and can show changes in these levels caused by environmental stimuli, drug treatment or different genetic backgrounds by measuring changes in cellular mRNA levels. In addition, qPCR is used for the detection and quantification of pathogens, microRNAs or GMOs as well

as for cancer phenotyping. The amplification part in qPCR is based on the same principle as standard PCR. The cDNA is amplified in three repeating steps: denaturation, annealing and elongation. The detection and quantification step in qPCR is based on fluorescence molecules that interact with the amplified DNA sequences.

There are two basic qPCR approaches:

(1) dye-based qPCR assays: the fluorescent dye (e.g. SYBR® Green) incorporates non-specifically into all double-stranded DNA (dsDNA) present in the reaction.
(2) probe-based qPCR: the fluorescence-labeled DNA probe binds specifically to the generated product.

In both cases, the measured fluorescence intensity is directly proportional to the amount of amplified product. During each PCR cycle, the fluorescence signal generated is measured providing an amplification plot (x=cycle number; y=fluorescence intensity) at the end of the reaction. The PCR process is initially exponential as the amount of PCR products doubles with each cycle, but eventually a non-exponential plateau phase is reached when one of the reagents becomes limited. The baseline of the plot is automatically generated by the machine and is the average fluorescence signal background. For analysis, the qPCR software calculates the Cq-value (quantification cycle) for each sample. The Cq-value corresponds to the amplification cycle in which the increasing fluorescence signal crosses the baseline for the first time. It not only shows the sensitivity of the assay, but is also related to the initial amount of cDNA used as a template. The lower the Cq-value, the earlier the fluorescence is above the baseline and the more template DNA is present at the beginning of the reaction. Thus, the Cq-value is indirectly proportional to the expression levels of the gene of interest.

The non-specific fluorescent dye SYBR® Green was used for all qPCR assays of this master thesis. SYBR® Green is characterized by weak background fluorescence, which is dramatically increased when intercalating into dsDNA. The SYBR® Green approach requires only a sequence-specific primer pair, but no probe, making it cost-effective, easy to design and set-up, and fast to perform. A disadvantage, however, is that SYBR® Green binds to any dsDNA present in the reaction. This also includes amplified non-specific products or primer dimers that can introduce a bias into the quantification. To check the specificity of the reaction, a high-resolution melting curve was performed at the end of each qPCR experiment.

The qPCR assays were used to quantify the expression levels of Ptger4 and adjacent genes (Ttc33, Prkaa1, Card6 and C7) in Ptger4-Enhancer-WT, -HET and –KO tissue and cell samples relative to the expression of the reference housekeeping gene B2M (beta-2-microglobulin). In addition, the effects of LPS-stimulation, luminal content and microbiome on the expression of Ptger4 were analyzed. Upregulation of Il-6 expression due to LPS-treatment was used as positive control for cell stimulation. The reference gene B2M is a subunit of the MHC-I complex and thus expressed on the surface of all nuclear cells. The level of its expression is constant between individuals, tissue and cells types and is not influenced by experimental interventions, making B2M a perfect reference housekeeping gene. Normalization to B2M was used as a correction method for uncontrolled variables, such as different amounts of starting material in the samples or differences between tissues, individuals or experimental conditions.

For the four adjacent genes Ttc33, Prkaa1, Card6 and C7 and Il-6, pre-designed primer pairs from Sigma-Aldrich were used for the qPCR assays. However, for Ptger4 the pre-designed primers showed

non-reproducible results, a low PCR efficiency and a high variance of the Cq-values of duplicates. Therefore new primers were designed using Primer3 and the NCBI-primer tool for an amplicon of 100-200 bp length. In order to exclude the amplification of potentially contaminating gDNA, exon-spanning primers were designed, where the forward primer binds to a different exon than the reverse primer (exon 2 and 3 of Ptger4). The NCBI-blast search was used to verify the uniqueness und specificity of the primer pairs.

The expression levels of target and reference genes were quantified in singleplex reactions. For more information about the method see Eurogentec (2008) and Thermo Fisher Scientific.

- The synthesized cDNA templates were diluted 1:10 (organoids and crypts samples) or 1:20 (tissue and cell samples) in DEPC-water prior to qPCR.
- To set up the amplification reaction, the diluted cDNA templates were pipetted in duplicates into the wells of a 96-well or 384-well qPCR-plate. For the no template controls (NTCs), MilliQ-water was added to two wells instead of the cDNA template. A standard curve was pipetted in duplicates for each gene. An untreated WT-sample was used as standard and diluted 10-, 20-, 40- and 80 fold to cover the range of expected gene expression.
- A reaction mix for each gene was prepared by mixing the respective primer pair (50 ng) with the 2x SYBR®Green Mastermix (Bio-Rad) which contains Taq-polymerase, $MgCl_2$, dNTPS, SYBR®Green and inert colored dye. The reaction mixtures were pipetted into the corresponding wells of the plate.
- The plate was carefully sealed with a special adhesive film (Bio-Rad) to prevent evaporation. It was briefly placed on a shaking platform and centrifuged to mix the reaction components and collect them at the bottom of the wells.
- The reaction was run immediately after preparation in a qPCR-thermocycler (Bio-Rad) equipped with fluorescence detection modules (see tab. 1).

Table 1: Standard settings for qPCR

Temperature	Time	Step	
95°C f	3 min	Activation of the Taq polymerase	
95°C	15 sec	Denaturation of dsDNA	} x40
60°C	45°sec	Primer annealing + primer extension by the Taq polymerase	
60°C-95°C		Melting curve to check for amplification specificity	

- The collected data was analyzed with the Biored-qPCR-analysis-software.
- The melting curve was checked for a single dissociation peak of dsDNA, indicating a specific amplification of the target.
- The standard curve of each gene provided information on the overall-performance of the qPCR-assay (linearity (R^2), sensitivity (Cq-values), reproducibility (duplicates)) and also showed the PCR-efficiency (slope of the curve). The experimental setup was optimized when the PCR-efficiency was lower than 85% or higher than 115%.
- Duplicates were eliminated from the analysis if the difference between their Cq-values was greater than 0.5.
- The relative expression values were calculated using the ΔΔCq-method with PCR efficiency correction. This method is based on the normalization of target gene expression to reference gene expression and also takes PCR efficiencies into account. An untreated WT-sample with low variance between the Cq-values of its duplicates was selected as calibrator. To calculate

the relative expression levels, the calibrator becomes the 1xsample, and all other quantities are expressed as an n-times the difference to the calibrator.

$$\text{Ratio} = (\text{Efficiency}_{\text{target}})^{\Delta Cq \text{ target (calibrator – sample)}} / (\text{Efficiency}_{\text{reference}})^{\Delta Cq \text{ reference (calibrator – sample)}}$$

2.4 Thymus - Flow cytometry analysis of T-cell development

The thymus is a primary lymphatic organ of the immune system. Within the thymus, the thymocytes mature sequentially into naïve T-cells. For this experiment, thymus cells were isolated from Ptger4-Enh-WT and –KO mice and stained for specific surface glycoproteins (CD45, CD4, CD8, CD25 and CD44) to investigate possible effects of the Ptger4-enhancer on T-cell development.

In the animal procedure room

- Two six-week-old mice (1x Enh-WT and 1x Enh-KO) were selected for the isolation of thymic cells.
- The mice were euthanized by CO_2-asphyxiation. A cervical dislocation was performed to ensure the death of the animals.
- The thymus, which is located above the heart in the thoracic cavity, was harvested using surgical scissors and tweezers (see Fig.6 for location information). The tissue was transfer to a 50 ml falcon tube filled with ice-cold HBSS buffer. The thymus tissue was transported on ice to the laboratory to isolate the thymus cells

In the laboratory

Isolation of thymic cells

- The thymus tissues were placed on a 70 µm cell strainer (Falcon) on a 50 ml conical tube. The tissues were gently pressed through the strainer using a syringe plunger. Fat tissue and debris couldn't pass through the filter and were discarded.
- The cells were washed by adding 20 ml FACS buffer (PBS+2%FBS+0.5mM EDTA) to the resulting single cell suspensions and the tubes were spun for 5 min at 1500 rpm at 4°C.
- The supernatant was removed completely and the cell pellets were resuspended in 4 ml ACK-lysis buffer by pipetting up- and down to destroy the erythrocytes.
- After 2 min of incubation the reaction was stopped by adding 20 ml FACS buffer and the tubes were centrifugated again.
- The supernatant was discarded and the clotted erythrocytes were removed with a P1000 pipette tip. For washing, the cell pellets were resuspended in 1 ml FACS buffer and centrifuged for 5 min at 1500 rpm and 4°C.
- The supernatant was removed completely and the cells were stained with PB-anti-CD4-antibody, PE-Cy7-anti-CD8-antibody, APC-anti-CD25-antibody, PE-anti-CD44-antibody and FITC-anti-CD45-antibody by resuspending the cells in 450µl staining solution. For the staining solution all five ABs were diluted 1:200 in 1 ml of FACS buffer.
- The tubes were incubated for 20 min in the dark at 4°C. The staining was top by adding 2 ml FACS buffer to each tube. The cells were spun down in 5 min at 1500 rpm and 4°C.
- The cells were fixed with 4% formaldehyde fixing solution and incubated for 20 min at RT.
- Another washing step was performed to remove residual fixing solution.

- The cell pellets were resuspended in 500 µl PBS and the proportion of maturing thymocytes and naïve T-cells was determined by flow cytometry analysis. First, forward and side scatter were used to select for living single cells. Then the CD4-fluorescence signal was plotted against the CD8-signal. The CD4, CD8-double-negative cells were analyzed further by plotting the CD44 signal against the CD25 signal. This enabled to assign the thymocytes to the four different early developmental stages of T-cells.

2.5 Statistical analysis

Statistical analyses were performed with Graph Pad Prism. For all animal studies, results are expressed in mean ± SEM. Statistically significant differences between gene expression levels, body weight changes or pathological scores of inflamed intestines of the two groups Enh-WT and Enh-KO were assessed by using a 2-tailed unpaired student's *t* test. P-values <0.05 were considered statistically significant.

3 Results

3.1 Identifying associated target genes of the putative enhancer region

The region of interest consists of non-coding elements located approx. 300- kb upstream of the *PTGER4* gene on chromosome 5. Several independent genome-wide association studies (GWAS) and associated fine-mapping studies showed a significant association of this ~250 kb region with colorectal cancer (CRC), ulcerative colitis (UC), Crohn's disease (CD) and other autoimmune diseases (Huyghe et al. 2019; Jostins et al. 2012a; Libioulle et al. 2007; Ellinghaus et al. 2016), underscoring its importance for numerous complex diseases. Previous unpublished work in the lab has shown that the risk locus features nine highly conserved H3K27Ac peaks in tissues of the gastrointestinal tract (GI-tract) and various immune cell lines (Sup. Fig. 1[A]). The histone acetylation pattern indicates a putative enhancer activity of the region of interest in the aforementioned tissues and cell types in human and mice (Schernthanner 2019; Creyghton et al. 2010). To identify associated target genes and to assess the functional properties of the putative enhancer *in vivo* and *in vitro* a novel enhancer knockout mouse line (Enh-KO) was created with the CRISPR/Cas9 system. Enh-KO-mice exhibit a genetic deletion of the putative regulatory elements of about 100 kp (5.437.707-5.542.206) on chromosome 15 upstream of *Ptger4* (see Fig 7[A]).

A study on enhancer activity in *Drosophila melanogaster* showed that >95% of the enhancers regulate genes in their immediate environment (88% of enhancers regulated the nearest gene, another 8% regulated the next nearest gene) (Kvon et al. 2014). Furthermore, the HiChIP data analysis of the region of interest in human Jurkat cells (T-lymphocyte cell line) performed prior to this study revealed a direct interaction of the *PTGER4* gene with the putative enhancer elements via the ubiquitous TF YY1 (Weintraub et al. 2017). A GWA-study comparing expression patterns of adjacent genes with the different genetic variants of the *PTGER4* risk locus showed that high-risk variants for

CD correlated with increased expression of *PTGER4* (Libioulle et al. 2007). *PTGER4* encodes the prostaglandin E_2(PGE) receptor protein 4 (EP4), which is implicated in anti- and pro-inflammatory responses as well as post-injury regeneration process, making *PTGER4* a strong candidate gene to be regulated by the risk locus as it might be involved in the pathogenesis of IBD and CRC (see 1.3 for more information). All together, we decided to evaluate the regulatory potential of the risk locus by studying the expression pattern of *Ptger4* and four neighboring genes (*Ttc33*, *Prkaa1*, *Card6* and *C7*) in the small intestine and colon of Enh-WT –HET and –KO mice (see Fig. 7[A]).

3.1.1 *Ptger4* identified as target gene of the putative enhancer elements in mice

Since *PTGER4* was highlighted as a promising target gene regulated by the putative enhancer elements, its relative expression values in tissues derived from Enh-mice were investigated first. Three independent experiments with one mouse per genotype (Enh-WT, -HET and -KO) were performed. Five ~1 cm pieces of the ileum (=the last part of the small intestine) and four ~2 cm pieces of the colon were collected (see Fig. 7[B]). The two major forms of inflammatory bowel diseases (IBD), UC and CD, and colorectal cancer predominantly affect these parts of the GI-tract. We assumed that an effect of the enhancer elements on gene expression is particularly pronounced in disease- relevant intestinal tissues.

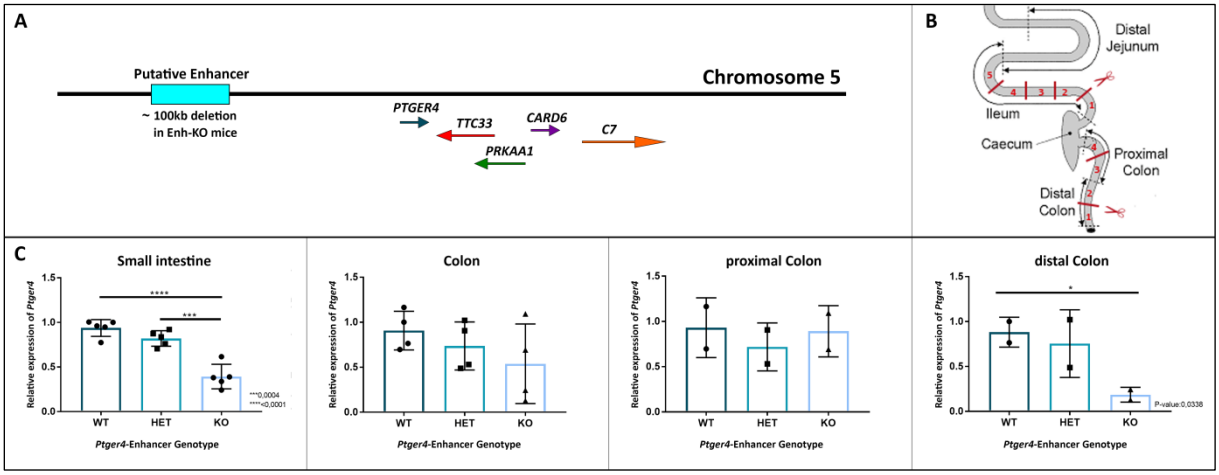

Figure 7: The putative enhancer regulates expression of Ptger4 in small intestine and distal colon of mice. [A] Scheme of the putative enhancer region and adjacent genes. **[B]** Tissue sampling for the experiment: ileum (five tissue pieces) and the entire colon (four tissues pieces – proximal and distal colon – two pieces each) were collected from *Ptger4*-Enhancer-WT, -HET and –KO mice. **[C]** Relative expression levels of *Ptger4* in small intestine and colon samples derived from *Ptger4*-Enhancer-WT, -HET and –KO mice. B2M was used as reference house keeping gene. Ptger4-expression is significantly reduced in the small intestine and the distal colon of Enh-KO mice. Data represent the mean ±SEM. *p-value <0.05; ***p-value <0.001; ****p-value <0.0001, five technical replicates of small intestine samples, four technical replicates of colon samples, n=1 mouse per genotype, three independent experiments

Indeed, the ablation of the enhancer elements in Enh-KO mice led to a significant reduction in Ptger4-expression compared to the expression levels of Enh-WT mice in the small intestine and distal colon. Levels of expression in the proximal colon, however, remained unchanged Figure 7[C]. These results validate the enhancer activity of the genetic elements prioritized by fine-mapping and bioinformatic analysis, as their genetic deletion resulted in reduced gene expression. Moreover, *Ptger4* was confirmed as possible target gene of the enhancer region as suggested by Libioulle et al. (2007). The discrepancy in downregulation of *Ptger4* expression between proximal and distal colon, could be explained by the activation of an otherwise latent enhancer triggered by a stimulus

exclusively present in the distal colon (Ostuni et al. 2013). Possible microbial stimuli of the enhancer region are addressed in chapter 3.3.

3.1.2 None of the other adjacent genes appears to be regulated by the enhancer region

Since the presence of active enhancer elements in the disease risk locus was confirmed, we wanted to know whether other genes are regulated by this enhancer region. Several studies have shown that enhancers can regulate gene expression irrespective of their distance, orientation or position to the target promoter (Rickels and Shilatifard 2018b). This phenomenon is based on DNA looping mechanisms that bring the enhancer in close physical proximity to its target promoter (Bulger and Groudine 2011a). Nevertheless, an emerging concept in enhancer biology is that *cis*-regulation of transcription via enhancers occurs locally in discrete chromosomal domains (Dekker and Mirny 2016; Sanyal et al. 2012; Kvon et al. 2014). Therefore, long-ranging interaction between enhancers and target gene most likely occurs in the immediate surroundings.

We decided to analyze the expression levels of the next four genes closest to the risk locus, *TTC33*, *PRKAA1*, *CARD6* and *C7* (see Fig 8[A]), as two of them are promising candidate genes with regard to IBD-pathogenesis. *CARD6* (Caspase Recruitment Domain Protein 6), belongs to the same family as *CARD15* (=NOD2), the first CD susceptibility gene discovered by linkage mapping featuring a very strong disease association (see Fig. 5[A]) (Hugot et al. 2001). *CARD15* is an intracellular pattern recognition receptor expressed in the epithelium and various immune cells. It is involved in the regulation of innate immune responses to intracellular pathogens and injury-associated stimuli (Kobayashi et al. 2005) but also plays a role in autophagy by interacting with *ATG16L1* during autophagosome formation (Homer et al. 2010). Also *C7*, a protein of the complement system, might play a role in the dysregulated innate immune response observed in IBD (Libioulle et al. 2007).

The relative expression levels of all four adjacent genes determined by qPCRs showed no significant differences between Enh-WT and Enh-KO tissue samples of small intestine and colon as would have been expected for at least *Card6* or *C7* (see Fig.8 [A] and [B]). The results suggest that these four genes are not regulated by the enhancer region of the risk locus in mice. This, however, doesn't exclude the involvement of the enhancer in humans, since devolved differences in the biology of humans and mice often affect networks that link genes to diseases (Perlman 2016).

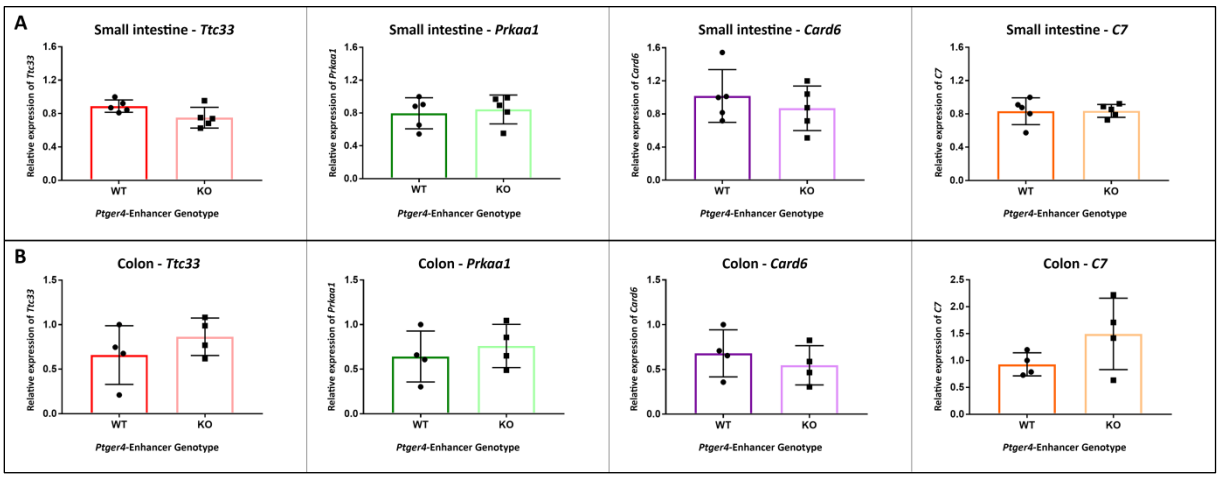

Figure 8: Expression levels of genes adjacent to the GWAS-risk locus. Relative expression levels of *Ttc33*, *Prkaa1*, *Card6* and *C7* in the small intestine **[A]** and the colon **[B]** are not affected by the ablation of the enhancer region. No significant differences in expression are visible between Enh-WT and Enh-KO tissue samples. Data represent the mean ±SEM. Five

technical replicates of small intestine samples, four technical replicates of colon samples, n=1 mouse per genotype, three independent experiments.

The firs functional analysis of the genetic region of interest provided evidence that the enhancer elements influence the expression levels of the nearest gen, *Ptger4*. Thus, the enhancer region could be assigned to at least one of its possible target genes and is henceforth referred to as *Ptger4* enhancer.

3.2 Tissue and cell type-specificity of *Ptger4*-Enhancer activity

3.2.1 Various tissues

The expression analysis experiments of genes adjacent to the genomic region of interest showed that the disease-associated genetic variants in the *PTGER4*- risk locus most likely impact IBD and CRC pathophysiology by perturbing transcription of the PGE_2 receptor protein 4.To follow up on this hypothesis, we investigated the expression levels of PTGER4 in disease-relevant tissues in Enh-WT and –KO mice: duodenum, ileum and colon as tissues of the GI- tract and spleen, thymus and mesenteric lymph node (MLN) as organs of the immune system.
In mice, EP4 is predominantly expressed in the ileum, colon, duodenum and thymus and in lesser extent in spleen, lung, kidney, ovary and heart (UniProt, 2019). Thus, we decided to extend our investigation of *Ptger4* expression levels to lung, kidney and liver tissues.
Analysis of histone acetylation (H3K27Ac) patterns obtained from the Roadmap Epigenomics project and Mouse ENCODE project already indicated highly conserved enhancer activity of the *PTGER4*-risk locus in tissues of the GI-tract (small intestine, colon) and the immune system (spleen and thymus) in humans and mice (Schernthanner 2019) (see Supp. Fig. 1[A]).
The expression analysis of *Ptger4* in the duodenum, terminal ileum and distal colon by qPCR, indeed, displayed the expected reduction in the mRNA levels of the Enh-KO-samples (see Fig. 9[A]). However, the differences in gene expression between Enh-WT and –KO samples weren't significant and therefore represent only a trend of reduced *Ptger4* transcription in KO-mice. The loss of significance in the reduction of *Ptger4* expression in ileum and distal colon compared to the first experiment (see Fig 7 [C]) might be explained by different tissue sampling strategies. In the first experiment five ~1 cm pieces of the ileum of one Enh-WT and –KO mouse were harvested and compared, whereas in this experiment only the most distal ~2cm of the terminal ileum of three Enh-WT and –KO mice were collected and compared. This would indicate that the *Ptger4*-enhancer is more active in the proximal than in the terminal ileum most likely due to stimuli predominantly presented in the proximal ileum (e.g. microbial factors or food particle). For the colon, the most distal part and its microbiome composition seems to be the decisive factor for enhancer regulated *Ptger4*-expression, as *Ptger4* transcription levels are extensively reduced in this colonic region in KO-mice. The strongly scattered expression values between individuals predominantly observed in the Enh-WT mice might be explained by the individual's unique composition of the intestinal microbiome supporting the stimulation hypothesis of the *Ptger4* enhancer by microbial factors.
The reduced expression of *Ptger4* in the duodenum of KO-mice may contribute to the pathological effect of the risk locus in IBD. Larsen et al. (2005) and Takeuchi (2010) showed that activation of EP4 receptors via PGE_2 binding in the epithelial cells of the duodenum mediates secretion of bicarbonate ($HCO3^-$) in mice and humans. Bicarbonate neutralizes the acidic fluid flowing from the stomach and thereby might accelerate the healing process of gastric ulcers and intestinal lesions seen in UC and CD.

The deletion of the *Ptger4*-enhancer region led to a significant reduction of the expression levels of *Ptger4* in all three investigated organs of the immune system (see Fig. 9 [B]). The downregulation was most profound in the thymus samples, suggesting a strong effect of the enhancer elements in T-cell development and differentiation. Several studies support a role of PGE_2-EP4 signaling in increased production of IL-23, thereby promoting expansion and maintenance of T_h17-cell (Maseda et al. 2018; Reinoso Webb et al. 2018). This T- cell subset comprise proinflammatory T-helper cells involved in maintaining mucosal barriers by clearing mucosal surfaces of pathogens but these cells also secrete the proinflammatory cytokine IL-17 implicated in the pathogenesis of IBD and other chronic inflammatory disorders (Geremia and Jewell 2012)

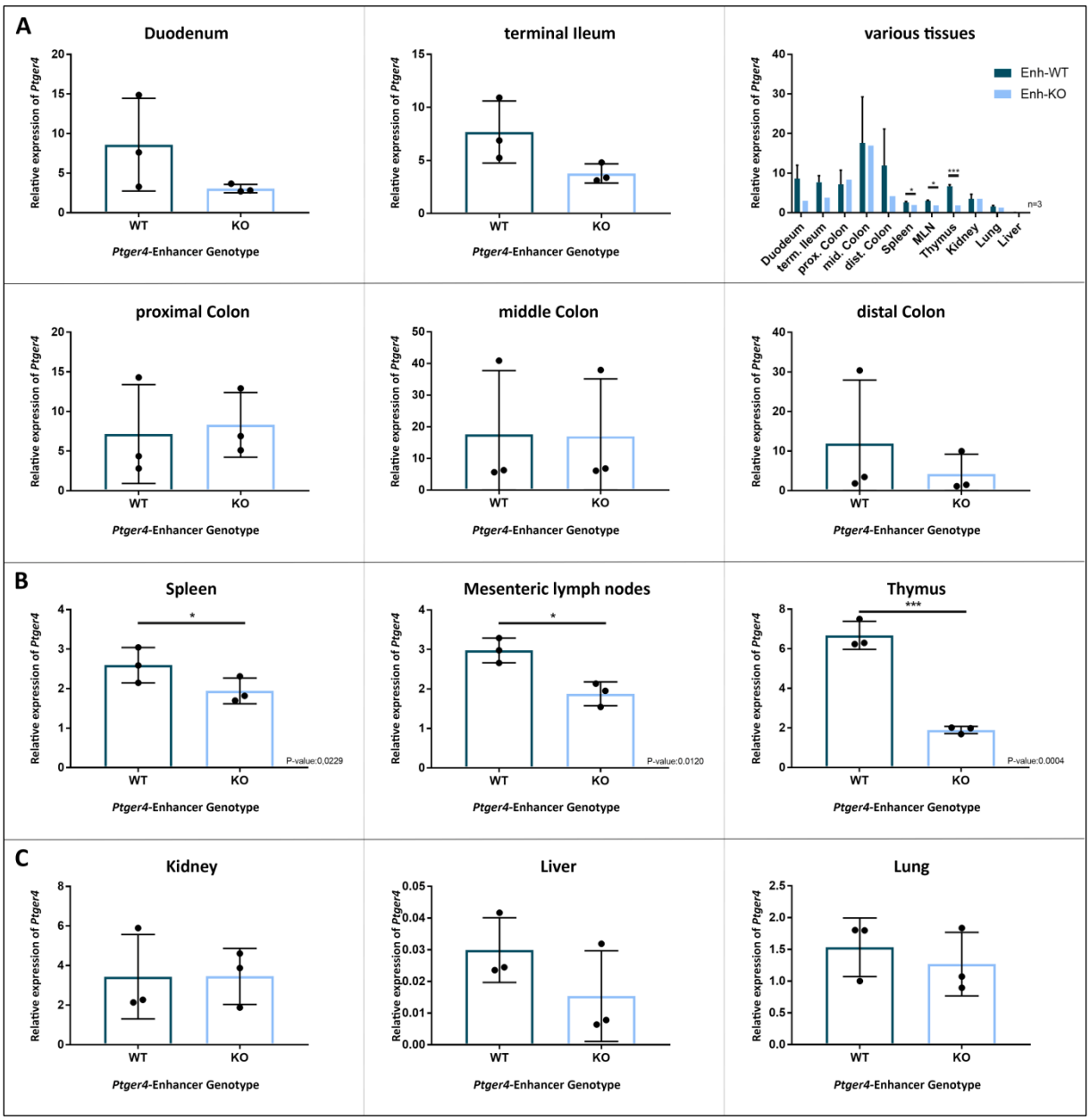

Figure 9: Relative expression levels of Ptger4 in various tissues of Enh-WT and –KO mice. [A] Gastrointestinal tract: duodenum, small intestine and proximal-, middle- and distal colon. **[B]** Organs of the immune system: spleen, mesenteric lymph nodes, thymus**. [C]** Excretory and respiratory organs: kidney, liver and lung**.** n=3 mice per genotype

Besides pain, fever mucosal integrity and inflammation PGE_2 signaling exert complex and diverse function in the regulation of renal function (Konya et al. 2013). Via EP4 signaling PGE_2 regulates renal

homeostasis by controlling cell proliferation, vascular tone and secretion of angiotensinogenase (=renin) (Friis et al. 2005; Schweda et al. 2004). In the liver, PGE_2-EP4 signaling provides protection against hepatic injury caused by reducing hepatic injury markers and inhibiting the release of proinflammatory cytokines such as TNF-α and INF-γ (Kuzumoto et al. 2005). PGE_2-EP4 signaling in the lung is involved in apoptosis of lung fibroblasts, inhibition of smooth muscle cell proliferation and migration and bronchoprotective actions (Sastre et al. 2011; Huang et al. 2009). Despite the numerous important and different functions of PGE_2 mediated via EP4 receptor in these three tissues, we did not determine any effect of the *Ptger4*-enahncer on *Ptger4* mRNA levels (see Fig. 9[C]).

3.2.2 Epithelial, stromal and immune cells

In the course of an immune response, PGE_2 is predominantly produced by epithelial cells, stromal cells (mainly fibroblasts) and infiltrating inflammatory immune cells (Kalinski 2012). It was also shown that PGE_2- signaling via EP4 receptors is increased in the same cell types in CRC (Hull et al. 2004; Gupta and Dubois 2001) underscoring their importance for disease status. As PGE_2 exert its effect through autocrine and/or paracrine) stimulation of its receptor proteins (Markovič et al. 2017), we decided to take a closer look at EP4 expression pattern and its regulation by the *Ptger4*-enhancer in the aforementioned cell types: intestinal mesenchymal cells (stromal cells), bone marrow-derived macrophages (immune cells) and intestinal crypts and organoids (epithelial cells) (see Fig. 10 and 11).

Intestinal mesenchymal cells (IMCs), excluding lymphocytes and endothelial cells, consist mainly of fibroblasts and myofibroblasts, but also include pericytes, stromal stem cells and smooth muscle cells. In recent years, IMCs have moved into the focus of biomedical research as they play a central role in the development and homeostasis of the intestine and interacting with the innate and adaptive immune system. They provide structural support, release growth factors and cytokines, act as nonprofessional immune cells (present antigens, express co-stimulatory and immune check-point molecules) and are involved in wound healing processes (Powell et al. 2011). IMCs are important regulators of pathologic conditions such as inflammation, carcinogenesis, fibrosis and tissue repair (Pinchuk et al. 2010). Roulis et al. (2011) propose that IMCs are involved in the initiation of IBD via dysregulated expression of extracellular matrix remodeling mediators, as seen in $Tnf^{\Delta ARE/+}$ mice, a murine model of CD. Besides alteration of matrix deposition, Pinchuk et al. (2010) showed that IMCs may also cause IBD via upregulation of proinflammatory cytokines, disruption in the balance of inflammatory cells in the mucosa and dysregulated secretion of immunoregulatory mediators, thereby preventing resolution of acute inflammation.

Figure 10 [A] display a significant reduction of *Ptger4*-mRNA levels in IMCs derived from Enh-KO mice, indicating an important regulatory effect of the Ptger4-enhancer in IMCs. Altered expression patterns of EP4 and thus PGE_2-EP4 signaling caused by disease-associated genetic variants in the *Ptger4*-ehnacer region might lead to incorrect regulation of matrix remodeling mediator, cytokines or immunoregulatory mediators resulting in IBD

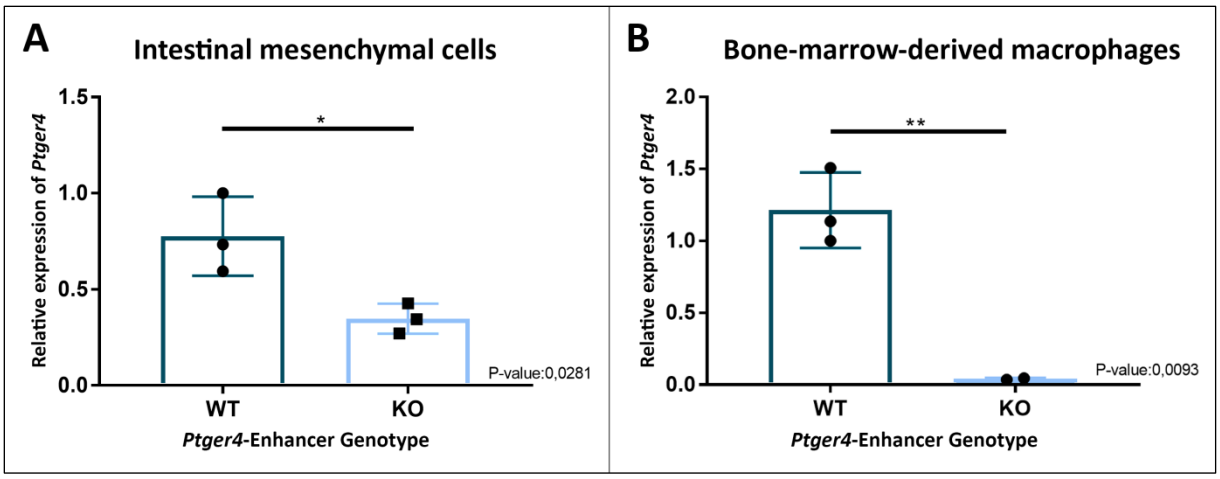

Figure 10: Relative expression levels of *Ptger4* in Enh-WT and KO-mice. [A] Intestinal mesenchymal cells (IMCs) **[B]** Bone-marrow-derived macrophages (BMDMs). Three technical replicates of IMCs and BMDMs per genotype; n=1 mouse per genotype

BMDMs are primary macrophage cells isolated from the bone marrow of adult mice. They differentiate *in vitro* from myeloid precursor cells in the presence of the M-CSF growth factor (macrophage colony-stimulating factor). BMDMs are a crucial component in innate and adaptive immune responses and are an excellent model for the study of innate immune mechanisms of colitis and host-microbial interactions in the intestine (Weischenfeldt and Porse 2008; Manzanero 2012). As displayed in Fig. 10[B], in BMDMs the *Ptger4* gene is strongly regulated by its enhancer. In the BMDMs derived from Enh-KO mice the expression of *Ptger4* is nearly undetectable at steady state. The IBD-association of the *Ptger4*-enahncer region found in GWAs might be connected to this pronounced effect of the enhancer in BMDMs leading to immune system dysfunction.

Intestinal organoids represent an *in vitro* multi-cellular, organotypic 3D culture system with strong physiological relevance to the adult intestine compared to conventional monolayer cell cultures. They not only consist of all cell types found in an adult intestinal epithelium (enterocytes, goblet cells, Paneth cells, enteroendocrine cells and stem cells) but also feature a polarized epithelium, a crypt-villus organization and a functional lumen. Moreover, intestinal organoids recapitulate most inter- and intra-epithelial cell dynamics that occur *in vivo* making them a powerful *in vitro* tool to the role of the intestinal epithelium in IBD. Intestinal cells are important for the host-microbiome interaction and represent the first line of pathogen defense, the mucosal barrier (Lukovac et al. 2014).

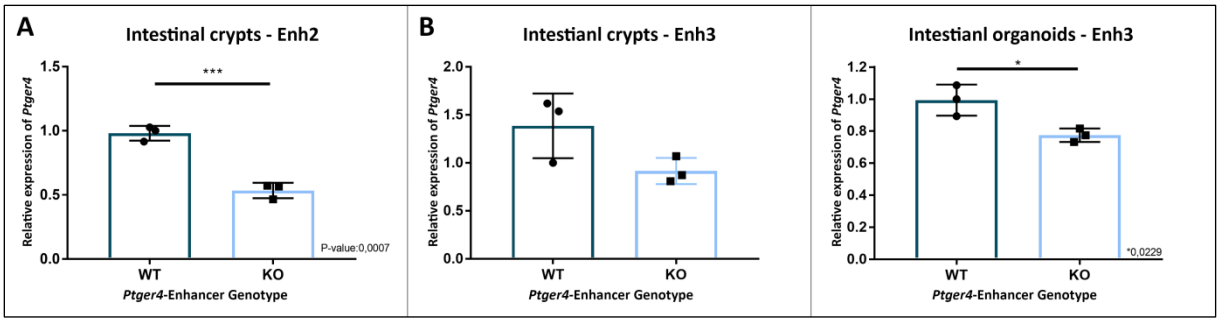

Figure 11: Relative expression levels of *Ptger4* in Enh-WT and KO-mice. [A] Intestinal crypts (experimental group 2) **[B]** Intestinal crypts and organoids (experimental group 3). Three technical replicates of organoids per genotype; n=1 mouse per genotype.

Figure 11[A] and [B] shows that ablation of the *Ptger4*-enhancer results in a significant decrease in the expression of *Ptger4* in intestinal crypts and organoids. The effect seems more pronounced in

organoids than in crypts derived from the same animal (see Fig. 11[B]). Since crypt samples always contain a certain percentage of debris and non-epithelial cells this result suggests that the enhancer is predominantly active in the intestinal epithelial cells. Moreover Fig. 11 also displays huge differences in the observed downregulation of *Ptger4* via its enhancer between individual mice. The reduction of *Ptger4*-transcription in crypts of the second experimental group is much more pronounced than in the crypts of the third experimental group, supporting the hypothesis of the intestinal microbiome as stimulator of the enhancer.

3.3 Possible microbial stimuli of the Ptger4-Enahncer

The mechanisms underlying IBD represent a complex interplay between genetic, environmental and intestinal microbial factors with the host immune system. It is believed that intestinal inflammation is caused by dysregualted auto-inflammatory immune responses triggered most likely by the intestinal microbiome and environmental factors, such as food particles or stress. To study the role of the gut microbiota in more detail, we decided to perform stimulation experiments with microbial factors (LPS- lipopolysaccharides) and the intestinal microbiome (germfree mice vs. conventional mice) to see if *Ptger4* expression is up – or downregulated.

3.3.1 LPS-stimulation experiment of BMDMs

Ostuni et al. (2013) showed that latent enhancers, defined as TF-unbound regions of the genome in terminally differentiated cells, can acquire histone marks (e.g. H3K27Ac, H3K4me1) of active enhancers and TF-binding in response to stimulation. In macrophages LPS-stimulation of toll-like-receptor 4 (TLR4) induced activation of latent enhancers trough cooperative binding of the TFs PU.1 and NF-κB (Kaikkonen et al. 2013). Lipopolysaccharides (LPS) are a component of the outer membrane of gram-negative bacteria and are able to stimulate the expression of the proinflammatory agent NF-κB as well as COX-2 and PGE-Synthases resulting in an upregulation of PGE_2-signaling (Simmons et al. 2004). The human *PTGER4*-gene contains several motifs responsive to proinflammatory agents such as IL-6, NF-κB and H-apf-1 in addition to a Y-box and activated activator protein-1 and -2 (AP-1, AP-2) binding sites (Foord et al. 1996). The murine *Ptger4* gene locus also features AP-1/2 sites and NF-κB and IL-6 elements but also contains a TATA box, and a glucocorticoid-responsive element (Arakawa et al. 1996). As IL-6 is rapidly upregulated after LPS-stimulation (see Fig. 13 [C]) and NF-κB is known to be activated in response to proinflammatory cytokines such as IL-6 and IL-1 (Li and Verma 2002), we expected an upregulation of *Ptger4* in LPS-stimulated BMDMs derived from Enh-WT, -HET and –KO mice as the gene region contains both NF-κB and IL-6 binding sites.

Figure 13[C] and Sup. Fig. 2[A] show that BMDMs off all three genetic backgrounds (Enh-WT, -HET and KO) responded fairly equal to the LPS-stimulation by a rapid upregulation of IL-6. The upregulation of *Ptger4*-transcription, however, differed significantly between the different genetic backgrounds. In BMDMs derived from an Enh-WT mouse the increase in the relative expression of *Ptger4* was the most pronounced and reached its peak after 1 hour of LPS-stimulation (see Fig. 13[A]). The Enh-KO BMDMs on the contrary showed only a small upregulation of Ptger4-expression (4-fold less than in Enh-WT) and time-delayed in comparison to the Enh-WT control since expression peaked after 3 hours of LPS-stimulation. BMDMs derived from an Enh-HET mouse displayed an intermediate phenotype with a less pronounced expression peak compared to Enh-WT-BMDMs (2-fold smaller) after 1 hour of stimulation. These significant differences in the response of Enh-WT and

–KO BMDMs to LPS-stimulation with regard to *Ptger4*-transcription (see Fig. 13[B]) indicate that the *Ptger4*-enhancer can be stimulated by microbial components like LPS. This represents a link between the immune system and the intestinal microbiota that might malfunction in case of pathologically changed PGE_2-EP4 signaling resulting in overactive, proinflammatory macrophages.

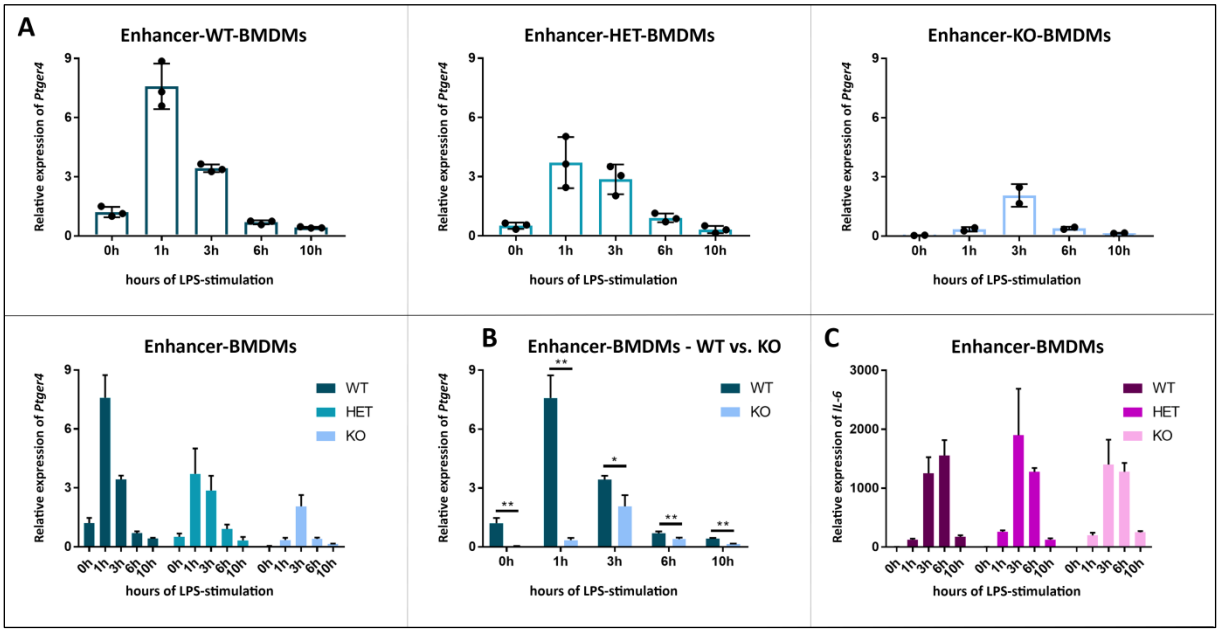

Figure 12: LPS-stimulation of bone-marrow derived macrophages (BMDMs) derived from Enh-WT, -HET and –KO mice. **[A]** Upregulation of Ptger4 expression in response to the stimulation in Enh-WT, -HET and –KO BMDMS. **[B]** The upregulation of Ptger4 is significantly lower in Enh-KO mice compared to Enh-WT mice. **[C]** Upregulation of IL-6 levels in response to LPS-stimulation in Enh-WT, -HET and –KO mice. Three technical replicates per timepoint for Enh-WT and –HET BMDMs, and two technical replicates per timepoint for Enh-KO BMDMs. n= 1 mouse per genotype.

Although Enh-KO BMDMs feature a delayed upregulation of Ptger4-expression in response to LPS-stimulation they are still able to increase transcription rates, suggesting that activated TFs not exclusively bind to the *Ptger4*-enhancer region but also to other regulatory elements of the *Ptger4* gene. Since IL-6 reaches its expression peak after 3 hours of LPS-stimulation it is a likely candidate to interact with its binding site in the *Ptger4* gene locus in mice. Also NF-κB most probably interacts with the NF-κB element in the *Ptger4* gene locus (Arakawa et al. 1996). Nevertheless, our results indicate that the *Ptger4*-enhancer is an important region for the interaction of the *Ptger4* gene with microbial factors as upregulation is the strongest in BMDMs derived from Enh-WT mice featuring two alleles with intact *Ptger4*-enhancer regions. A bioinformatic analysis of possible TF-binding sites in the enhancer region would shed some light on the possible stimulating molecules involved in the observed upregulation of *Ptger4.*

3.3.2 Ptger4 expression in germ-free and conventional mice

To see if the intestinal microbiome plays a role in the regulation of *Ptger4* expression in general, we analyzed gene expression in terminal Ileum and distal colon samples of germ-free and conventional mice. As shown in Fig. 9[A] Ptger4 is predominantly expressed in the small intestine and distal colon in mice (UniProt: a worldwide hub of protein knowledge 2019), therefore we expected the effect of bacteria on gene expression to be the most pronounced in these tissues. The germ-free mice show no tissue-specific expression of Ptger4 (see Fig. 14[A]) as transcription levels are about the same in the terminal ileum and the distal colon. In conventional mice (germ-free mice gavaged with Enh-WT

feces), however, *Ptger4* expression is significantly lower in the distal colon, suggesting a repressive effect of the colonic microflora on *Ptger4* expression (see Fig. 14[B]). The comparison of germ-free with conventional mice revealed that the microbiota of the GI-tract strongly regulates Ptger4-expression, resulting in a significant decrease of *Ptger4*-transcription in terminal ileum and distal colon of conventional mice (see Fig. 14[C]).

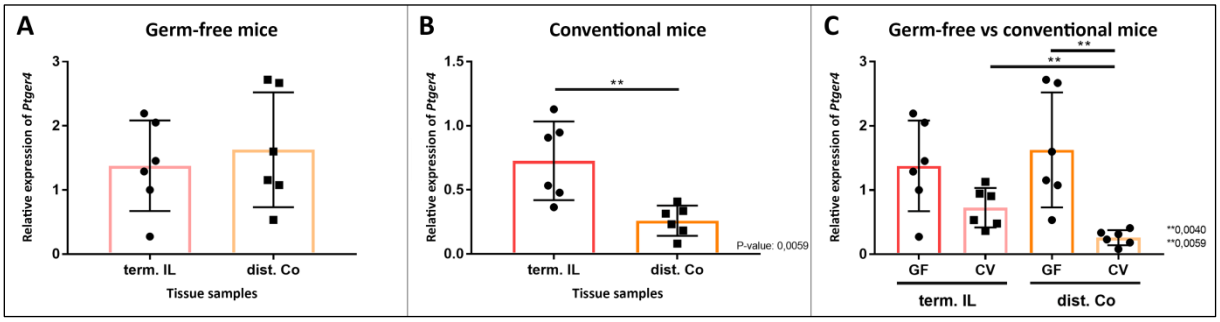

Figure 13: Expression of *Ptger4* in terminal ileum and distal colon of germ-free and conventional mice. [A] Germ-free mice, **[B]** conventional mice and **[C]** comparison of germ-free and conventional mice. Ptger4-expression is downregulated in terminal ileum and colon of conventional mice. n=6 mice per group, *p-value <0.05; **p-value >0.001

These results implicate that an increase of PGE_2-EP4 signaling due to the IBD-associated risk variants in the *Ptger4*-enhancer may be caused by repeal of transcription-suppression mediated by the intestinal microbiome.

3.4 The roleof the Ptger4-Enhancer in two colitis model

3.4.1 Chemically-induced dextran sodium sulfate (DSS)-model

Dextran sodium sulfate (DSS) is a water-soluble, negatively charged sulfated polysaccharide with anticoagulant properties and is used for the chemical induction of experimental colitis in mice. This model of colitis mimics clinical and histopathological features of human IBD, in particular of ulcerative colitis (UC). Although the exact mechanisms by which DSS causes inflammation of the intestinal mucosa are not fully understood, it is generally accepted that DSS toxicity leads to the destruction of the intestinal epithelial monolayer, resulting in the loss of its barrier function. The associated increase in mucosal permeability allows microbial entry into the intestinal mucosa and thus exposes cells of the lamina propria to luminal antigens and microorganisms, causing acute local inflammation. The inflammatory responses are mainly based on the activation and infiltration of neutrophils, macrophages and lymphocytes into the colon. Furthermore, an increased production of proinflammatory mediators can be observed not only by immune cells but also by epithelial cells. It is believed that these inflammatory responses cause further epithelial degeneration as well as ulceration and necrosis (Eichele and Kharbanda 2017; Yan et al. 2009).

DSS-Colitis was induced in Enhancer-WT and –KO mice to investigate, if the loss of the *Ptger4*-enhancer region and associated reduction in EP4 expression affect the course of the disease. As seen in Figure 15[A] the DSS-concentration of 1.5% (w/v) was too low to induce severe colitis in any of the male Enhancer mice. In the female mice, however, the expected weight loss was observed as displayed in Figure 15[B]. Although DSS concentration, duration of DSS-administration as well as DSS-manufacturer and batch were exactly the same differences in the respond are clearly visible between sexes. The composition of the intestinal microbiome might vary between sexes and also the initial

weight at the start of the experiment can be decisive for onset and severity of colitis (Perše and Cerar 2012).

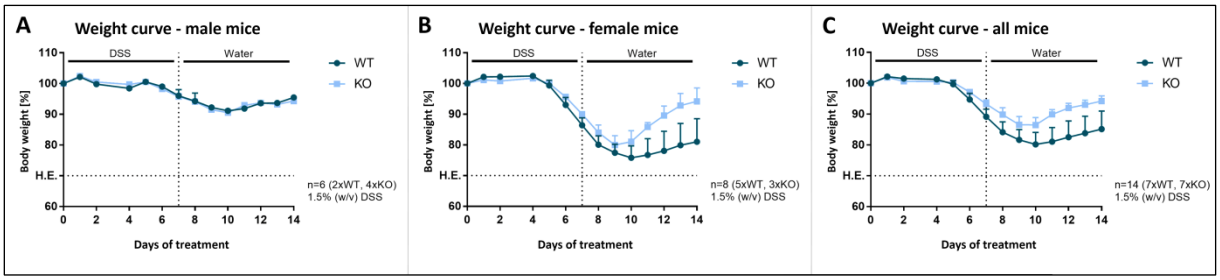

Figure 14: Enhancer-KO mice perform better in chemically induced DSS-model of colitis. Male **[A]** and female **[B]** Enhancer-WT and –KO mice were administered to 1.5% (w/v) DSS by drinking water for 7 days. **[C]** Weight curve of all animals (female + male). Two independent experiments with >6 mice per genotype were performed. Body weight changes are depicted as means ± SEM**.**

In Figure 15[B] it is also shown that Enh-KO mice perform considerably better in this colitis model compared to their WT-littermate-controls. Their weight loss is less severe and they also start to gain weight one day earlier and faster than the WT-mice. Both groups started to significantly lose weight around day 5 of DSS-treatment and continue to lose weight until day 9 (KO) or day 10 (WT) respectively. Following day 9/10 the mice stared to gain weight and the KO-mice nearly reached their initial body weight (~95% of initial weight) at the end of the experiment, whereas the end weight of the WT-mice was around 85% of the initial body weight.

This result would indicate a deleterious, proinflammatory role of the PGE_2-EP4 signaling pathway in inflammatory disorders of the GI-tract. This contradicts the findings of Kabashima et al. (2002), who proposed a beneficial effect of EP4 on colitis course. They showed that EP4-deficient mice developed exacerbated colitis, whereas WT-mice only feature marginal colitis. The phenotype was mimicked in WT-mice using EP4-selective antagonists (AE3-208). However, given the absence of littermate controls and the mixed genetic background of the mice (129/Ola x C57BL/6) to ensure their survival (incomplete closure of the ductus arteriosus) (Chang et al. 2010), might have biased the results.

Further DSS-colitis with higher DSS-concentration (probably 2% DSS (w/v)) will be necessary to validate the deleterious effect of PGE_2-EP4 signaling on the colitis course observed in our experiment.

3.4.2 T-cell dependent transfer colitis model

The T-cell transfer model of chronic colitis is based on the transfer of naïve $CD4^+$ $CD45RB^{high}$-T-cells from healthy mice into immunocompromised mice. The animals develop autoimmune colitis due to the homeostatic expansion of the donor T-cells and the associated inflammatory responses to the microbiome and self-antigens of the host animal. A large number of naïve T-cell convert into pathogenic effector T-cells (mainly T_h1- and T_h17-cells) that produced proinflammatory cytokines like INF-γ, IL-12, IL-17 and IL-23. Disease-attenuating regulatory T-cells (T_{reg}), however, are generated very rarely or not at all.

This widely used transfer colitis model mimics many aspects of human IBD pathology, in particular of Crohn's disease, such as intestinal hyperplasia, abnormal crypt morphology, goblet cell depletion, transmural inflammation and ulcers, and infiltration of inflammatory cells (mostly lymphocytes and macrophages). It is a useful tool to understand immunopathological and immunoregulatory

mechanisms of chronic intestinal inflammation by studying the role of causative effector T-cells and suppressive regulatory T-cells (Reinoso Webb et al. 2018; Chen et al. 2016).

For the T-cell dependent model of colitis, effector T-cells ($CD4^+$, $CD45RB^{high}$) from Enh-WT- and KO mice were isolated, purified and transferred to recombinase activating gene-deficient ($RAG^{-/-}$) recipient mice. The mice were monitored and evaluated for colitis progression for 10 subsequent weeks after transfer. The experiment was conducted to see whether the knock-out of the Ptger4-enhancer region in the transferred T-cells alters the onset and severity of induced colitis by interfering of PGE_2-EP4 signaling with phenotype and pathogenic potential of the T-cells.

As seen in Figure 16[A]-[C] the body weight of both $RAG^{-/-}$ that received Enh-WT effector T-cells and those that received Enh-KO effector T-cells showed no changes until week 4. While the Enh-KO group featured little to no weight loss, the mice that received Enh-WT effector T-cells displayed significant loss of body weight of up to 15-20% of the initial weight. The decrease in body weight between Enh-WT and Enh-KO group was more pronounced at the latter phases of disease and in the male $RAG^{-/-}$ mice, indicating that male animals are more susceptible for this model of colitis. Overall, the differences in body weight loss were significant between Enh-KO and –WT groups at week 8 and 9 after T-cell transfer (Fig. 16[C]).

The observed variation in the body weight curves are reflected in the endoscopy scores. In general, the Enh-WT group of $RAG^{-/-}$ mice showed a higher endoscopy score than the Enh-KO group, with a significant difference at week 10 post transfer in the male mice. The mice of the Enh-KO group largely showed normal blood vessel structure, a smooth and translucent mucosal surface and solid stool. In contrast, the Enh-WT mice showed multiple signs of mucosal inflammation such as thickened intestinal wall (less translucent), bleeding, loss of normal blood vessel architecture and diarrhea.

Our results support a proinflammatory, colitogenic role of PGE_2-EP4 signaling in this colitis model. This is consistent with the findings of Maseda et al. (2018), who showed that $CD4^+$ effector T-cells either deficient in mPGES-1 or EP4 are less colitogenic in immunodeficient mice. The reduction in colitogenicity was associated with an increase in $CD4^+ROR\gamma t^+$ cells (T_h17-cells) in the lamina propria.

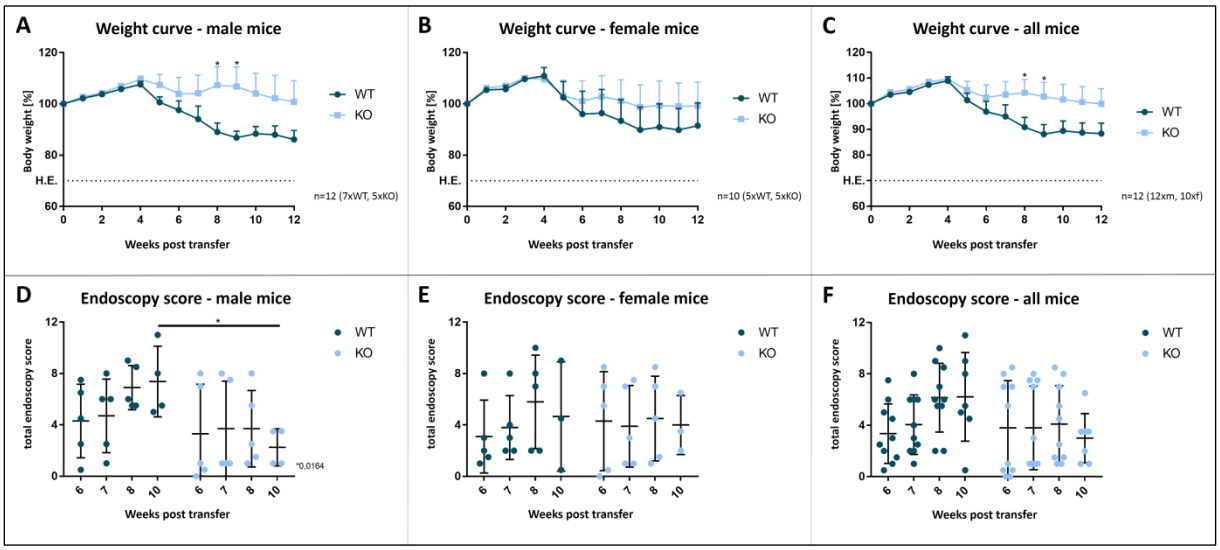

Figure 15: Immune-deficient $Rag^{-/-}$ mice recipients of Enh-KO effector T-cells perform better in the T-cell dependent transfer colitis model. Body weight curves of **[A]** male mice, **[B]** female mice and **[C]** all mice (male + female animals).

Endoscopy score of **[D]** male mice, **[E]** female mice and **[F]** all mice. Body weight changes are depicted as means ± SEM. *p-value <0.05

To investigate if the attenuation of colitis observed in the Enh-KO group was also due to an altered phenotype of the transferred T-cells, we analyzed proinflammatory phenotypes of T-cells isolated from colon samples via flow cytometry: INF-γ-expressing T_h1 cells, IL-17-expressing T_h17 cells and strongly proinflammatory T-cells expressing both cytokines (see Fig. 17[A]). As displayed in Fig. 17 [B-D] the flow cytometry analysis revealed a significant increase of IL-17 expressing T-cells in the $RAG^{-/-}$ mice that received Enh-KO effector T-cells. Our results are consistent with the T-cell phenotype distribution observed in mPGES-1 deficient T-cell transfer colitis experiment performed by Maseda et al. (2018). Furthermore, INF-γ expressing T-cells and strong proinflammatory T-cells expressing both IL-17 and INFγ were slightly down-regulated in the Enh-KO group. Our results suggest that PGE_2-signaling via EP4 influences expansion of T-cell phenotypes resulting in a shift towards IL-17 expressing T-cells. The role of T_h17 cells in IBD is controversial; they can either enhance protective immune responses and accelerate epithelial regeneration or mediate inflammation by overexpression of proinflammatory cytokines such as IL-17 and IL-23. Further experimental analyses of the role of T_h17-cells in inflammatory disorders of the bowel have to be performed to clarify the precise effect of this T-cell subpopulation.

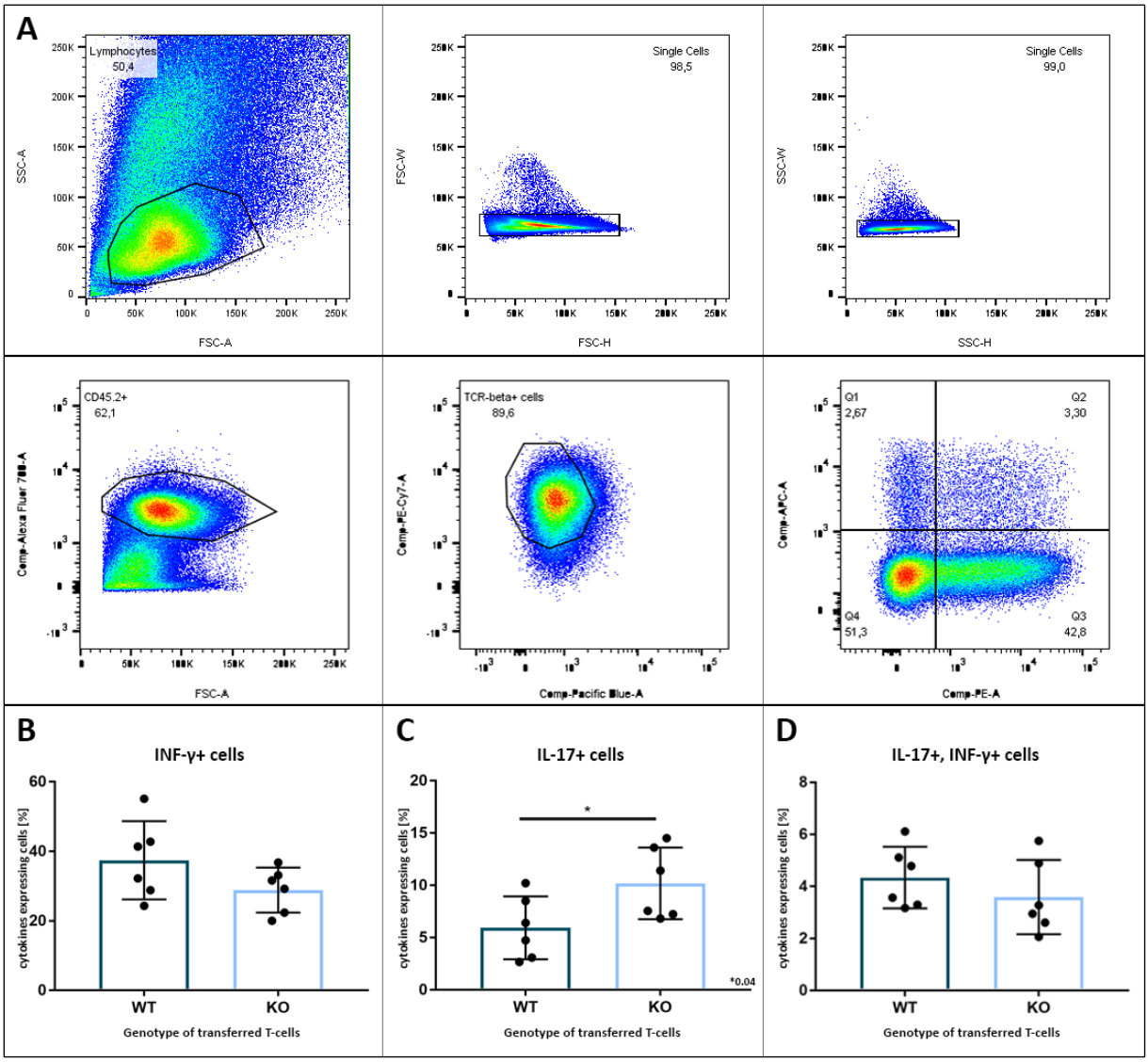

Figure 16 Flow cytometry analysis of T-cell phenotypes isolated from colon samples of T-cell recipient mice in the transfer colitis model. [A] Flow cytometer gating strategy: Living cells → single cells → transferred T-cells (CD45.2$^+$)→ effector T-cells (TCR-beta, CD4$^+$ cells) → proinflammatory T-cells (INF-γ, IL-17 expressing cells) **[B]** INF-γ expressing T-**cells [C]** IL-17 expressing T-cells **[D]** INF-γ, IL-17 expressing T-cells. *p-value <0.05

3.4.3 Role of the Ptger4-enhancer in the development of T-cells

The transfer colitis experiment showed that the *Ptger4*-enhancer plays an important part in expansion of specific T-cell subpopulation. Also expression analysis of *Ptger4* in thymus samples indicated a pronounced effect of the enhancer in T-cell development and differentiation (see Fig. 11[C]). Therefore, we started a pilot experiment to investigate the effect of the Ptger4-enhancer on early stages of T-cell development in the thymus. The thymus is a primary lymphatic organ of the immune system. Within the thymus, the thymocytes mature sequentially into naïve T-cells expressing specific surface proteins according to their stage of development (CD44$^+$ →CD44$^+$ CD25$^+$ → CD25$^+$ → double-negative cells) (Famili et al. 2017; Simons and Caton 2011).

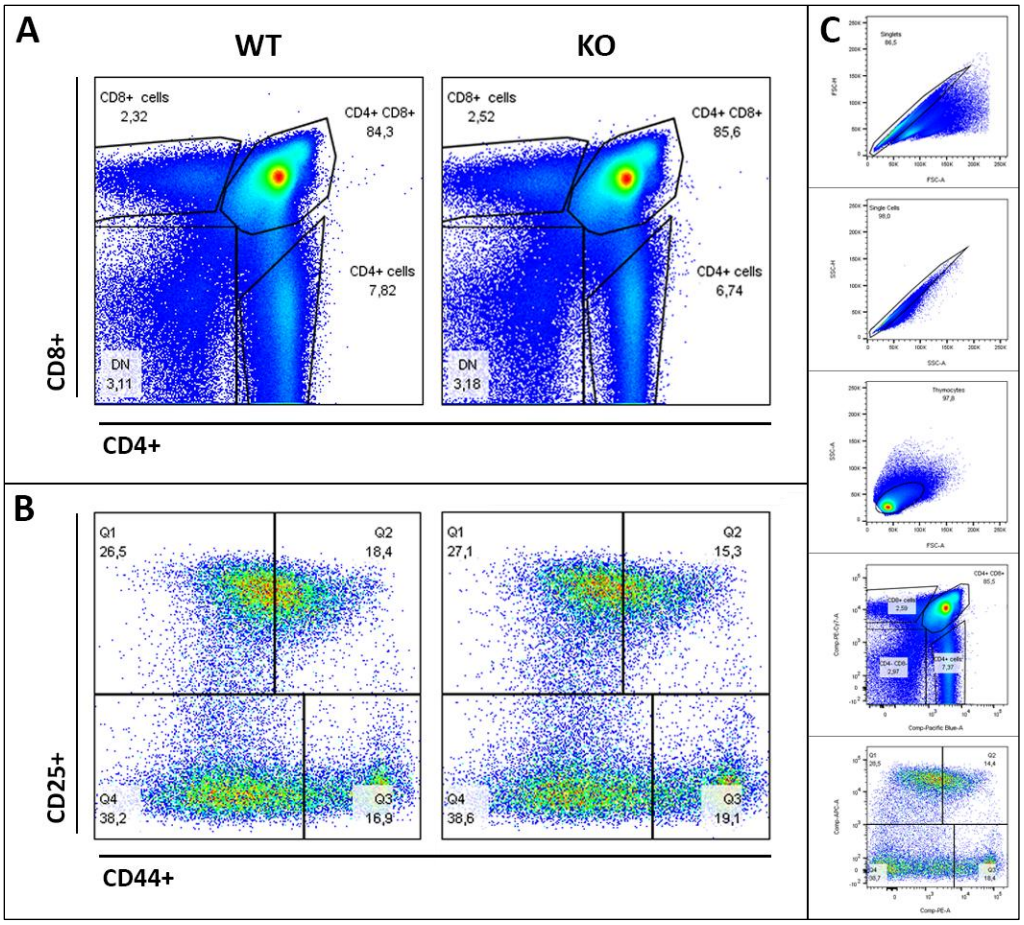

Figure 17: Flow cytometry analysis of early developmental stages of T-cell in Enh-WT and Enh–KO mice. [A] naïve T-cell populations **[B]** early stages of T-cell development **[C]]** Flow cytometer gating strategy: Living cells → single cells → thymocytes→naïve T-cell populations ($CD4^+$ cells, $CD8^+$ cells, DP cells, DN cells) → early developmental stages ($CD44^+$ cells, DP cells, $CD25^+$ cells, DN cells)

As displayed in Fig. 18 [A-B] and Tab. 2 the Ptger4-enhancer has no effect on early T-cell development. No significant differences are visible in thymus samples derived from Enh-WT and Enh-KO mice. To validate this result further investigation of T-cell development (thymus) and differentiation (T-cell differentiation experiment – Spleen, LNs) are necessary.

Table 2: Early stages of T-cell development in Enh-WT and Enh-KO mice.

Freq.of Parent	Q1 (DN3): CD25+, CD44-/lo	Q2 (DN2): CD25+, CD44+	Q3 (DN1): CD25-, CD44+	Q4 (DN4): CD25-, CD44-/lo
Thymus_KO_002.fcs	28,5 %	14,4 %	18,4 %	38,7 %
Thymus_WT_001.fcs	27,8 %	17,8 %	16,3 %	38,1 %
Count				
Thymus_KO_002.fcs	8268	4185	5352	11231
Thymus_WT_001.fcs	8133	5200	4751	11120

4 Publication bibliography

Altshuler, David; Daly, Mark J.; Lander, Eric S. (2008): Genetic mapping in human disease. In *Science (New York, N.Y.)* 322 (5903), pp. 881–888. DOI: 10.1126/science.1156409.

Arakawa, T.; Laneuville, O.; Miller, C. A.; Lakkides, K. M.; Wingerd, B. A.; DeWitt, D. L.; Smith, W. L. (1996): Prostanoid receptors of murine NIH 3T3 and RAW 264.7 cells. Structure and expression of the murine prostaglandin EP4 receptor gene. In *The Journal of biological chemistry* 271 (47), pp. 29569–29575. DOI: 10.1074/jbc.271.47.29569.

Basu, Dhiman; Lopez, Ivelisse; Kulkarni, Aparna; Sellin, Joseph H. (2005): Impact of race and ethnicity on inflammatory bowel disease. In *The American journal of gastroenterology* 100 (10), pp. 2254–2261. DOI: 10.1111/j.1572-0241.2005.00233.x.

Becker, C.; Fantini, M. C.; Neurath, M. F. (2006): High resolution colonoscopy in live mice. In *Nature protocols* 1 (6), pp. 2900–2904. DOI: 10.1038/nprot.2006.446.

Bos, Johannes L. (2003): Epac: a new cAMP target and new avenues in cAMP research. In *Nature reviews. Molecular cell biology* 4 (9), pp. 733–738. DOI: 10.1038/nrm1197.

Brant, Steven R.; Okou, David T.; Simpson, Claire L.; Cutler, David J.; Haritunians, Talin; Bradfield, Jonathan P. et al. (2017): Genome-Wide Association Study Identifies African-Specific Susceptibility Loci in African Americans With Inflammatory Bowel Disease. In *Gastroenterology* 152 (1), 206-217.e2. DOI: 10.1053/j.gastro.2016.09.032.

Brückner, Markus; Lenz, Philipp; Nowacki, Tobias M.; Pott, Friederike; Foell, Dirk; Bettenworth, Dominik (2014): Murine endoscopy for in vivo multimodal imaging of carcinogenesis and assessment of intestinal wound healing and inflammation. In *Journal of visualized experiments : JoVE* (90). DOI: 10.3791/51875.

Buchanan, F. Gregory; Gorden, D. Lee; Matta, Pranathi; Shi, Qiong; Matrisian, Lynn M.; DuBois, Raymond N. (2006): Role of beta-arrestin 1 in the metastatic progression of colorectal cancer. In *Proceedings of the National Academy of Sciences of the United States of America* 103 (5), pp. 1492–1497. DOI: 10.1073/pnas.0510562103.

Bulger, Michael; Groudine, Mark (2011a): Functional and mechanistic diversity of distal transcription enhancers. In *Cell* 144 (3), pp. 327–339. DOI: 10.1016/j.cell.2011.01.024.

Bulger, Michael; Groudine, Mark (2011b): Functional and mechanistic diversity of distal transcription enhancers. In *Cell* 144 (3), pp. 327–339. DOI: 10.1016/j.cell.2011.01.024.

Chang, Hee-Yoon; Locker, Joseph; Lu, Run; Schuster, Victor L. (2010): Failure of postnatal ductus arteriosus closure in prostaglandin transporter-deficient mice. In *Circulation* 121 (4), pp. 529–536. DOI: 10.1161/CIRCULATIONAHA.109.862946.

Chassaing, Benoit; Aitken, Jesse D.; Malleshappa, Madhu; Vijay-Kumar, Matam (2014): Dextran sulfate sodium (DSS)-induced colitis in mice. In *Current protocols in immunology* 104, Unit 15.25. DOI: 10.1002/0471142735.im1525s104.

Chen, Yu-Ling; Chen, Yi-Ting; Lo, Cheng-Feng; Hsieh, Ching-I; Chiu, Shang-Yi; Wu, Chang-Yen et al. (2016): Early Detection of T cell Transfer-induced Autoimmune Colitis by In Vivo Imaging System. In *Scientific reports* 6, p. 35635. DOI: 10.1038/srep35635.

Cho, Judy H.; Brant, Steven R. (2011): Recent insights into the genetics of inflammatory bowel disease. In *Gastroenterology* 140 (6), pp. 1704–1712. DOI: 10.1053/j.gastro.2011.02.046.

Corradin, Olivia; Scacheri, Peter C. (2014): Enhancer variants: evaluating functions in common disease. In *Genome medicine* 6 (10), p. 85. DOI: 10.1186/s13073-014-0085-3.

Creyghton, Menno P.; Cheng, Albert W.; Welstead, G. Grant; Kooistra, Tristan; Carey, Bryce W.; Steine, Eveline J. et al. (2010): Histone H3K27ac separates active from poised enhancers and predicts developmental state. In *Proceedings of the National Academy of Sciences of the United States of America* 107 (50), pp. 21931–21936. DOI: 10.1073/pnas.1016071107.

Das, Srustidhar; Batra, Surinder; Rachagani, Satyanarayana (2017): Mouse Model of Dextran Sodium Sulfate (DSS)-induced Colitis. In *BIO-PROTOCOL* 7 (16). DOI: 10.21769/BioProtoc.2515.

Dekker, Job; Mirny, Leonid (2016): The 3D Genome as Moderator of Chromosomal Communication. In *Cell* 164 (6), pp. 1110–1121. DOI: 10.1016/j.cell.2016.02.007.

Desai, Snehal; Ashby, Barrie (2001): Agonist-induced internalization and mitogen-activated protein kinase activation of the human prostaglandin EP4 receptor. In *FEBS Letters* 501 (2-3), pp. 156–160. DOI: 10.1016/s0014-5793(01)02640-0.

Duchmann, R.; Kaiser, I.; Hermann, E.; Mayet, W.; Ewe, K.; Zum Meyer Büschenfelde, K. H. (1995): Tolerance exists towards resident intestinal flora but is broken in active inflammatory bowel disease (IBD). In *Clinical and experimental immunology* 102 (3), pp. 448–455. DOI: 10.1111/j.1365-2249.1995.tb03836.x.

Duerr, Richard H.; Taylor, Kent D.; Brant, Steven R.; Rioux, John D.; Silverberg, Mark S.; Daly, Mark J. et al. (2006): A genome-wide association study identifies IL23R as an inflammatory bowel disease gene. In *Science (New York, N.Y.)* 314 (5804), pp. 1461–1463. DOI: 10.1126/science.1135245.

Edwards, Stacey L.; Beesley, Jonathan; French, Juliet D.; Dunning, Alison M. (2013): Beyond GWASs: illuminating the dark road from association to function. In *American journal of human genetics* 93 (5), pp. 779–797. DOI: 10.1016/j.ajhg.2013.10.012.

Eichele, Derrick D.; Kharbanda, Kusum K. (2017): Dextran sodium sulfate colitis murine model: An indispensable tool for advancing our understanding of inflammatory bowel diseases pathogenesis. In *World journal of gastroenterology* 23 (33), pp. 6016–6029. DOI: 10.3748/wjg.v23.i33.6016.

Ellinghaus, David; Jostins, Luke; Spain, Sarah L.; Cortes, Adrian; Bethune, Jörn; Han, Buhm et al. (2016): Analysis of five chronic inflammatory diseases identifies 27 new associations and highlights disease-specific patterns at shared loci. In *Nature genetics* 48 (5), pp. 510–518. DOI: 10.1038/ng.3528.

Ephgrave, Kimberly (2007): Extra-intestinal manifestations of Crohn's disease. In *The Surgical clinics of North America* 87 (3), pp. 673–680. DOI: 10.1016/j.suc.2007.03.003.

Eurogentec (2008): qPCR guide. Eurogentec. Available online at www.eurogentec.com, checked on 8/30/2019.

Famili, Farbod; Wiekmeijer, Anna-Sophia; Staal, Frank Jt (2017): The development of T cells from stem cells in mice and humans. In *Future science OA* 3 (3), FSO186. DOI: 10.4155/fsoa-2016-0095.

Farh, Kyle Kai-How; Marson, Alexander; Zhu, Jiang; Kleinewietfeld, Markus; Housley, William J.; Beik, Samantha et al. (2015): Genetic and epigenetic fine mapping of causal autoimmune disease variants. In *Nature* 518 (7539), pp. 337–343. DOI: 10.1038/nature13835.

Felder, J. B.; Korelitz, B. I.; Rajapakse, R.; Schwarz, S.; Horatagis, A. P.; Gleim, G. (2000): Effects of nonsteroidal antiinflammatory drugs on inflammatory bowel disease: a case-control study. In *The American journal of gastroenterology* 95 (8), pp. 1949–1954. DOI: 10.1111/j.1572-0241.2000.02262.x.

Foord, S. M.; Marks, B.; Stolz, M.; Bufflier, E.; Fraser, N. J.; Lee, M. G. (1996): The structure of the prostaglandin EP4 receptor gene and related pseudogenes. In *Genomics* 35 (1), pp. 182–188. DOI: 10.1006/geno.1996.0337.

Friis, Ulla G.; Stubbe, Jane; Uhrenholt, Torben R.; Svenningsen, Per; Nüsing, Rolf M.; Skøtt, Ole; Jensen, Boye L. (2005): Prostaglandin E2 EP2 and EP4 receptor activation mediates cAMP-dependent hyperpolarization and exocytosis of renin in juxtaglomerular cells. In *American journal of physiology. Renal physiology* 289 (5), F989-97. DOI: 10.1152/ajprenal.00201.2005.

Fujino, S.; Andoh, A.; Bamba, S.; Ogawa, A.; Hata, K.; Araki, Y. et al. (2003): Increased expression of interleukin 17 in inflammatory bowel disease. In *Gut* 52 (1), pp. 65–70. DOI: 10.1136/gut.52.1.65.

Geremia, Alessandra; Jewell, Derek P. (2012): The IL-23/IL-17 pathway in inflammatory bowel disease. In *Expert review of gastroenterology & hepatology* 6 (2), pp. 223–237. DOI: 10.1586/egh.11.107.

Goessling, Wolfram; North, Trista E.; Loewer, Sabine; Lord, Allegra M.; Lee, Sang; Stoick-Cooper, Cristi L. et al. (2009): Genetic interaction of PGE2 and Wnt signaling regulates developmental specification of stem cells and regeneration. In *Cell* 136 (6), pp. 1136–1147. DOI: 10.1016/j.cell.2009.01.015.

Gupta, R. A.; Dubois, R. N. (2001): Colorectal cancer prevention and treatment by inhibition of cyclooxygenase-2. In *Nature reviews. Cancer* 1 (1), pp. 11–21. DOI: 10.1038/35094017.

Ha, Francis; Khalil, Hanan (2015): Crohn's disease: a clinical update. In *Therapeutic advances in gastroenterology* 8 (6), pp. 352–359. DOI: 10.1177/1756283X15592585.

Haas, Kelly; Rubesova, Erika; Bass, Dorsey (2016): Role of imaging in the evaluation of inflammatory bowel disease: How much is too much? In *World journal of radiology* 8 (2), pp. 124–131. DOI: 10.4329/wjr.v8.i2.124.

Hanna, Violette Said; Hafez, Ebtisam Abdel Aziz (2018): Synopsis of arachidonic acid metabolism: A review. In *Journal of advanced research* 11, pp. 23–32. DOI: 10.1016/j.jare.2018.03.005.

Hazan-Eitan, Zahit; Weinstein, Yacob; Hadad, Nurit; Konforty, Aviva; Levy, Rachel (2006): Induction of Fc gammaRIIA expression in myeloid PLB cells during differentiation depends on cytosolic phospholipase A2 activity and is regulated via activation of CREB by PGE2. In *Blood* 108 (5), pp. 1758–1766. DOI: 10.1182/blood-2006-05-021881.

Homer, Craig R.; Richmond, Amy L.; Rebert, Nancy A.; Achkar, Jean-Paul; McDonald, Christine (2010): ATG16L1 and NOD2 interact in an autophagy-dependent antibacterial pathway implicated in Crohn's disease pathogenesis. In *Gastroenterology* 139 (5), 1630-41, 1641.e1-2. DOI: 10.1053/j.gastro.2010.07.006.

Hristovska, Ana-Marija; Rasmussen, Lasse E.; Hansen, Pernille B. L.; Nielsen, Susan S.; Nüsing, Rolf M.; Narumiya, Shuh et al. (2007): Prostaglandin E2 induces vascular relaxation by E-prostanoid 4 receptor-mediated activation of endothelial nitric oxide synthase. In *Hypertension (Dallas, Tex. : 1979)* 50 (3), pp. 525–530. DOI: 10.1161/HYPERTENSIONAHA.107.088948.

Huang, Hailiang; Fang, Ming; Jostins, Luke; Umićević Mirkov, Maša; Boucher, Gabrielle; Anderson, Carl A. et al. (2017): Fine-mapping inflammatory bowel disease loci to single-variant resolution. In *Nature* 547 (7662), pp. 173–178. DOI: 10.1038/nature22969.

Huang, Steven K.; White, Eric S.; Wettlaufer, Scott H.; Grifka, Heather; Hogaboam, Cory M.; Thannickal, Victor J. et al. (2009): Prostaglandin E(2) induces fibroblast apoptosis by modulating

multiple survival pathways. In *FASEB journal : official publication of the Federation of American Societies for Experimental Biology* 23 (12), pp. 4317–4326. DOI: 10.1096/fj.08-128801.

Hugot, J. P.; Chamaillard, M.; Zouali, H.; Lesage, S.; Cézard, J. P.; Belaiche, J. et al. (2001): Association of NOD2 leucine-rich repeat variants with susceptibility to Crohn's disease. In *Nature* 411 (6837), pp. 599–603. DOI: 10.1038/35079107.

Hull, Mark A.; Ko, Stanley C. W.; Hawcroft, Gillian (2004): Prostaglandin EP receptors: targets for treatment and prevention of colorectal cancer? In *Molecular cancer therapeutics* 3 (8), pp. 1031–1039.

Huyghe, Jeroen R.; Bien, Stephanie A.; Harrison, Tabitha A.; Kang, Hyun Min; Chen, Sai; Schmit, Stephanie L. et al. (2019): Discovery of common and rare genetic risk variants for colorectal cancer. In *Nature genetics* 51 (1), pp. 76–87. DOI: 10.1038/s41588-018-0286-6.

Iida, Tomoya; Yokoyama, Yoshihiro; Wagatsuma, Kohei; Hirayama, Daisuke; Nakase, Hiroshi (2018): Impact of Autophagy of Innate Immune Cells on Inflammatory Bowel Disease. In *Cells* 8 (1). DOI: 10.3390/cells8010007.

Jostins, Luke; Ripke, Stephan; Weersma, Rinse K.; Duerr, Richard H.; McGovern, Dermot P.; Hui, Ken Y. et al. (2012a): Host-microbe interactions have shaped the genetic architecture of inflammatory bowel disease. In *Nature* 491 (7422), pp. 119–124. DOI: 10.1038/nature11582.

Jostins, Luke; Ripke, Stephan; Weersma, Rinse K.; Duerr, Richard H.; McGovern, Dermot P.; Hui, Ken Y. et al. (2012b): Host-microbe interactions have shaped the genetic architecture of inflammatory bowel disease. In *Nature* 491 (7422), pp. 119–124. DOI: 10.1038/nature11582.

Kabashima, Kenji; Saji, Tomomi; Murata, Takahiko; Nagamachi, Miyako; Matsuoka, Toshiyuki; Segi, Eri et al. (2002): The prostaglandin receptor EP4 suppresses colitis, mucosal damage and CD4 cell activation in the gut. In *The Journal of clinical investigation* 109 (7), pp. 883–893. DOI: 10.1172/JCI14459.

Kaikkonen, Minna U.; Spann, Nathanael J.; Heinz, Sven; Romanoski, Casey E.; Allison, Karmel A.; Stender, Joshua D. et al. (2013): Remodeling of the enhancer landscape during macrophage activation is coupled to enhancer transcription. In *Molecular cell* 51 (3), pp. 310–325. DOI: 10.1016/j.molcel.2013.07.010.

Kalinski, Pawel (2012): Regulation of immune responses by prostaglandin E2. In *Journal of immunology (Baltimore, Md. : 1950)* 188 (1), pp. 21–28. DOI: 10.4049/jimmunol.1101029.

Kaufmann, H. J.; Taubin, H. L. (1987): Nonsteroidal anti-inflammatory drugs activate quiescent inflammatory bowel disease. In *Annals of internal medicine* 107 (4), pp. 513–516. DOI: 10.7326/0003-4819-107-4-513.

Khor, Bernard; Gardet, Agnès; Xavier, Ramnik J. (2011): Genetics and pathogenesis of inflammatory bowel disease. In *Nature* 474 (7351), pp. 307–317. DOI: 10.1038/nature10209.

Kirsner, J. B. (2001): Historical origins of current IBD concepts. In *World journal of gastroenterology* 7 (2), pp. 175–184. DOI: 10.3748/wjg.v7.i2.175.

Kobayashi, Koichi S.; Chamaillard, Mathias; Ogura, Yasunori; Henegariu, Octavian; Inohara, Naohiro; Nuñez, Gabriel; Flavell, Richard A. (2005): Nod2-dependent regulation of innate and adaptive immunity in the intestinal tract. In *Science (New York, N.Y.)* 307 (5710), pp. 731–734. DOI: 10.1126/science.1104911.

Kodani, Tomohiro; Rodriguez-Palacios, Alex; Corridoni, Daniele; Lopetuso, Loris; Di Martino, Luca; Marks, Brian et al. (2013): Flexible colonoscopy in mice to evaluate the severity of colitis and colorectal tumors using a validated endoscopic scoring system. In *Journal of visualized experiments : JoVE* (80), e50843. DOI: 10.3791/50843.

Koliaraki, Vasiliki; Kollias, George (2016): Isolation of Intestinal Mesenchymal Cells from Adult Mice. In *BIO-PROTOCOL* 6 (18). DOI: 10.21769/BioProtoc.1940.

Konya, Viktoria; Marsche, Gunther; Schuligoi, Rufina; Heinemann, Akos (2013): E-type prostanoid receptor 4 (EP4) in disease and therapy. In *Pharmacology & therapeutics* 138 (3), pp. 485–502. DOI: 10.1016/j.pharmthera.2013.03.006.

Kuzumoto, Yukiyasu; Sho, Masayuki; Ikeda, Naoya; Hamada, Kaoru; Mizuno, Takashi; Akashi, Satoru et al. (2005): Significance and therapeutic potential of prostaglandin E2 receptor in hepatic ischemia/reperfusion injury in mice. In *Hepatology (Baltimore, Md.)* 42 (3), pp. 608–617. DOI: 10.1002/hep.20827.

Kvon, Evgeny Z.; Kazmar, Tomas; Stampfel, Gerald; Yáñez-Cuna, J. Omar; Pagani, Michaela; Schernhuber, Katharina et al. (2014): Genome-scale functional characterization of Drosophila developmental enhancers in vivo. In *Nature* 512 (7512), pp. 91–95. DOI: 10.1038/nature13395.

Lakatos, Peter-Laszlo (2006): Recent trends in the epidemiology of inflammatory bowel diseases: up or down? In *World journal of gastroenterology* 12 (38), pp. 6102–6108. DOI: 10.3748/wjg.v12.i38.6102.

Lange, Katrina M. de; Moutsianas, Loukas; Lee, James C.; Lamb, Christopher A.; Luo, Yang; Kennedy, Nicholas A. et al. (2017): Genome-wide association study implicates immune activation of multiple integrin genes in inflammatory bowel disease. In *Nature genetics* 49 (2), pp. 256–261. DOI: 10.1038/ng.3760.

Larsen, R.; Hansen, M. B.; Bindslev, N. (2005): Duodenal secretion in humans mediated by the EP4 receptor subtype. In *Acta physiologica Scandinavica* 185 (2), pp. 133–140. DOI: 10.1111/j.1365-201X.2005.01471.x.

Lee, Seung Bum; Han, Sung-Hoon; Park, Sunhoo (2018): Long-Term Culture of Intestinal Organoids. In *Methods in molecular biology (Clifton, N.J.)* 1817, pp. 123–135. DOI: 10.1007/978-1-4939-8600-2_13.

Li, Qiutang; Verma, Inder M. (2002): NF-kappaB regulation in the immune system. In *Nature reviews. Immunology* 2 (10), pp. 725–734. DOI: 10.1038/nri910.

Libioulle, Cécile; Louis, Edouard; Hansoul, Sarah; Sandor, Cynthia; Farnir, Frédéric; Franchimont, Denis et al. (2007): Novel Crohn disease locus identified by genome-wide association maps to a gene desert on 5p13.1 and modulates expression of PTGER4. In *PLoS genetics* 3 (4), e58. DOI: 10.1371/journal.pgen.0030058.

Liu, Jimmy Z.; van Sommeren, Suzanne; Huang, Hailiang; Ng, Siew C.; Alberts, Rudi; Takahashi, Atsushi et al. (2015): Association analyses identify 38 susceptibility loci for inflammatory bowel disease and highlight shared genetic risk across populations. In *Nature genetics* 47 (9), pp. 979–986. DOI: 10.1038/ng.3359.

Liu, Ta-Chiang; Stappenbeck, Thaddeus S. (2016): Genetics and Pathogenesis of Inflammatory Bowel Disease. In *Annual review of pathology* 11, pp. 127–148. DOI: 10.1146/annurev-pathol-012615-044152.

Lukovac, Sabina; Belzer, Clara; Pellis, Linette; Keijser, Bart J.; Vos, Willem M. de; Montijn, Roy C.; Roeselers, Guus (2014): Differential modulation by Akkermansia muciniphila and Faecalibacterium prausnitzii of host peripheral lipid metabolism and histone acetylation in mouse gut organoids. In *mBio* 5 (4). DOI: 10.1128/mBio.01438-14.

Manichanh, Chaysavanh; Borruel, Natalia; Casellas, Francesc; Guarner, Francisco (2012): The gut microbiota in IBD. In *Nature reviews. Gastroenterology & hepatology* 9 (10), pp. 599–608. DOI: 10.1038/nrgastro.2012.152.

Manzanero, Silvia (2012): Generation of mouse bone marrow-derived macrophages. In *Methods in molecular biology (Clifton, N.J.)* 844, pp. 177–181. DOI: 10.1007/978-1-61779-527-5_12.

Marim, Fernanda M.; Silveira, Tatiana N.; Lima, Djalma S.; Zamboni, Dario S. (2010): A method for generation of bone marrow-derived macrophages from cryopreserved mouse bone marrow cells. In *PloS one* 5 (12), e15263. DOI: 10.1371/journal.pone.0015263.

Markovič, Tijana; Jakopin, Žiga; Dolenc, Marija Sollner; Mlinarič-Raščan, Irena (2017): Structural features of subtype-selective EP receptor modulators. In *Drug discovery today* 22 (1), pp. 57–71. DOI: 10.1016/j.drudis.2016.08.003.

Maseda, Damian; Banerjee, Amrita; Johnson, Elizabeth M.; Washington, Mary Kay; Kim, Hyeyon; Lau, Ken S.; Crofford, Leslie J. (2018): mPGES-1-Mediated Production of PGE2 and EP4 Receptor Sensing Regulate T Cell Colonic Inflammation. In *Frontiers in immunology* 9, p. 2954. DOI: 10.3389/fimmu.2018.02954.

M'Koma, Amosy E. (2013): Inflammatory bowel disease: an expanding global health problem. In *Clinical medicine insights. Gastroenterology* 6, pp. 33–47. DOI: 10.4137/CGast.S12731.

Momozawa, Yukihide; Dmitrieva, Julia; Théâtre, Emilie; Deffontaine, Valérie; Rahmouni, Souad; Charloteaux, Benoît et al. (2018a): IBD risk loci are enriched in multigenic regulatory modules encompassing putative causative genes. In *Nature communications* 9 (1), p. 2427. DOI: 10.1038/s41467-018-04365-8.

Momozawa, Yukihide; Dmitrieva, Julia; Théâtre, Emilie; Deffontaine, Valérie; Rahmouni, Souad; Charloteaux, Benoît et al. (2018b): IBD risk loci are enriched in multigenic regulatory modules encompassing putative causative genes. In *Nature communications* 9 (1), p. 2427. DOI: 10.1038/s41467-018-04365-8.

Morteau, O.; Morham, S. G.; Sellon, R.; Dieleman, L. A.; Langenbach, R.; Smithies, O.; Sartor, R. B. (2000): Impaired mucosal defense to acute colonic injury in mice lacking cyclooxygenase-1 or cyclooxygenase-2. In *The Journal of clinical investigation* 105 (4), pp. 469–478. DOI: 10.1172/JCI6899.

Nakase, Hiroshi; Fujiyama, Yoshihide; Oshitani, Nobuhide; Oga, Toru; Nonomura, Kimiko; Matsuoka, Toshiyuki et al. (2010): Effect of EP4 agonist (ONO-4819CD) for patients with mild to moderate ulcerative colitis refractory to 5-aminosalicylates: a randomized phase II, placebo-controlled trial. In *Inflammatory Bowel Diseases* 16 (5), pp. 731–733. DOI: 10.1002/ibd.21080.

Neurath, Markus F.; Wittkopf, Nadine; Wlodarski, Alexandra; Waldner, Maximilian; Neufert, Clemens; Wirtz, Stefan et al. (2010): Assessment of tumor development and wound healing using endoscopic techniques in mice. In *Gastroenterology* 139 (6), 1837-1843.e1. DOI: 10.1053/j.gastro.2010.10.007.

Ostuni, Renato; Piccolo, Viviana; Barozzi, Iros; Polletti, Sara; Termanini, Alberto; Bonifacio, Silvia et al. (2013): Latent enhancers activated by stimulation in differentiated cells. In *Cell* 152 (1-2), pp. 157–171. DOI: 10.1016/j.cell.2012.12.018.

Park, Jean Y.; Pillinger, Michael H.; Abramson, Steven B. (2006): Prostaglandin E2 synthesis and secretion: the role of PGE2 synthases. In *Clinical immunology (Orlando, Fla.)* 119 (3), pp. 229–240. DOI: 10.1016/j.clim.2006.01.016.

Perlman, Robert L. (2016): Mouse models of human disease: An evolutionary perspective. In *Evolution, medicine, and public health* 2016 (1), pp. 170–176. DOI: 10.1093/emph/eow014.

Perše, Martina; Cerar, Anton (2012): Dextran sodium sulphate colitis mouse model: traps and tricks. In *Journal of biomedicine & biotechnology* 2012, p. 718617. DOI: 10.1155/2012/718617.

Pinchuk, I. V.; Mifflin, R. C.; Saada, J. I.; Powell, D. W. (2010): Intestinal mesenchymal cells. In *Current gastroenterology reports* 12 (5), pp. 310–318. DOI: 10.1007/s11894-010-0135-y.

Powell, D. W.; Pinchuk, I. V.; Saada, J. I.; Chen, Xin; Mifflin, R. C. (2011): Mesenchymal cells of the intestinal lamina propria. In *Annual review of physiology* 73, pp. 213–237. DOI: 10.1146/annurev.physiol.70.113006.100646.

Qiagen GmbH (2014): RNeasy Plus Micro Handbook. Protocol: Purification of Total RNA from Animal and Human Cells. Edited by Qiagen GmbH, checked on 8/31/2019.

Rahmani, Sara; Breyner, Natalia M.; Su, Hsuan-Ming; Verdu, Elena F.; Didar, Tohid F. (2019): Intestinal organoids: A new paradigm for engineering intestinal epithelium in vitro. In *Biomaterials* 194, pp. 195–214. DOI: 10.1016/j.biomaterials.2018.12.006.

Reinoso Webb, Cynthia; den Bakker, Hendrik; Koboziev, Iurii; Jones-Hall, Yava; Rao Kottapalli, Kameswara; Ostanin, Dmitry et al. (2018): Differential Susceptibility to T Cell-Induced Colitis in Mice: Role of the Intestinal Microbiota. In *Inflammatory Bowel Diseases* 24 (2), pp. 361–379. DOI: 10.1093/ibd/izx014.

Rickels, Ryan; Shilatifard, Ali (2018a): Enhancer Logic and Mechanics in Development and Disease. In *Trends in cell biology* 28 (8), pp. 608–630. DOI: 10.1016/j.tcb.2018.04.003.

Rickels, Ryan; Shilatifard, Ali (2018b): Enhancer Logic and Mechanics in Development and Disease. In *Trends in cell biology* 28 (8), pp. 608–630. DOI: 10.1016/j.tcb.2018.04.003.

Rodriguez-Rodriguez, Luis; Ivorra-Cortes, Jose; Carmona, F. David; Martín, Javier; Balsa, Alejandro; van Steenbergen, Hanna W. et al. (2015): PTGER4 gene variant rs76523431 is a candidate risk factor for radiological joint damage in rheumatoid arthritis patients: a genetic study of six cohorts. In *Arthritis research & therapy* 17, p. 306. DOI: 10.1186/s13075-015-0830-z.

Roulis, Manolis; Armaka, Maria; Manoloukos, Menelaos; Apostolaki, Maria; Kollias, George (2011): Intestinal epithelial cells as producers but not targets of chronic TNF suffice to cause murine Crohn-like pathology. In *Proceedings of the National Academy of Sciences of the United States of America* 108 (13), pp. 5396–5401. DOI: 10.1073/pnas.1007811108.

Rubin, Deborah C.; Shaker, Anisa; Levin, Marc S. (2012): Chronic intestinal inflammation: inflammatory bowel disease and colitis-associated colon cancer. In *Frontiers in immunology* 3, p. 107. DOI: 10.3389/fimmu.2012.00107.

Ruel, Joannie; Ruane, Darren; Mehandru, Saurabh; Gower-Rousseau, Corinne; Colombel, Jean-Frédéric (2014): IBD across the age spectrum: is it the same disease? In *Nature reviews. Gastroenterology & hepatology* 11 (2), pp. 88–98. DOI: 10.1038/nrgastro.2013.240.

Russel, M.G.V.M (2000): Changes in the incidence of inflammatory bowel disease. What does it mean? In *European journal of internal medicine* 11 (4), pp. 191–196. DOI: 10.1016/S0953-6205(00)00090-X.

Sanyal, Amartya; Lajoie, Bryan R.; Jain, Gaurav; Dekker, Job (2012): The long-range interaction landscape of gene promoters. In *Nature* 489 (7414), pp. 109–113. DOI: 10.1038/nature11279.

Sastre, Beatriz; Fernández-Nieto, Mar; López, Esther; Gámez, Cristina; Aguado, Erica; Quirce, Santiago et al. (2011): PGE(2) decreases muscle cell proliferation in patients with non-asthmatic eosinophilic bronchitis. In *Prostaglandins & other lipid mediators* 95 (1-4), pp. 11–18. DOI: 10.1016/j.prostaglandins.2011.03.002.

Schernthanner, Marina (2019): The role of PGE2 signaling at the epithelial-mesenchymal interface in Colorectal Cancer and Inflammatory Bowel Disease. Edited by University of Innsbruck. Innsbruck, checked on 9/15/2019.

Schweda, Frank; Klar, Jürgen; Narumiya, Shuh; Nüsing, Rolf M.; Kurtz, Armin (2004): Stimulation of renin release by prostaglandin E2 is mediated by EP2 and EP4 receptors in mouse kidneys. In *American journal of physiology. Renal physiology* 287 (3), F427-33. DOI: 10.1152/ajprenal.00072.2004.

Sheibanie, Amir F.; Yen, Jui-Hung; Khayrullina, Tanzilya; Emig, Frances; Zhang, Ming; Tuma, Ronald; Ganea, Doina (2007): The proinflammatory effect of prostaglandin E2 in experimental inflammatory bowel disease is mediated through the IL-23--IL-17 axis. In *Journal of immunology (Baltimore, Md. : 1950)* 178 (12), pp. 8138–8147. DOI: 10.4049/jimmunol.178.12.8138.

Shivananda, S.; Lennard-Jones, J.; Logan, R.; Fear, N.; Price, A.; Carpenter, L.; van Blankenstein, M. (1996): Incidence of inflammatory bowel disease across Europe: is there a difference between north and south? Results of the European Collaborative Study on Inflammatory Bowel Disease (EC-IBD). In *Gut* 39 (5), pp. 690–697. DOI: 10.1136/gut.39.5.690.

Simmons, Daniel L.; Botting, Regina M.; Hla, Timothy (2004): Cyclooxygenase isozymes: the biology of prostaglandin synthesis and inhibition. In *Pharmacological reviews* 56 (3), pp. 387–437. DOI: 10.1124/pr.56.3.3.

Simons, Donald M.; Caton, Andrew J. (2011): Flow cytometric profiling of mature and developing regulatory T cells in the thymus. In *Methods in molecular biology (Clifton, N.J.)* 707, pp. 55–69. DOI: 10.1007/978-1-61737-979-6_5.

Sohrabpour, Amir Ali; Malekzadeh, Reza; Keshavarzian, Ali (2010): Current therapeutic approaches in inflammatory bowel disease. In *Current pharmaceutical design* 16 (33), pp. 3668–3683. DOI: 10.2174/138161210794079155.

Souza, Heitor S. P. de; Fiocchi, Claudio (2016): Immunopathogenesis of IBD: current state of the art. In *Nature reviews. Gastroenterology & hepatology* 13 (1), pp. 13–27. DOI: 10.1038/nrgastro.2015.186.

Stange, Eduard F.; Wehkamp, Jan (2016): Recent advances in understanding and managing Crohn's disease. In *F1000Research* 5, p. 2896. DOI: 10.12688/f1000research.9890.1.

STEMCELL Technologies Inc. (2016): Intestinal Epithelial Organoid Culture with IntestiCult™ Organoid Growth Medium (Mouse). 2.0.1st ed. Edited by Stemcell Technologies (28223). Available online at https://www.stemcell.com/intestinal-epithelial-organoid-culture-with-intesticult-organoid-growth-medium-mouse-lp.html, checked on 8/29/2019.

STEMCELL Technologies Inc. (2019): EasySep Mosue T-Cell Isolation Kit. 1_1_5. Edited by Stemcell Technologies (#29286). Available online at www.stemcell.com/PIS, checked on 9/10/2019.

Swiatecka, Dominika; Mackie, Alan (2015): The Impact of Food Bioactives on Health: In Vitro and Ex Vivo Models. [Erscheinungsort nicht ermittelbar]: Springer.

Takeuchi, Koji (2010): Prostaglandin EP receptors and their roles in mucosal protection and ulcer healing in the gastrointestinal tract. In *Advances in clinical chemistry* 51, pp. 121–144.

Tam, Vivian; Patel, Nikunj; Turcotte, Michelle; Bossé, Yohan; Paré, Guillaume; Meyre, David (2019): Benefits and limitations of genome-wide association studies. In *Nature reviews. Genetics* 20 (8), pp. 467–484. DOI: 10.1038/s41576-019-0127-1.

Tao, Yulong; Zhu, Sang; Yang, Hong; Huang, Fei; Fu, Hui; Tao, Xia (2016): Isolation and characterization of putative mesenchymal stem cells from mammalian gut. In *Cytotechnology* 68 (6), pp. 2753–2759. DOI: 10.1007/s10616-016-9992-z.

Thermo Fisher Scientific: Real-Time PCR Handbook. Edited by Thermo Fisher Scientific.

Thermo Fisher Scientific: TURBO DNA-free Kit User Guide. TURBO DNase Treatment and Removal Reagents. Edited by Thermo Fisher Scientific (1907M), checked on 8/31/2019.

Thermo Fisher Scientific (2016): TRIzol Reagent. User Guide. Edited by Thermo Fisher Scientific (MAN0001271). Available online at thermofisher.com, checked on 9/12/2019.

Torres, Joana; Billioud, Vincent; Sachar, David B.; Peyrin-Biroulet, Laurent; Colombel, Jean-Frédéric (2012): Ulcerative colitis as a progressive disease: the forgotten evidence. In *Inflammatory Bowel Diseases* 18 (7), pp. 1356–1363. DOI: 10.1002/ibd.22839.

UniProt: a worldwide hub of protein knowledge (2019). In *Nucleic acids research* 47 (D1), D506-D515.

Verstockt, Bram; Smith, Kenneth Gc; Lee, James C. (2018): Genome-wide association studies in Crohn's disease: Past, present and future. In *Clinical & translational immunology* 7 (1), e1001. DOI: 10.1002/cti2.1001.

Walfish, Aaron E.; Ching Companioni, Rafael A. (2019): Overview of Inflammatory Bowel Disease. Professional Version. MSD Manual. Available online at https://www.msdmanuals.com/professional/gastrointestinal-disorders/inflammatory-bowel-disease-ibd/overview-of-inflammatory-bowel-disease, checked on 9/19/2019.

Weintraub, Abraham S.; Li, Charles H.; Zamudio, Alicia V.; Sigova, Alla A.; Hannett, Nancy M.; Day, Daniel S. et al. (2017): YY1 Is a Structural Regulator of Enhancer-Promoter Loops. In *Cell* 171 (7), 1573-1588.e28. DOI: 10.1016/j.cell.2017.11.008.

Weischenfeldt, Joachim; Porse, Bo (2008): Bone Marrow-Derived Macrophages (BMM): Isolation and Applications. In *CSH protocols* 2008, pdb.prot5080. DOI: 10.1101/pdb.prot5080.

Yan, Yutao; Kolachala, Vasantha; Dalmasso, Guillaume; Nguyen, Hang; Laroui, Hamed; Sitaraman, Shanthi V.; Merlin, Didier (2009): Temporal and spatial analysis of clinical and molecular parameters

in dextran sodium sulfate induced colitis. In *PloS one* 4 (6), e6073. DOI: 10.1371/journal.pone.0006073.

Yokoyama, Utako; Iwatsubo, Kousaku; Umemura, Masanari; Fujita, Takayuki; Ishikawa, Yoshihiro (2013): The prostanoid EP4 receptor and its signaling pathway. In *Pharmacological reviews* 65 (3), pp. 1010–1052. DOI: 10.1124/pr.112.007195.

Zhang, Yushan; Daaka, Yehia (2011): PGE2 promotes angiogenesis through EP4 and PKA Cγ pathway. In *Blood* 118 (19), pp. 5355–5364. DOI: 10.1182/blood-2011-04-350587.

Zidar, Nina; Odar, Katarina; Glavac, Damjan; Jerse, Maja; Zupanc, Tomaz; Stajer, Dusan (2009): Cyclooxygenase in normal human tissues--is COX-1 really a constitutive isoform, and COX-2 an inducible isoform? In *Journal of cellular and molecular medicine* 13 (9B), pp. 3753–3763. DOI: 10.1111/j.1582-4934.2008.00430.x.

5 Supplementary material

5.1 Aberrations

AB	**a**nti**b**ody
AC	**a**denylate **c**yclase
ACK	**a**mmonium-chloride-**p**otassium
APC	**a**llo**p**hyco**c**yanin
AWAR	**A**nimal **W**elfare **A**ct **R**egulations
BMDMs	**b**one **m**arrow **d**erived **m**acrophage**s**
β-ME	**β**-**m**ercapto**e**thanol
B2M	**b**eta-**2**-**m**icroglobulin
cAMP	**c**yclic **a**denosine **m**ono**p**hosphate
CD	**c**luster of **d**ifferentiation
CD	**C**rohn's **d**isease
cDNA	**c**omplementary **DNA**
COX-2	**c**yclo**ox**ygenase-**2**
Cq	**q**uantification **c**ycle
DB-1	**d**igestion **b**uffer-**1**
DEPC-water	**di**e**t**hyl**p**yro**c**arbonate-treated **water**

DMEM	**D**ulbecco's **m**odified **e**agle **m**edium
dNTPs	**d**eoxy**n**ucleotide **t**ri**p**hosphate
dsDNA	**d**ouble-**s**tranded **DNA**
DTT	**di**thio**t**hreitol
EDTA	**e**thylene**d**iamine**t**etraacetic **a**cid
Enh-KO	Ptger4-**Enh**ancer **k**nock-**o**ut mouse line
EP4	prostaglandin $\mathbf{E_2}$ receptor **p**rotein **4**
FBS	**f**etal **b**ovine **s**erum
FITC	**f**luorescein **i**so**t**hio**c**yanate
GCDR	**G**entle **C**ell **D**issociation **R**eagent
gDNA	**g**enomic **DNA**
GI-tract	**g**astro**i**ntestinal **tract**
GWAS	**g**enome-**w**ide **a**ssociation **s**tudy
HBSS	**H**ank's **b**alanced **s**alt **s**olutions
HEPES	4-(2-**h**ydroxy**e**thyl)-1-**p**iperazine**e**thane**s**ulfonic acid
IBD	**I**nflammatory **B**owel **D**isease
IC-medium	complete **I**ntesti**C**ult™ Organoid Growth **Medium**
IL	**i**nter**l**eukin
IMCs	**i**ntestinal **m**esenchymal **c**ell**s**
INF-γ	**in**ter**f**eron **γ**
i.p.	**i**ntra-**p**eritoneal
Kbp	**k**ilo **b**ase**p**air
LPS	**l**ipo**p**oly**s**accharides
M-CSF	**m**acrophage **c**olony **s**timulating **f**actor
MHC-1	**m**ajor **h**istocompatibility **c**omplex – class **1**
MLN	**m**esenteric **l**ymph **n**odes
mRNA	**m**essenger **RNA**
NSAIDs	**n**on-**s**teroidal **a**nti-**i**nflammatory **d**rug**s**

NTCs	**n**o **t**emplate **c**ontrols
PB	**P**acific **B**lue
PCR	**p**oly**c**hain **r**eaction
PE	**p**hyco**e**rythrin
Pen/Strep	**pen**icillin**/strep**tomycin
PGE_2	**p**rosta**g**landin **E_2**
qPCR	**q**uantitative **p**oly**c**hain **r**eaction
RPMI medium	**R**oswell **P**ark **M**emorial **I**nstitute medium
RT	**r**everse **t**ranscriptase
RT	**r**oom **t**emperature
SNPs	**s**ingle-**n**ucleotide **p**olymorphism**s**
TNF	**t**umor **n**ecrosis **f**actor
UC	**u**lcerative **c**olitis

5.2 Supplementary figures

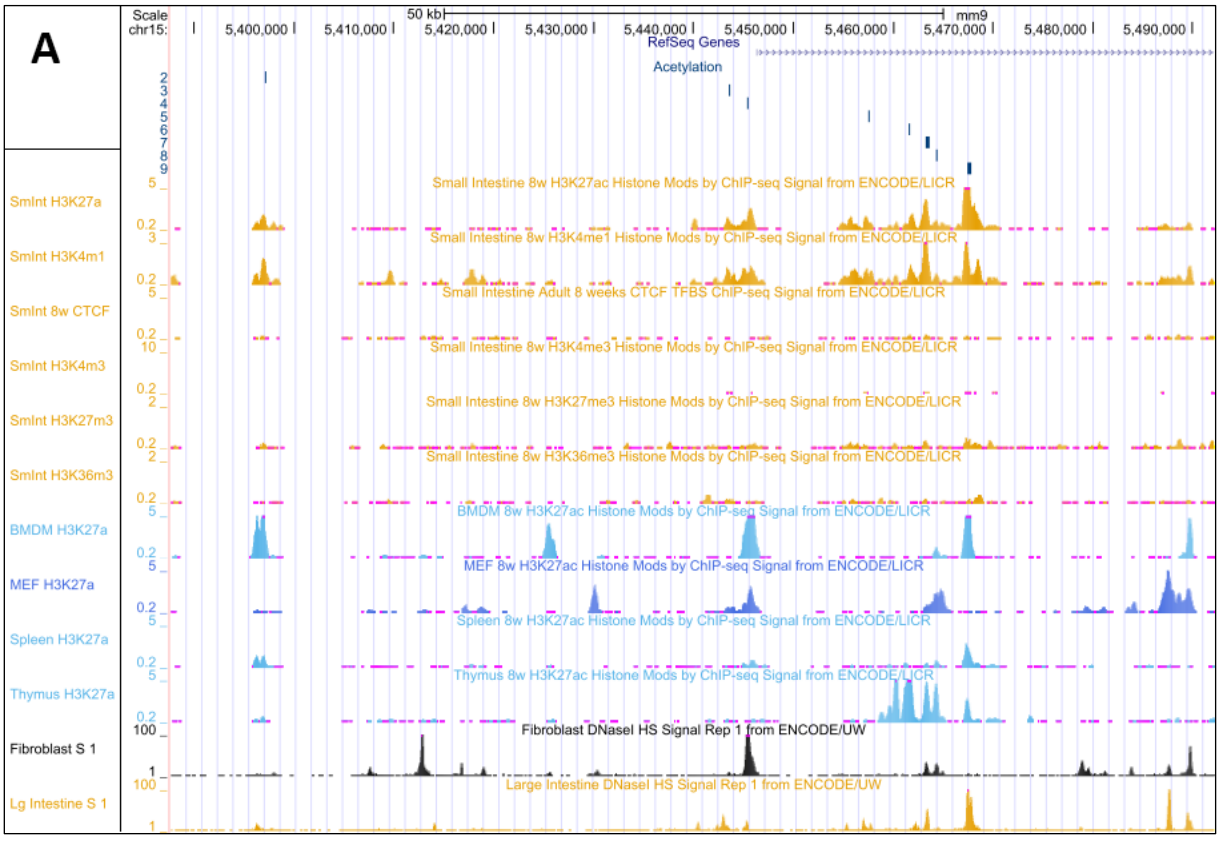

Supp.-Figure 1: Visualization of the potential enhancer region upstream of Ptger4 in various tissues. Histone acetylation pattern, indicating active enhancer elements were found in this region in tissues and cell types of the GI-tract and the immune system. The enhancer elements are conserved between humans and mice.

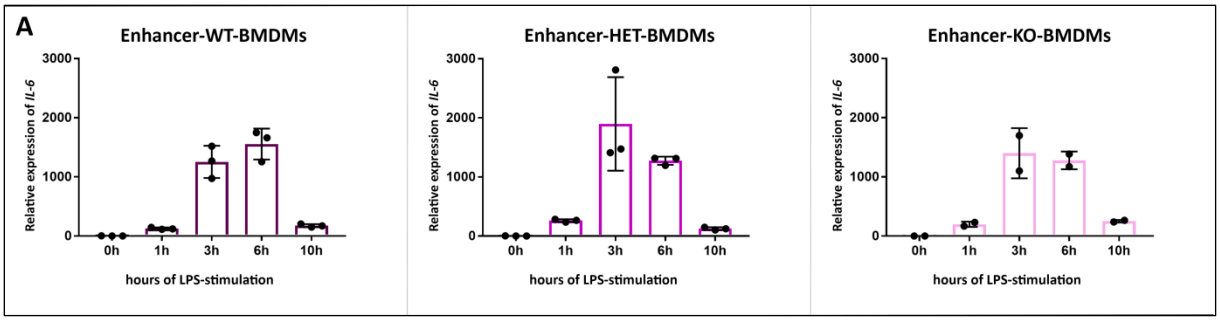

Supp.-Figure 2: Upregulation of IL-6 in LPS stimulated BMDMs derived from Enh-WT, -HET and –KO cells. Three technical replicates per timepoint for Enh-WT and –HET BMDMs, and two technical replicates per timepoint for Enh-KO BMDMs. n= 1 mouse per genotype.